

---

Geneva, Switzerland 6 - 16 Sept 2011

Question: 4/15

SOURCE<sup>1</sup>: TNO

TITLE: G.fast: Wideband modeling of twisted pair cables as two-ports

---

### ABSTRACT

This contribution is a covering letter for the attached research report, that elaborates on wideband modeling of twisted pair cables. It introduces a new class of parametric models suitable for G.fast performance studies up to hundreds of MHz. The attached report describes in great detail the underlying modeling theory and contains lots of measurement evidence about the validity of the proposed models. This report is provided to the ITU-T to assist in the development of G.fast solutions. This contribution is for information only.

### 1. Introduction:

Recently, the new project G.fast has been initiated within ITU-T SG15. In order for this project to become a success, it is of importance to realistically characterize and model the channels between the last distribution point and the end-user premises equipment.

G.fast transceivers are envisaged to work over twisted pair cabling and to utilize frequencies up to hundreds of Megahertz. To develop transceivers for this, detailed knowledge is needed about the transmission properties of the last copper drop of such loops at these high frequencies. These properties include insertion loss, impedance, crosstalk coupling, etc. Such knowledge is commonly available for frequencies up to 30 MHz but this does not hold for frequencies up to hundreds of MHz.

Due to the lack of such models, an initial performance studies from ASSIA [6] and CopperGate [8] simply extended existing channel and crosstalk models to use above 30 MHz with no modification. However the lack of any validation at higher frequencies makes such studies unreliable. We agree with Alcatel-Lucent [7] that extrapolation of known models may not be sufficient for the purpose of technology evaluation, and agree with CopperGate [\*] to put a call for papers focusing on wire models above 30MHz and FEXT models relevant for the G.fast deployment scenarios.

TNO identified in a previous contribution [2] the need for realistic wideband cable models that are validated up to hundreds of MHz, and unveiled [1,3] the results of an extensive cable measurement campaign on different cable types. Performance studies are to be based on such models, and their validity should be demonstrated by a good match between predicted and measured cable properties.

A first step is the development of full two-port models, describing the transmission and reflection/impedance of a cable section. With such models, the transmission and reflection of arbitrary loop topologies can easily be simulated via a composition of loop segments. And when needed the two-port models can be combined with two-port measurements on irregularities (like splices and manipulation points) to make the simulation more realistic. The development of wideband crosstalk models should follow as well.

---

1

---

**Author:** Rob van den Brink  
TNO

---

Tel:+31 88 86 67059  
Email: rob.vandenbrink@tno.nl

---

**Contact:** Bas van den Heuvel  
TNO

---

Tel: +31 88 86 67126  
Email: bas.vandenheuvel@tno.nl

## **2. Study into wideband modeling of twisted pair cables**

The present contribution, unveils the results of an extensive study into wideband cable modeling of twisted pair cables as two-ports. It is a covering letter for the attached research report, and that report introduces a new class of parametric cable models and describes the underlying theory in detail. Subsequently, it shows what parameter values have been extracted from cable measurements and how good the models can match with the measurements.

The research was conducted in the Celtic 4GBB project [5], and the document is the TNO part of a multi-document 4GBB deliverable. It is the intention of TNO to assist with the development of the reference models needed for predicting loops

## **3. Summary**

This paper should be presented under the G.fast agenda item, and addresses issue 5.1

The paper highlights the need for reference models to describe the various wiring elements within a twisted pair cable topology, suitable for frequencies up to hundreds of MHz, and unveils the results of an extensive study into wideband cable modeling of twisted pair cabling.

This contribution provides the motivation and proof of the reference models being proposed in another contribution [4], and is therefore for information only

It is proposed to agree to add the following new issue to the G.fast issues list:

## **4. References**

- [1] Rob F.M. van den Brink, “*Enabling 4GBB via Hybrid-FttH*”, Broadband Forum presentation bbf2010.1395.00 , San Francisco, dec 2010.
- [2] TNO (Rob van den Brink, Bas van den Heuvel), “*G.fast: The need for wideband reference models of loop segments within twisted pair cable topologies*”, ITU contribution 11BM-020, April 18, 2011.
- [3] TNO (Rob van den Brink, Bas van den Heuvel), “*G.fast: Wideband transfer and crosstalk measurements on twisted pair cables*”, ITU contribution 11BM-021, April 18, 2011.
- [4] TNO (Rob van den Brink, Bas van den Heuvel), “*G.fast: Parametric cable models for specifying reference loops*”, ITU contribution 11GS3-029, Geneva Sept 2011
- [5] 4GBB Consortium, cooperating as a project under the EUREKA CELTIC cluster. See [www.4gbb.eu](http://www.4gbb.eu) for further details.
- [6] Assia (Ken Kerpez), “*G.fast: Fast Maximum Number of Bits/Hz*”, ITU contribution 11BM-028, Bedford, June 2011.
- [7] Alcatel-Lucent (Danny Van Bruyssel), “*G.fast: Observations On Channel Characteristics Measurements*”, ITU contribution 11BM-048, Bedford, June 2011.
- [8] CopperGate (Erez Ben-Tovim), “*G.fast: G.hn performance preliminary predictions*”, ITU contribution 11BM-071, Bedford, June 2011.
- [9] Ikanos (Massimo Sorbara), “*G.fast: Proposal to define reference loop topologies for G.fast*”, ITU contribution 11BM-077, Bedford, June 2011.

## WIDEBAND MODELING OF TWISTED PAIR CABLES AS TWO-PORTS PART 3 – TNO APPROACH

### DOCUMENT IDENTIFICATION

<b>Doc number:</b>	WP3_0142_V04_CableModel2port_TNO
<b>Title:</b>	<b>Milestone M3.1C.1 / Part 2 (Interim report):</b> Wideband modeling of twisted pair cables as two-ports, part 3 – TNO approach
<b>Author(s):</b>	Rob van den Brink (TNO, The Netherlands) - <a href="mailto:Rob.vandenBrink@tno.nl">Rob.vandenBrink@tno.nl</a>
<b>Abstract:</b>	<p>Modeling cable characteristics like transmission, reflection and crosstalk coupling is an essential step in enabling performance studies by means of simulations. A two-port approach is adequate for performance studies on individual lines, but a multi-port approach is preferred in performance studies on coordinated transmission solutions (with names like vectoring, phantoming, MIMO, etc). However, in some cases a multi-port approach may complicate more than it contributes, so a two-port approach is still valuable.</p> <p>This document is the third part of a multi-document report, providing the TNO approach on cable modeling. It proposes a new class of parametric models, suitable for frequency domain studies up to hundreds of MHz, and suitable for time domain studies. It elaborates in detail on the theory as well as the extraction of model parameters from many cable measurements, and demonstrates how effective the new models are. In addition, this document proposes suitable reference models for four different cable types: a high quality CAT5 cable, a medium quality telephony cable use in buildings, a low quality telephony cable for in-house wiring, and for an access cable typical used in the Netherlands by KPN.</p> <p><i>NOTE: This milestone document reflects the current status of text that is to be updated into a deliverable before the end of 2011.</i></p>

### DOCUMENT HISTORY

	Date	Author	org	modification
<b>V01</b>	Feb 2011	Rob van den Brink	TNO	Creation from scratch.
<b>V02</b>	June 2011	Rob van den Brink	TNO	Completion of the modeling theory
<b>V03</b>	Aug 2011	Rob van den Brink	TNO	Extraction of parameter values for various cable models
<b>V04</b>	Sept 2011	Rob van den Brink	TNO	Update after TNO-internal review by Bas van den heuvel

**TABLE OF CONTENT**

<b>1</b>	<b>INTRODUCTION</b> .....	<b>4</b>
<b>2</b>	<b>WIDEBAND MODELLING OF TWISTED PAIR CABLING</b> .....	<b>6</b>
2.1	Modeling cables via impedances and admittances .....	6
2.2	The proposed class of parametric models .....	7
2.3	Consequences for series impedances .....	8
2.4	Consequences for shunt admittances .....	8
2.5	Consequences for impulse responses .....	9
2.6	Alternative parametric description for fitting the models.....	9
2.7	From primary cable parameters to matrix parameters .....	10
<b>3</b>	<b>FURTHER DETAILS ON MODELLING CABLES</b> .....	<b>12</b>
3.1	Shaping functions for modeling impedances .....	12
3.1.1	<i>Overview of analyzed shaping functions</i> .....	12
3.1.2	<i>Definition of elaborated shaping functions</i> .....	14
3.2	Shaping functions for modeling admittance .....	15
3.2.1	<i>Example shaping function #1</i> .....	16
3.2.2	<i>Example shaping function #2</i> .....	17
3.3	Finding starting values for skin frequency .....	18
<b>4</b>	<b>MODELING HIGH QUALITY, CAT 5 CABLING</b> .....	<b>20</b>
4.1	Match with two-port parameters.....	20
4.2	Match with secondary cable parameters (per unit length) .....	22
4.3	Match with primary cable parameters (per unit length) .....	23
4.4	Extracted parameter values for various models and sections .....	25
4.4.1	<i>Loop section of 232m</i> .....	25
4.4.2	<i>Loop section of 61m</i> .....	25
4.4.3	<i>Loop section of 10m</i> .....	26
4.4.4	<i>Virtual loop section of 2 ´ 232m in cascade</i> .....	27
4.5	Common reference model for this CAT5 cable.....	27
<b>5</b>	<b>MODELING MEDIUM QUALITY CABLING FOR TELEPHONY</b> .....	<b>28</b>
5.1	Match with two-port parameters.....	28
5.2	Match with secondary cable parameters (per unit length) .....	31
5.3	Match with primary cable parameters (per unit length) .....	32
5.4	Extracted parameters for various models and sections.....	33
5.4.1	<i>Quad #1, 378m</i> .....	33
5.4.2	<i>Quad #2, 378m</i> .....	34
5.4.3	<i>Quad #5, 378m</i> .....	35
5.4.4	<i>Virtual loop section of 6 ´ 378m in cascade</i> .....	35
5.5	Common reference model for this cable.....	36
<b>6</b>	<b>MODELING LOW QUALITY CABLING FOR TELEPHONY</b> .....	<b>37</b>
6.1	Match with two-port parameters.....	37
6.2	Match with secondary cable parameters (per unit length) .....	39
6.3	Match with primary cable parameters (per unit length) .....	41
6.4	Extracted parameters for various models and sections.....	42
6.4.1	<i>Loop section of 50m</i> .....	42
6.4.2	<i>Virtual loop section of 2 ´ 50m in cascade</i> .....	43
6.5	Common reference model for this cable.....	43
<b>7</b>	<b>MODELING KPN ACCES CABLING FOR TELEPHONY</b> .....	<b>44</b>
7.1	Match with two-port parameters.....	44
7.2	Match with secondary cable parameters (per unit length) .....	46
7.3	Match with primary cable parameters (per unit length) .....	47
7.4	Extracted parameters for various models and wire pairs .....	49
7.4.1	<i>Individual wire pairs (104.1m)</i> .....	49
7.4.2	<i>Virtual loop section of 6 ´ 100m in cascade</i> .....	51
7.5	Common reference model for this cable.....	51
<b>8</b>	<b>REFERENCES</b> .....	<b>52</b>

## MANAGEMENT SUMMARY

*Problem to be solved:* The maximum data rate that can be transported through a given access network is highly dependent on the characteristics of the used (twisted pair) cabling, being designed for transporting analog telephony signals. Insertion loss and crosstalk coupling in these cables are the key factors of these limitations, and they have been studied in the past for ADSL and VDSL applications (typically up to 30MHz). But the transportation of a 4GBB service package requires modem signals that are much higher in frequency and very little is known on these cables beyond 30MHz. This troubles the prediction of the maximum attainable data rate that can be delivered via such access networks.

*Aims:* The aim of modeling of twisted pair cables as two-ports is to predict the maximum attainable data rate by means of realistic simulations. These models are to be an extension to existing two-port models that are commonly used for ADSL and VDSL studies. They should not only be valid in the frequency domain over a wide frequency range (up to hundreds of MHz) but also be valid in the time domain (causal system). The predictions with these models should result in causal predictions of impulse response, meaning that the output depends on past/current inputs but not future inputs. In other words: nothing should come out of the cable before any impulse has been injected.

*Results:*

The TNO approach is focused on developing parametric models that are defined such that they are realistic by nature for both time domain and frequency domain studies up to hundreds of MHz. This document introduces a new class of parametric models suitable for performance studies with G.fast modems. It elaborates in detail on the theory as well as the extraction of model parameters from many cable measurements, and demonstrates how applicable the new models are. In addition, this document proposes suitable reference models for four different cable types: a high quality CAT5 cable, a medium quality telephony cable use in buildings, a low quality telephony cable for in-house wiring, and for a typical access cable used in the Netherlands by KPN.

*Follow up:* The next step is to create multi-port computer models as well, and to use them in a variety of performance studies. Such studies are to predict the maximum data rate that can be transported through a given access network.

# 1 INTRODUCTION

Modeling cable properties is an essential step in enabling performance studies to the transportation of a 4GBB service package via G.fast modems. Such studies are needed for analyzing what bitrates are achievable for 4GBB in a given access network.

Many different parametric cable models have been developed in the past [\*] to enable performance studies for HDSL, ADSL and VDSL, but they were often restricted to 30 MHz or less. Several of these models were only designed for studies in the frequency domain and these models are predicting unrealistic (non-real) impulse functions when applied to time domain studies. It may be obvious from this that new parametric models are needed to enable adequate studies for G.fast.

This deliverable elaborates on a new class of parametric models for cables as two-ports, that are applicable for performance studies up to 500MHz, and that are also suitable for time domain studies. Parametric models with these properties are essential for studies in 4GBB work package 4 where new modulation schemes are being studied and in ITU-T-SG15 where a standard for G.fast is created. Models that are currently commonly used, like the BT#1-model [\*] used in TP100 [\*] and the KPN#1 model [\*] used in TP150 [\*] are predicting unrealistic (non-real) impulse responses and therefore not considered as suitable.

The first few chapters are dedicated to a theoretical foundation of these parametric models, while the remaining chapters are dedicated to the extraction of parameter values for these models from cable measurements up to 500 MHz. These chapters demonstrate how effective the proposed parametric models are, and provide for each cable type being studied an adequate reference model for the cable as a whole.

## Parametric models

Two of the proposed parametric models have demonstrated to be very useful in practice. A simple one offering a good compromise between simplicity and good match with measurements, and an advanced model with more parameters to improve the match with measurements

*Simple model, with square root function, 6+1 parameters:*

$$[Z_s, Y_p] = \text{Model\_01} (Z_{0\mu}, \eta_{VF}, R_{s0}, q_L, q_H, f, f_d)$$

$$Z_s(j\omega) = j\omega \cdot L_{s\infty} + R_{s0} \times \left( 1 - q_s + \text{sqrt} \left( q_s^2 + 2 \cdot \frac{j\omega}{w_s} \right) \right)$$

$$Y_p(j\omega) = j\omega \cdot C_{p0} \times \left( 1 + \frac{j\omega}{w_d} \right)^{-2f/p}$$

*More advanced model, with square root of rational function, 8+1 parameters:*

$$[Z_s, Y_p] = \text{Model\_02} (Z_{0\mu}, \eta_{VF}, R_{s0}, q_L, q_H, q_x, q_y, f, f_d)$$

$$Z_s(j\omega) = j\omega \cdot L_{s\infty} + R_{s0} \times \left( 1 - q_s \cdot q_x + \text{sqrt} \left( q_s^2 \cdot q_x^2 + 2 \cdot \frac{j\omega}{w_s} \cdot \left( \frac{q_s^2 + j\omega/w_s \cdot q_y}{q_s^2/q_x + j\omega/w_s \cdot q_y} \right) \right) \right)$$

$$Y_p(j\omega) = j\omega \cdot C_{p0} \times \left( 1 + \frac{j\omega}{w_d} \right)^{-2f/p}$$

Where:

$$L_{s\infty} = \frac{1}{h_{VF} \cdot c_0} \times Z_{0\infty}$$

$$C_{p0} = \frac{1}{h_{VF} \cdot c_0} \times \frac{1}{Z_{0\infty}}$$

$$q_s = \frac{1}{q_H^2 \cdot q_L}$$

$$w_s = q_H^2 \cdot w_{s0} = q_H^2 \cdot \left( \frac{4p \cdot R_{s0}}{m_0} \right)$$

$$w_d = 2p \cdot f_d$$

$$c_0 = 3 \cdot 10^8 \text{ [m/s]}$$

$$m_0 = 4\pi \cdot 10^{-7} \text{ [H/m].}$$

**Reference models.**

The parametric modeling approach has been applied to extract the associated parameters from many cable measurements, to find “typical” values that can be used as a reference model for the cables being studied. So far four different cable types have been analyzed in the next chapters, and the above mentioned parametric model (the one with square root of a rational function) was chosen to serve as reference model. The associated parameters found for the different cable types are:

Cable type	Parametric model	Parameters of reference model
HQ_CAT5	[ASYMP.sqrt.rat]	Z0_inf=98.000000; VF=0.690464; Rs0=165.900000e-3; qL=2.150000; qH=0.859450; qX=0.500000; qY=0.722636; Phi=0.973846e-3; Fd=1.000000;
MQ_TelCable_30q	[ASYMP.sqrt.rat]	Z0_inf=132.348256; VF=0.675449; Rs0=170.500000e-3; qL=1.789725; qH=0.725776; qX=0.799306; qY=1.030832; Phi=0.005222e-3; Fd=1.000000
LQ_Gamma	[ASYMP.sqrt.rat]	Z0_inf=98.369783; VF=0.681182; Rs0=170.800000e-3; qL=1.700000; qH=0.650000; qX=0.777307; qY=1.500000; Phi=3.023930e-3; Fd=1.000000
KPN_acc#1	[ASYMP.sqrt.rat]	Z0_inf=125.636455; VF=0.729623; Rs0=180.000000e-3; qL=1.666050; qH=0.740000; qX=0.848761; qY=1.207166; Phi=1.762056e-3; Fd=1.000000

**Validity of the reference models.**

The transfer measurements of the HQ\_CAT5 cable show an excellent match up to 500MHz, and this is due to the high quality construction of the cable. This makes the model applicable for up to hundreds of MHz.

However, the transfer measurements of the other cables show some resonant behavior (notches) at frequencies between 30 and 100MHz, and this is currently not well understood. See the associated chapters for further details. And above about 100MHz, the transmission becomes even a bit random in nature, which is assumed to be caused by the imperfect homogeneous construction of the twisted-pair cable.

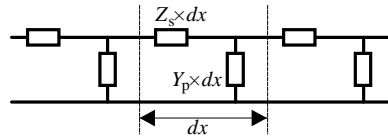
It is assumed that this resonant + random behavior is caused by the fact that their construction isn't as perfect as for HQ\_CAT5 cable, and that behavior puts a fundamental upper frequency limit to what ever can be matched with a pure homogeneous cable model. However if these notches are assumed to be deterministic in nature they might be modeled separately in a deterministic manner as well.

Therefore the proposed homogeneous models are assumed to be applicable up to 100 MHz if resonant effects are handled separately. And if the models are augmented with random variations above 100 MHz, then the results may even be applicable beyond 100 MHz, but those refinements are left for further study.

## 2 WIDEBAND MODELLING OF TWISTED PAIR CABLING

### 2.1 Modeling cables via impedances and admittances

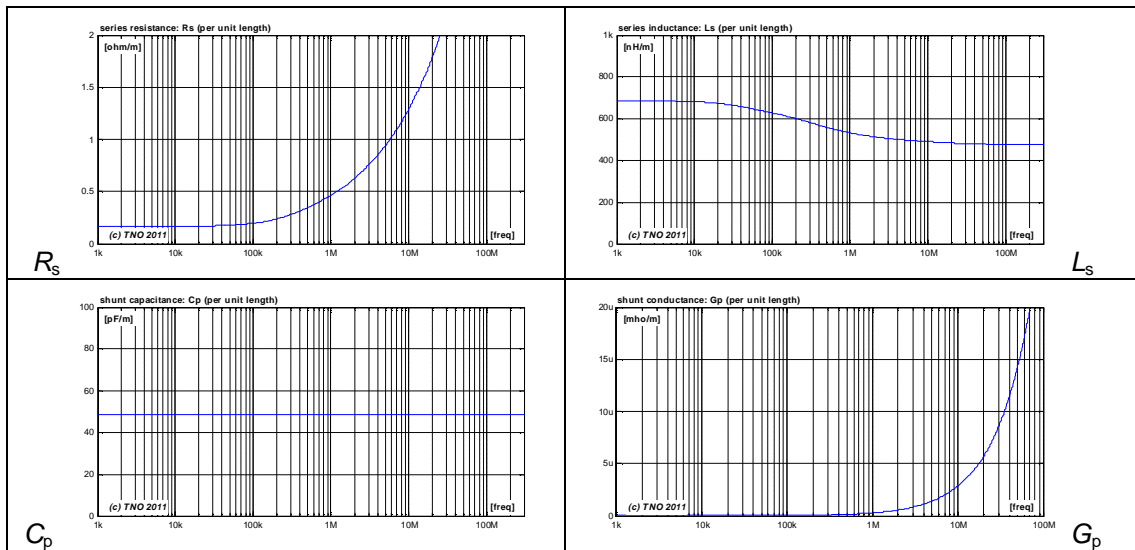
A twisted pair copper cable of length  $x$  can be modeled as a cascade of  $N$  homogeneous segments of length  $dx = x / N$ , when  $N \rightarrow \infty$ . Each segment can then be represented by a series impedance  $Z_s \cdot dx$  and a shunt admittance  $Y_p \cdot dx$ , as illustrated below:



$$R_s(j\omega) = \text{real}(Z_s(j\omega)) \quad L_s(j\omega) = \text{imag}(Z_s(j\omega))/(j\omega)$$

$$G_p(j\omega) = \text{real}(Y_p(j\omega)) \quad C_p(j\omega) = \text{imag}(Y_p(j\omega))/(j\omega)$$

A simple representation is to assume that the associated  $R_s$ ,  $L_s$ ,  $C_p$ ,  $G_p$  are frequency independent but this is too simple in practice. Therefore a more generic representation is to express  $Z_s$  and  $Y_p$  via a parametric (frequency dependent) descriptions. The values for these parameters may be found from theory or, more likely, by means of curve fitting from measurements. This is the basis of various cable models of twisted pair cables that are being used for describing loops for DSL. Typical curves for  $R_s$ ,  $L_s$ ,  $C_p$ ,  $G_p$  as function of the frequency are shown below.



There are many ways to express  $Z_s$  and  $Y_p$ , and even the standardized test loops for VDSL2 [\*] are based on different approaches. Cable TP100, originally extracted from a BT cable [\*], is defined via independent parametric functions  $R_s(\omega)$ ,  $L_s(\omega)$ ,  $G_p(\omega)$  and  $C_p(\omega)$ . And cable TP150, originally extracted from a KPN cable [\*], models  $Z_s(j\omega)$  as a whole and  $G_p$  and  $C_p$  individually. Other possibilities can be found as well, as in [\*] and [\*].

The problem with several of these legacy models is that they are adequate only in the frequency domain, but will predict non-real impulse responses (with imaginary parts) when used for time-domain calculations. The class of models proposed in this document are such that they all enable a good match over many decades in the frequency domain and that the impulse responses predicted with these models are always real.

## 2.2 The proposed class of parametric models

The elements in the series impedance  $Z_s(j\omega) = R_s(j\omega) + j\omega \cdot L_s(j\omega)$  are frequency dependent due to mechanisms like the skin effect in wiring with imperfect conductivity. We propose a class of models for describing them, that all start from the same asymptotic characteristics for low and high frequencies. Several essential aspects of this approach was inspired by work from Musson [\*,\*], and evolved into a more generic approach. By definition the following applies for  $Z_s(j\omega)$ :

- $L_s(j\omega) \rightarrow L_{s0}$  for low frequencies, including DC
- $L_s(j\omega) \rightarrow L_{s\infty}$  for high frequencies, different from  $L_{s0}$
- $R_s(j\omega) \rightarrow R_{s0}$  for low frequencies, including DC
- $R_s(j\omega) \rightarrow R_{s0} \cdot \text{sqrt}(\omega/\omega_s)$  for high frequencies

All parameters  $\{L_{s\infty}, L_{s0}, R_{s0}, \text{ and } \omega_s\}$  in these expressions are representing constant (frequency independent) values, and these constants are typical for a specific cable. The scaling frequency  $\omega_s$  represents a break frequency from where the skin-effect becomes significant.

The elements in the shunt admittance  $Y_p(j\omega) = G_p(j\omega) + j\omega \cdot C_p(j\omega)$  are also frequency dependent due to mechanisms like dielectric losses in the insulation. The class of models for describing  $Y_p(j\omega)$  are therefore also starting from the same asymptotic characteristics but this time mainly for mid-band frequencies. By definition the following applies for  $Y_p(j\omega)$ :

- $C_p(j\omega) \rightarrow C_{p0}$  for most frequencies of interest, including DC
- $G_p(j\omega) \rightarrow 0$  for low frequencies, including DC
- $\text{arg}\{Y_p(j\omega)\} \rightarrow \pi/2 - f$  for most frequencies of interest, over many decades

The DC-capacitance  $C_{p0}$  and loss angle  $f$  are also representing constant (frequency independent) values, and are typical for a specific cable as well.

To create full parametric models for  $Z_s(j\omega)$  and  $Y_p(j\omega)$ , the proposed models are all starting from exactly the same asymptotic characteristics. The measurements in the following chapters show that these characteristics hold very well (even up to hundreds of MHz) for twisted pair cables. This implies that  $Z_s(j\omega)$  is to be expressed via at least four independent parameters, e.g.  $\{L_{s\infty}, L_{s0}, R_{s0}, \text{ and } \omega_s\}$ , and  $Y_p(j\omega)$  via at least two independent parameters, e.g.  $\{C_{p0}, f\}$ . The expressions are further completed via so called “shaping functions”, named  $Q_z(j\omega)$  and  $Q_y(j\omega)$ , to get an expression for each frequency, and these functions enable an additional fine tuning to find the best match between model and measurements.

When an alternative parameter  $q_s$  is used for  $L_{s0}$  via the substitution  $L_{s0} = L_{s\infty} + (R_{s0} / \omega_s) / q_s$  then the full parametric model can be expressed as:

$Z_s(j\omega) = j\omega \cdot L_{s\infty} + R_{s0} \times \left( 1 - q_s + q_s \cdot Q_z \left( \frac{j\omega}{q_s^2 \cdot \omega_s} \right) \right)$ $Y_p(j\omega) = j\omega \cdot C_{p0} \times \left[ Q_y \left( \frac{j\omega}{\omega_d} \right) \right]^f$
<p>The shaping function <math>Q_z(j\omega)</math> is to be an analytical function, that complies with the following set of requirements:</p> <p>for <math>w \rightarrow 0</math>     <math>Q_z(j\omega) \rightarrow 1 + jw</math></p> <p>for <math>w \rightarrow \infty</math>     <math>Q_z(j\omega) \rightarrow \text{sqrt}(2 \times jw) = (1 + j) \times \text{sqrt}(w)</math></p> <p>for all <math>w</math>     <math>Q_z(j\omega) \equiv \text{conj}(Q_z(-j\omega))</math></p>
<p>The shaping function <math>Q_y(j\omega)</math> is to be another analytical function, that complies with the following set of requirements:</p> <p>for <math>w = 0</math>     <math>Q_y(j\omega) = +1</math></p> <p>for <math>w &gt; 1</math>     <math>\text{abs}\{Q_y(j\omega)\} &lt; +1</math></p> <p>for all <math>w</math>     <math>\text{arg}\{Q_y(j\omega)\} \rightarrow -1</math> (over many decades)</p> <p>for all <math>w</math>     <math>Q_y(j\omega) \equiv \text{conj}(Q_y(-j\omega))</math></p>

Many functions  $Q_Z(j\omega)$  and  $Q_Y(j\omega)$  are capable of meeting the specified requirements, and several possible functions are discussed in chapter [\*] and [\*]. Examples of such functions are:

- $Q_Z(j\omega) = \text{sqrt}(1+2 \cdot j\omega)$
- $Q_Y(j\omega) = (1+j\omega)^{2/p}$

Both are often adequate (at least to start with) but can both be refined to achieve a better match. The scaling frequency  $\omega_d$  is a bit meaningless since the desired characteristics of  $Y_p(j\omega)$  are more or less frequency independent, but is essential for dimensional reasons. Therefore the use of a default value of  $\omega_d=2\pi$  is often preferred.

The additional requirements of  $Q(j\omega)=\text{conj}\{Q(-j\omega)\}$  ensures that impulse responses predicted via these cable models are always real (without imaginary values) since it ensures that the same behavior applies for  $Z_s(-j\omega)$  and  $Y_p(-j\omega)$ .

### 2.3 Consequences for series impedances

The full definition of  $Z_s$  now equals to:

$$Z_s(j\omega) = j\omega \cdot L_{s\infty} + R_{s0} \times (1 - q_s + q_s \cdot Q_Z(j\Omega)) \quad \text{where } j\Omega = \frac{j\omega}{q_s^2 \cdot \omega_s}$$

Due to the (asymptotic) requirements of the shaping function  $Q_Z(j\omega)$ , the following applies:

$$\begin{aligned} L_s(j\omega) &\rightarrow L_{s\infty} + \frac{R_{s0}}{q_s \cdot \omega_s} = L_{s\infty} + \Delta L_{s0} \quad \text{for low frequencies} \\ L_s(j\omega) &\rightarrow L_{s\infty} \quad \text{for high frequencies} \\ R_s(j\omega) &\rightarrow R_{s0} \quad \text{for low frequencies} \\ R_s(j\omega) &\rightarrow R_{s0} \times \text{sqrt}\left(\frac{\omega}{\omega_s}\right) \quad \text{for high frequencies} \end{aligned}$$

- $R_{s0}$  represents a DC loop resistance of the wire pair.
- $L_{s\infty}$  represent a series inductance which is approximated at high frequencies.
- $L_{s\infty} + \Delta L_{s0}$  represents a series inductance which is approximated at low frequencies.
- $\omega_s$  represents a break frequency from above the skin-effect becomes significant.

### 2.4 Consequences for shunt admittances

The full definition of  $Y_p$  now equals to:

$$Y_p(j\omega) = j\omega \cdot C_{p0} \times \left[ Q_Y\left(\frac{j\omega}{\omega_d}\right) \right]^f$$

Due to the requirements of the shaping function  $Q_Y(j\omega)$  then  $Q_Y(j\omega)^f \rightarrow 1 - j \cdot f$  applies for a wide frequency band when  $f \ll 1$ . This can be demonstrated by:

If  $q = \ln(\text{abs}(Q_Y))$  then  $\ln\{Q_Y\} \rightarrow \ln(\text{abs}(Q_Y) \cdot \exp(-j)) = q - j$  (by definition, over many decades).  
 So  $Q_Y(j\omega)^f = \exp(f \times \ln(Q_Y)) \rightarrow \exp(f \times (q - j)) = \exp(f \cdot q) \times \exp(-j \cdot f)$ , also over many decades.  
 Since  $q < 1$  (by "definition") then  $\exp(f \cdot q) \rightarrow 1$  when  $f \ll 1$ , making  $Q_Y(j\omega)^f \rightarrow \exp(-j \cdot f) \rightarrow 1 - j \cdot f$ .

Since  $f \ll 1$  in practical situations, the above approximation usually holds many decades of  $\omega$  and yields:

$$\begin{aligned} C_p(j\omega) &\rightarrow C_{p0} \\ G_p(j\omega) &\rightarrow \omega \times f \cdot C_{p0} \end{aligned}$$

- $C_{p0}$  represents a low frequency capacity between the wire pairs.
- $f$  represents a dielectric loss angle between real and imaginary parts of  $Y_p(j\omega)$ .
- $\omega_d$  represents a break frequency, for above this loss effect becomes noticeable.

In practice,  $\omega_d$  is so low that it cannot be extracted from AC-measurements, but simply putting  $\omega_d=2\pi$  gives adequate results.

## 2.5 Consequences for impulse responses

The proposed class of models facilitates that impulse responses predicted by these models are real by nature, and this property prevents that the models are unrealistic from the beginning. To ensure real impulse responses, the real and imaginary parts of  $Z_s$  and  $Y_p$ , should have a special relation [\*], and it is not obvious that a model ensures that relation. For instance, it does not hold for several well-known legacy models like the above mentioned TP100 and TP150 cable models.

This property can be found as follows: If  $h(t)$  is the (real) impulse response (in the time domain) of a device, and  $H(j\omega)$  is the (complex) transfer function (in the frequency domain) of the same device, then they are related via the following inverse Fourier transform:

$$h(t) = \int_{-\infty}^{+\infty} H(j\omega) e^{j\omega t} \cdot d \frac{\omega}{2\pi} = \int_{-\infty}^{+\infty} \overline{H(j\omega)} e^{-j\omega t} \cdot d \frac{\omega}{2\pi} = \int_{-\infty}^{+\infty} H(-j\omega) e^{j\omega t} \cdot d \frac{\omega}{2\pi} = \int_{-\infty}^{+\infty} \overline{H(-j\omega)} e^{j\omega t} \cdot d \frac{\omega}{2\pi}$$

This yields the well-known condition that when the impulse response  $h(t)$  of a device is real the relation  $\text{conj}(H(-j\omega)) \equiv H(j\omega)$  should hold for all (real) angular frequencies  $\omega$ .

Something similar holds for devices constructed from a cascade of  $N$  homogeneous segments, where each segment is described with a simple linear circuit diagram. If all current responses on a voltage impulse are real, then all impedances should comply with  $\text{conj}(Z_s(-j\omega)) \equiv Z_s(j\omega)$  and all admittances should comply with  $\text{conj}(Y_p(-j\omega)) \equiv Y_p(j\omega)$  for all real values of  $\omega$ . And if this holds for the impulse response of an infinitesimal cable segment then it will also hold for an infinite cascade of these segments.

In other words, if  $\text{conj}(Z_s(-j\omega)) \equiv Z_s(j\omega)$ , and  $\text{conj}(Y_p(-j\omega)) \equiv Y_p(j\omega)$  for all (real) angular frequencies  $\omega$  then such cable model will predict real impulse responses.

It is plausible that the reverse is also true and that the above condition is a necessary requirement. Such a mathematic proof is beyond the scope of this report but a details analysis on this topic can be found in [\*]. The proposed models might be causal as well [\*], but mathematical proof was not elaborated on this.

## 2.6 Alternative parametric description for fitting the models

So far, the models are being described with 6+1 parameters  $\{L_{s\infty}, C_{p0}, R_{s0}, q_s, \omega_s, f, w_d\}$  and two shaping functions, in a manner that is convenient for describing theory. For fitting such models to measured data in an iterative manner, it is preferred to rework these parameters a bit to estimate their starting values more easily from measurements. The following expressions describe the same model but with a slightly revised set of 6+1 parameters  $\{Z_{0\infty}, \eta_{VF}, R_{s0}, q_H, q_L, f, w_d\}$ .

$$\begin{aligned} Z_s(j\omega) &= \frac{j\omega}{h_{VF} \cdot c_0} \times Z_{0\infty} + R_{s0} \times (1 - q_s + q_s \times Q_Z(j\Omega)) \\ Y_p(j\omega) &= \frac{j\omega}{h_{VF} \cdot c_0} / Z_{0\infty} \times \left[ Q_Y \left( \frac{j\omega}{w_d} \right) \right]^f \end{aligned}$$

Where

$$L_{s\infty} = \frac{1}{h_{VF} \cdot c_0} \times Z_{0\infty} \quad \left| \quad j\Omega = \frac{j\omega}{q_s^2 \cdot w_s} = q_L^2 \cdot q_H^2 \cdot \frac{j\omega}{w_{s0}}$$

$$C_{p0} = \frac{1}{h_{VF} \cdot c_0} \times \frac{1}{Z_{0\infty}}$$

$$q_s = \frac{1}{q_H \cdot q_L}$$

$$w_s = q_H^2 \cdot w_{s0}$$

For instance with  $Q_{Z,sqrt}(j\omega) = \text{sqrt}(1 + 2 \cdot j\omega)$ , or any other shaping function suggested in chapter [\*].

For instance with  $Q_{Y,1}(j\omega, f) = (1 + j\omega)^{-2 \cdot f / p}$ , or any other shaping function suggested in chapter [\*].

If  $c_0$  is the speed of light and if  $\omega_{s0}$  is a fair estimate of  $\omega_s$  (for instance  $\omega_{s0}=4\pi \cdot R_{s0}/m_0$ , as discussed in a chapter [\*]) then the following interpretation applies:

- $Z_{o\infty}$  = characteristic impedance for high frequencies, typically in the range of 50-200  $\Omega$
- $\eta_{VF}$  = velocity factor, typically in the range of 0.6-0.8
- $R_{s\infty}$  = DC loop resistance of a wire pair, typically in the order of 0.15-0.2  $\Omega/m$  for 0.5mm wires
- $q_H$  = HF correction factor, typically in the range of 0.5-1 for the chosen estimate  $\omega_{s0}$  of  $\omega_s$
- $q_L$  = LF correction factor, typically in the range of 1.5-2.5

Constant parameters, to be set to a fixed value

- $c_0$  = speed of light  $\approx 3 \cdot 10^8$  [m/s]
- $m_0$  = permeability =  $4\pi \cdot 10^{-7}$  [H/m]
- $\omega_{s0}$  = fair estimate of  $\omega_s$ , defined as  $\omega_{s0}=4\pi \cdot R_{s0}/m_0 = R_{s0} \times (10^7$  [H/m])
- $\omega_d$  = a scaling frequency which is fixed at  $\omega_d=2\pi$  [rad/s]

The use of  $\{Z_{o\infty}, \eta_{VF}\}$ , instead of  $\{L_{s\infty}, C_{p0}\}$ , is because the characteristic impedance of a cable can be extracted easily, without the need for extracting primary cable parameters  $Z_s$  and  $Y_p$ . And the velocity factor is mainly fixed by the dielectric between the conductors and almost independent on the geometry and wire dimensions.

The use of  $\{q_H, q_L\}$  instead of  $\{q_s, L_{s0}, \omega_s\}$  is because they can be optimized independently. Factor  $q_L$  is a LF correction factor only affecting the series inductance at low frequencies, and  $q_H$  is a HF correction factor (only affecting the series resistance at high frequencies, as expressed below

$$\Delta L_{s0} = L_{s0} - L_{s\infty} = \frac{R_{s0}}{q_s \times \omega_s} = \frac{R_{s0}}{\omega_{s0}} \times q_L = \frac{m_0}{4p} \times q_L$$

$$R_s(j\omega) \rightarrow \frac{R_{s0}}{q_H} \cdot \sqrt{\frac{\omega}{\omega_{s0}}} = R_{s0} \cdot \sqrt{\frac{\omega}{\omega_s}}, \quad \text{for } \omega \rightarrow \infty$$

Factor  $q_H$  is only meaningful in combination with a well-defined estimate of  $\omega_{s0}$ . Such estimate is derived in chapter [\*] via an over-simplified model of the skin effect, and nevertheless very effective in practice.

## 2.7 From primary cable parameters to matrix parameters

A pair of primary cable parameters  $\{Z_s, Y_p\}$  per unit length enable an unambiguous calculation of two-port matrix parameters of a loop section with arbitrary length  $x$ . Table 1 summarizes the relations<sup>1</sup> between various cable parameters, as taken from [\*], where  $Z_{sx} = x \cdot Z_s$  and  $Y_{px} = x \cdot Y_p$  represent the primary cable parameters of the cable section with length  $x$ . The use of intermediate parameters like secondary cable parameters  $\{g_x, Z_0\}$ , where  $\gamma_x = g \cdot x$ , and characteristic transmission and reflection  $\{s_{Tx}, s_R\}$  usually simplifies the transformation between various matrix formats.

Cable parameters (symmetrical)		
analysis	synthesis	remarks
$Z_{sx} = g_x \cdot Z_0$ $Y_{px} = g_x / Z_0$	$g_x = \sqrt{Z_{sx} \cdot Y_{px}}$ $Z_0 = \sqrt{Z_{sx} / Y_{px}}$	primary cable parameters (series impedance and shunt-admittance)
$Z_{ocx} = Z_0 / \tanh(g_x)$ $Z_{scx} = Z_0 \cdot \tanh(g_x)$	$g_x = \operatorname{arctanh}(\sqrt{Z_{scx} / Z_{ocx}})$ $Z_0 = \sqrt{Z_{ocx} \cdot Z_{scx}}$	input impedance at open or short-circuited output of a cable, having length $x$ .
$s_{Tx} = \exp(-g_x)$ $s_R = (Z_0 - R_n) / (Z_0 + R_n)$	$g_x = -\ln(s_{Tx})$ $Z_0 = R_n \cdot (1 + s_R) / (1 - s_R)$	characteristic transmission and reflection, normalized to reference impedance $R_n$

Table 1: Relations between various two-port cable parameters

<sup>1</sup>  $\sinh(\gamma) = \frac{1}{2} \cdot (\exp(\gamma) - \exp(-\gamma))$   
 $\cosh(\gamma) = \frac{1}{2} \cdot (\exp(\gamma) + \exp(-\gamma))$   
 $\tanh(\gamma) = \sinh(\gamma) / \cosh(\gamma)$

Primary and secondary parameters are sometimes divided in their real and imaginary parts. These (real) parameters are defined in table 2. The default unit of  $a_x$  is in this document the Neper<sup>2</sup> [Np], and for  $b_x$  the radian<sup>3</sup> [rad]. Similarly are [Np/m] and [rad/m] the default units for  $a$  and  $b$  themselves.

$a_x = \text{real}(g_x)$	$R_{sx} = \text{real}(Z_{sx})$	$G_{px} = \text{real}(Y_{px})$
$b_x = \text{imag}(g_x)$	$L_{sx} = \text{imag}(Z_{sx} / w)$	$C_{px} = \text{imag}(Y_{px} / w)$

Table 2: Definition of real and imaginary parts of cable parameters

Table 3 summarizes the associated expressions for voltage, current and wave representations. The (wave) scattering and transfer parameters ( $s$ - and  $t$ - parameters) are normalized to an arbitrary chosen (real) *reference* impedance  $R_N$ . The theory about using these representation is beyond the scope of this document.

**THIS SUMMARY SHOULD BE DOUBLE CHECKED AGAINST TYPE-ERRORS**

<b>two-port matrix parameters</b>	
$\mathbf{Z} = \begin{bmatrix} z_{11} & z_{12} \\ z_{21} & z_{22} \end{bmatrix} = \begin{bmatrix} \frac{z_0}{\tanh(g_x)} & \frac{z_0}{\sinh(g_x)} \\ \frac{z_0}{\sinh(g_x)} & \frac{z_0}{\tanh(g_x)} \end{bmatrix}$	
$\mathbf{Y} = \begin{bmatrix} y_{11} & y_{12} \\ y_{21} & y_{22} \end{bmatrix} = \begin{bmatrix} \frac{1}{z_0 \cdot \tanh(g_x)} & \frac{-1}{z_0 \cdot \sinh(g_x)} \\ \frac{-1}{z_0 \cdot \sinh(g_x)} & \frac{1}{z_0 \cdot \tanh(g_x)} \end{bmatrix}$	
$\mathbf{S} = \begin{bmatrix} s_{11} & s_{12} \\ s_{21} & s_{22} \end{bmatrix} = \frac{1}{(Z_0 / R_N + R_N / Z_0) \cdot \tanh(g_x) + 2} \times \begin{bmatrix} (Z_0 / R_N - R_N / Z_0) \cdot \tanh(g_x) & 2 / \cosh(g_x) \\ 2 / \cosh(g_x) & (Z_0 / R_N - R_N / Z_0) \cdot \tanh(g_x) \end{bmatrix}$	
$\mathbf{A} = \begin{bmatrix} a_{11} & a_{12} \\ a_{21} & a_{22} \end{bmatrix} = \begin{bmatrix} \cosh(g_x) & \sinh(g_x) / Z_0 \\ \sinh(g_x) \cdot Z_0 & \cosh(g_x) \end{bmatrix} = \begin{bmatrix} A & C \\ B & D \end{bmatrix}$	
$\mathbf{T} = \begin{bmatrix} t_{11} & t_{12} \\ t_{21} & t_{22} \end{bmatrix} = \begin{bmatrix} \cosh(g_x) + \frac{(Z_0 / R_N + R_N / Z_0)}{2} \cdot \sinh(g_x) & \frac{(Z_0 / R_N - R_N / Z_0)}{2} \cdot \sinh(g_x) \\ \frac{(R_N / Z_0 - Z_0 / R_N)}{2} \cdot \sinh(g_x) & \cosh(g_x) - \frac{(Z_0 / R_N + R_N / Z_0)}{2} \cdot \sinh(g_x) \end{bmatrix}$	
$\mathbf{S} = \begin{bmatrix} s_{11} & s_{12} \\ s_{21} & s_{22} \end{bmatrix} = \frac{1}{1 - (s_{Tx} \cdot s_R)^2} \times \begin{bmatrix} s_R \cdot (1 - s_{Tx}^2) & s_{Tx} \cdot (1 - s_R^2) \\ s_{Tx} \cdot (1 - s_R^2) & s_R \cdot (1 - s_{Tx}^2) \end{bmatrix}$	
$\mathbf{T} = \begin{bmatrix} t_{11} & t_{12} \\ t_{21} & t_{22} \end{bmatrix} = \frac{1}{1 - s_R^2} \times \begin{bmatrix} 1 / s_{Tx} - s_R^2 \cdot s_{Tx} & s_R \cdot s_{Tx} - s_R / s_{Tx} \\ s_R \cdot s_{Tx} - s_R \cdot s_{Tx} & s_{Tx} - s_R^2 / s_{Tx} \end{bmatrix} = \begin{bmatrix} s_R & 1 \\ 1 & s_R \end{bmatrix} \times \begin{bmatrix} s_{Tx} & 1 \\ 1 & 1 / s_{Tx} \end{bmatrix} / \begin{bmatrix} s_R & 1 \\ 1 & s_R \end{bmatrix}$	

Table 3: Various expressions for matrix parameters

<sup>2</sup> The parameter  $a_x$  is in fact dimensionless, like any ratio number expressed in dB or %, The dB is not a suitable unit, but this does not hold if it is transformed into a 'loss' quantity. The characteristic loss magnitude  $|1/s_{Tx}| = \exp(a_x)$  can be expressed in dB by evaluating  $p_x = 20 \cdot \log(|1/s_{Tx}|) \approx 8.6859 \cdot a_x$ . The factor 8.6859, or more precisely  $20/\ln(10)$ , illustrates why the dB is not a suitable unit, so the Neper has took its place. Saying that  $a_x$  equals " $p_x$ "[dB] is therefore impure language for meaning:  $a_x = p_x / 8.6859$  [Np]. Be aware of this confusion.

<sup>3</sup> The characteristic loss phase  $\angle(1/s_{Tx})$  in radians equals  $b_x$  because  $1/s_{Tx} = \exp(a_x + j \cdot b_x)$ . Since it is not common to express a loss phase in radians, the loss phase  $\angle(1/s_{Tx})$  in degrees equals  $(180/\pi) \cdot b_x$ . Saying that  $b_x$  equals " $q_x$ " degrees is therefore impure language for meaning  $b_x = (\pi/180) \cdot q_x$ . Be aware of this confusion.

### 3 FURTHER DETAILS ON MODELLING CABLES

#### 3.1 Shaping functions for modeling impedances

The parametric model for  $Z_s(j\omega)$  is described via analytical shaping functions  $Q_Z(j\omega)$  that are to meet the following asymptotic requirements.

$$\begin{aligned} \text{for } j\omega \rightarrow 0 \quad Q_Z(j\omega) &\rightarrow 1 + j\omega \\ \text{for } j\omega \rightarrow \infty \quad Q_Z(j\omega) &\rightarrow \text{sqrt}(2 \times j\omega) = (1 + j) \times \text{sqrt}(\omega) \\ \text{for all } \omega \quad Q_Z(j\omega) &\equiv \text{conj}(Q_Z(-j\omega)) \end{aligned}$$

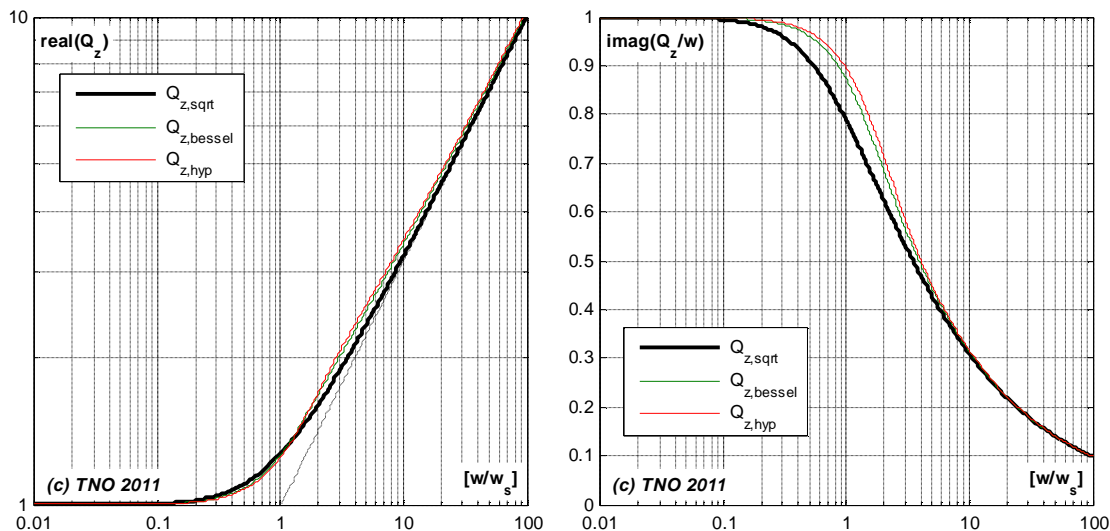
A simple function like  $Q_Z(j\omega) = \text{sqrt}(1 + 2 \cdot j\omega)$ , can already meet these requirements but it is certainly not the only possibility. This chapter discusses several options.

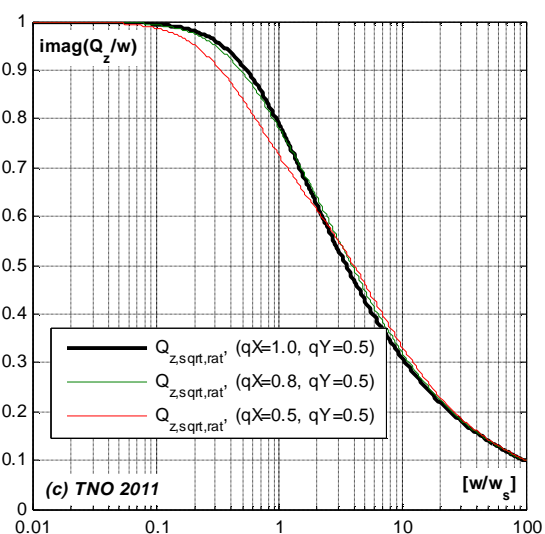
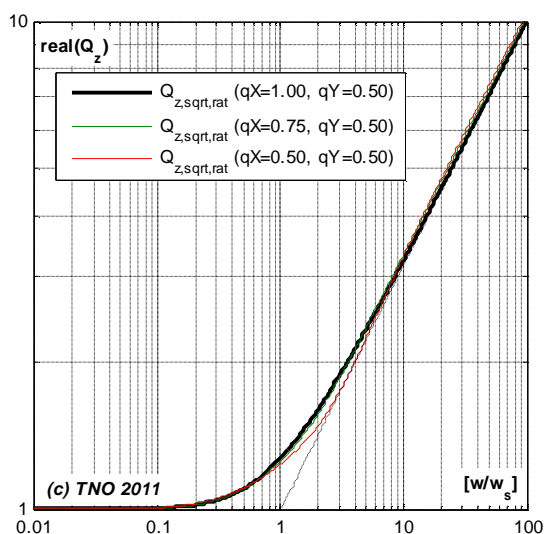
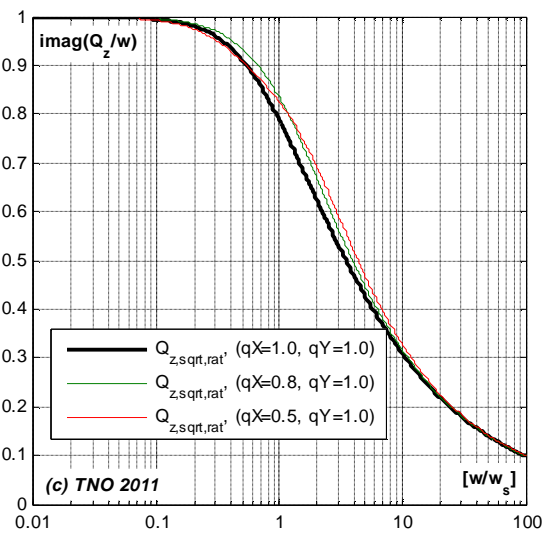
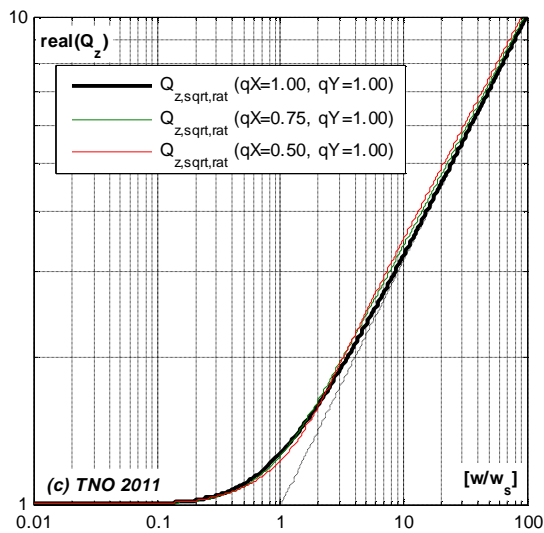
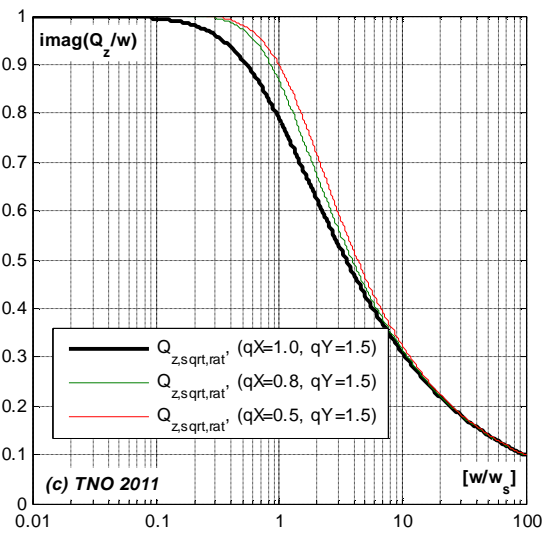
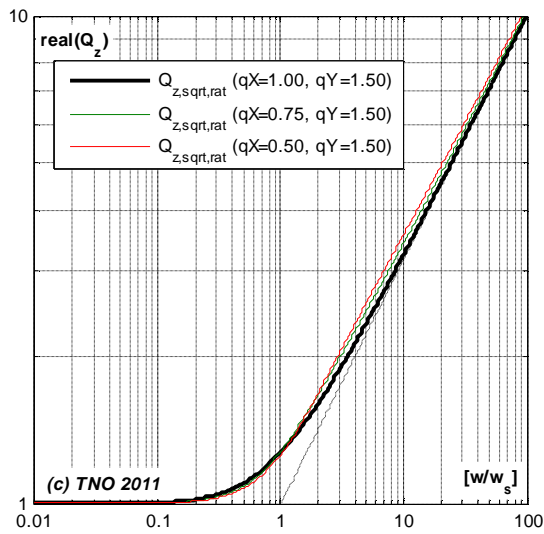
##### 3.1.1 Overview of analyzed shaping functions

The functions in table [\*] provide examples of different shaping functions that are all equal in asymptotic behavior (for low or high frequencies). If a selected shaping function results in only poor matches of  $Z_s(j\omega)$  at mid band frequencies, then one can select one of the others for achieving better results. This includes:

- $Q_{Z,\text{sqrt}}(j\omega)$ , which is defined via a square-root function) and is preferred to starting with since it is so simple to evaluate.
- $Q_{Z,\text{sqrt,rat}}(j\omega, q_x, q_y)$ , which is defined via a square root of rational functions, and has additional parameters for fine tuning its shape at mid band frequencies. It will be equal to  $Q_{Z,\text{sqrt}}(j\omega)$  when  $q_x = 1$  and was inspired by the cable modeling used within the MAR model in [\*].
- $Q_{Z,\text{bessel}}(j\omega)$ , which is more complicated and defined via Bessel functions. They are used in cable models like in [\*] or [\*], and could facilitate a better match. Note that the computational effort of evaluating Bessel functions can be significant.
- $Q_{Z,\text{hyp}}(j\omega)$  is defined via simple hyperbolic functions, and is inspired by the cable modeling used for TP150 in [\*].
- $Q_{Z,\text{mix}}(j\omega, q_B) = q_B \cdot Q_{Z,a}(j\omega) + (1 - q_B) \cdot Q_{Z,b}(j\omega)$  is a mix of one of the above curves. and has also an additional parameter for fine tuning its shape.

The figures [\*] to [\*] show the differences in shape of several of these functions  $Q_Z(j\omega)$ . They demonstrate that all these shapes are very similar, with only small difference at midband frequencies. Only  $Q_{Z,\text{sqrt,rat}}(j\omega)$  can offer very different shapes but most of them cannot be used for cable modelling. Parameter values that are too different from  $q_x = 1$  and  $q_y = 1$  cause shapes with multiple bends and are therefore not plausible for modeling of series impedance. The mix of  $q_B \cdot Q_{Z,\text{sqrt}}(j\omega) + (1 - q_B) \cdot Q_{Z,\text{hyp}}(j\omega)$  can even approximate  $Q_{Z,\text{bessel}}(j\omega)$  reasonably well for  $q_B = 0.25$ . The fact that they are all similar explains why even the simplest shaping function of table [\*] can often provide a match that can hardly be outperformed by one of the more complicated shaping functions. Using one of the others may even worsen the match. Our measurements shows that  $Q_{Z,\text{sqrt,rat}}(j\omega)$  is often preferred, and that the simplism of  $Q_{Z,\text{sqrt}}(j\omega)$  is often adequate as well.





### 3.1.2 Definition of elaborated shaping functions

#### 1. Shaping via Square-root of polynomial function:

$$Q_{Z,sqrt}(j\omega) = \text{sqrt}(1 + 2 \cdot j\omega)$$

$$\text{for } j\omega \rightarrow 0 \quad Q_{Z,sqrt}(j\omega) \rightarrow 1 + j\omega - 1/2 \cdot (j\omega)^2 + \dots$$

$$\text{for } j\omega \rightarrow \infty \quad Q_{Z,sqrt}(j\omega) \rightarrow \text{sqrt}(2 \times j\omega)$$

$$\text{for } j\omega = j \quad Q_{Z,sqrt}(j) \rightarrow 1.2720 + j \times 0.7862$$

Applying this shaping to  $Z_s$  brings:

$$Z_s(j\omega) = j\omega \cdot L_{s\infty} + R_{s0} \times \left( 1 - q_s + q_s \cdot \text{sqrt} \left( 1 + 2 \cdot \frac{j\omega}{q_s^2 \cdot w_s} \right) \right)$$

$$Z_s(j\omega) = j\omega \cdot L_{s\infty} + R_{s0} \times \left( 1 - q_s + \text{sqrt} \left( q_s^2 + 2 \cdot \frac{j\omega}{w_s} \right) \right)$$

#### 2. Shaping via Square-root of rational function:

$$Q_{Z,sqrt,rat}(j\omega; q_x, q_y) = 1 - q_x + q_x \times \text{sqrt} \left( 1 + 2 \cdot \frac{j\omega}{q_x} \cdot \left( \frac{1 + j\omega \cdot q_y}{1 + j\omega \cdot q_x \cdot q_y} \right) \right)$$

$$\text{for } j\omega \rightarrow 0 \quad Q_{Z,sqrt,rat}(j\omega, q_x, q_y) \rightarrow 1 + j\omega - \left( q_x \cdot q_y - q_y + \frac{1}{2 \cdot q_x} \right) \cdot (j\omega)^2 + \dots$$

$$\text{for } j\omega \rightarrow \infty \quad Q_{Z,sqrt,rat}(j\omega, q_x, q_y) \rightarrow \text{sqrt}(2 \times j\omega)$$

Applying this shaping to  $Z_s$  could also be formulated as:

$$Z_s(j\omega) = j\omega \cdot L_{s\infty} + R_{s0} \times \left( 1 - q_{sx} + q_{sx} \times \text{sqrt} \left( 1 + j\omega \cdot A \cdot \left( \frac{1 + j\omega \cdot B}{1 + j\omega \cdot C} \right) \right) \right)$$

$$\text{where } A = \frac{2}{q_x \cdot q_s^2 \cdot w_s}, \quad B = \frac{q_y}{q_s^2 \cdot w_s}, \quad C = \frac{q_x \cdot q_y}{q_s^2 \cdot w_s}, \quad q_{sx} = q_s \cdot q_x$$

For the special case when  $q_{sx} = q_s \cdot q_x = 0.75$ , the above formula approximates the series impedance being used within the MAR#1 model [\*]

**NOTE:** If  $q_x = 1$ , then  $Q_{Z,sqrt,rat}$  becomes equal to  $Q_{Z,sqrt}$  for all values of  $q_y$ . So if an iterative match results in a  $q_x$  close to 1 then the use of  $Q_{Z,sqrt,rat}$  will hardly make any sense.

#### 3. Shaping via Bessel functions:

$$Q_{Z,bessel}(j\omega) = \frac{I_0(2X)}{I_1(2X)} \cdot X \quad \text{where } X(j\omega) = \sqrt{2 \cdot j\omega}$$

$$\text{for } j\omega \rightarrow 0 \quad Q_{Z,bessel}(j\omega) \rightarrow 1 + j\omega - 1/3 \cdot (j\omega)^2 + 1/6 \cdot (j\omega)^3 \dots$$

$$\text{for } j\omega \rightarrow \infty \quad Q_{Z,bessel}(j\omega) \rightarrow \text{sqrt}(2 \times j\omega)$$

$$\text{for } j\omega = j \quad Q_{Z,bessel}(j) \rightarrow 1.2646 + j \times 0.8705$$

Applying this shaping to  $Z_s$  brings:

$$Z_s(j\omega) = j\omega \cdot L_{s\infty} + R_{s0} \times \left( 1 - q_s + q_s \cdot \frac{I_0(2X)}{I_1(2X)} \cdot X \right), \quad \text{where } X(j\omega) = \sqrt{2 \cdot j\omega} = \sqrt{2 \cdot \frac{j\omega}{q_s^2 \cdot w_s}}$$

Other ways to express the same function are:

$$Q_{Z,bessel}(j\omega) = \frac{J_0(j \cdot 2X)}{J_1(j \cdot 2X)} \cdot jX \quad \text{where } X(j\omega) = \sqrt{2 \cdot j\omega}$$

$$Q_{Z,bessel}(j\omega) = \frac{J_0(a)}{J_1(a)} \cdot \frac{a}{2} \quad \text{where } a(j\omega) = \sqrt{-8 \cdot j\omega}$$

#### 4. Shaping via Hyperbolic functions:

$$Q_{Z,hyp}(j\omega) = \coth(3/2 \times X) \times X + 1/3; \quad \text{where } X(j\omega) = \sqrt{2 \cdot j\omega}$$

$$\begin{aligned} \text{for } j\omega \rightarrow 0 \quad Q_{Z,hyp}(j\omega) &\rightarrow 1 + j\omega - 3/10 \cdot (j\omega)^2 + \dots \\ \text{for } j\omega \rightarrow \infty \quad Q_{Z,hyp}(j\omega) &\rightarrow \text{sqrt}(2 \times j\omega) \\ \text{for } j\omega = j \quad Q_{Z,hyp}(j) &\rightarrow 1.2521 + j \times 0.8932 \end{aligned}$$

Applying this shaping to  $Z_s$  brings:

$$Z_s(j\omega) = j\omega \cdot L_{s\infty} + R_{s0} \times \left(1 - \frac{2}{3} \cdot q_s + q_s \cdot \coth\left(\frac{3}{2} \times X\right) \times X\right), \quad \text{where } X(j\Omega) = \sqrt{2 \cdot j\Omega} = \sqrt{2 \cdot \frac{j\omega}{q_s^2 \cdot w_s}}$$

Other ways to express the same shaping function are:

$$Q_{Z,hyp}(j\omega) = \frac{1 + \exp(-3 \cdot X)}{1 - \exp(-3 \cdot X)} \cdot X + 1/3 \quad \text{where } X(j\omega) = \sqrt{2 \cdot j\omega} \quad \text{or}$$

and when  $X$  is substituted:

$$\begin{aligned} Q_{Z,hyp}(j\omega) &= \coth(\sqrt{9/2 \cdot j\omega}) \times \sqrt{2 \cdot j\omega} + 1/3 \\ Q_{Z,hyp}(j\omega) &= \left(\exp(\sqrt{18 \cdot j\omega}) + 1\right) / \left(\exp(\sqrt{18 \cdot j\omega}) - 1\right) \cdot \sqrt{2 \cdot j\omega} + 1/3 \end{aligned}$$

#### 5. Shaping via a Mix of square-root and hyperbolic function:

$$Q_{Z,mix}(j\omega, q_B) = q_B \cdot \text{sqrt}(1 + 2 \cdot j\omega) + (1 - q_B) \cdot (\coth(3/2 \times X) \times X + 1/3)$$

$$\text{where } X(j\omega) = \sqrt{2 \cdot j\omega}$$

$$\begin{aligned} \text{for } j\omega \rightarrow 0 \quad Q_{Z,mix}(j\omega, q_B) &\rightarrow 1 + j\omega - q_B/3 - 3/10 \cdot (1 - q_B) \cdot (j\omega)^2 \dots \\ \text{for } j\omega \rightarrow \infty \quad Q_{Z,mix}(j\omega, q_B) &\rightarrow \text{sqrt}(2 \times j\omega) \end{aligned}$$

## 3.2 Shaping functions for modeling admittance

The parametric model for  $Y_p(j\omega)$  is described via another type of analytical shaping functions  $Q_Y(j\omega)$  that are to meet the following asymptotic requirements.

$$\begin{aligned} \text{for } w = 0 \quad Q_Y(j\omega) &= +1 \\ \text{for } w > 1 \quad \text{abs}\{Q_Y(j\omega)\} &< +1 \\ &\text{arg}\{Q_Y(j\omega)\} \rightarrow -1 \quad (\text{over many decades}) \\ \text{for all } w \quad Q_Y(j\omega) &\equiv \text{conj}(Q_Y(-j\omega; f)) \end{aligned}$$

A simple function can already meet these requirements but it is certainly not the only possibility. This chapter discusses two options.

### 3.2.1 Example shaping function #1

The function shown in table [\*] meets the shaping requirements for admittance very well. The numerical values illustrates how close they are met over many decades of  $w$ .

	$Q_{y,1}(jw) = \left( \frac{1}{1+jw} \right)^{2/p}$		
$w$	$abs\{Q_{y,1}(jw)\}$	$arg\{Q_{y,1}(jw)\}+1$	$[Q_{y,1}(jw)]^f$ for $f = 0.01$
1	8.02e-1	5.00e-01	0.9973 -0.0061i
10	2.30e-1	6.35e-02	0.9820 -0.0113i
100	5.33e-2	6.37e-03	0.9645 -0.0118i
1k	1.23e-2	6.37e-04	0.9473 -0.0116i
10k	2.84e-3	6.37e-05	0.9303 -0.0114i
100k	6.56e-4	6.37e-06	0.9137 -0.0112i
1M	1.51e-4	6.37e-07	0.8974 -0.0110i
10M	3.50e-5	6.37e-08	0.8814 -0.0108i
100M	8.07e-6	6.37e-09	0.8656 -0.0106i
1G	1.86e-6	6.37e-10	0.8501 -0.0105i
10G	4.30e-7	6.37e-11	0.8350 -0.0103i

A simple Padé or even a Taylor approximation can predict these numerical values very close. For  $w \gg 1$  the following applies:

$$Q_{y,1}(jw)^f = \exp(f \cdot \ln(Q_y)) = \exp\left(\frac{2f}{p} \cdot \ln\left(\frac{1}{1+jw}\right)\right)$$

$$Q_{y,1}(jw)^f \rightarrow \exp\left(-\frac{2f}{p} \cdot \ln(jw)\right) = \exp\left(-\frac{2f}{p} \cdot \left(\ln(w) + \frac{jp}{2}\right)\right)$$

$$Q_{y,1}(jw)^f \rightarrow \exp\left(-\frac{2f}{p} \cdot \ln(w) - jf\right) = \exp(-jf) \times \exp\left(-\frac{2f}{p} \cdot \ln(w)\right)$$

Padé approximation:  $\exp(x) \rightarrow (1+x/2)/(1-x/2)$  for  $|x| < 1$

Taylor approximation:  $\exp(x) \rightarrow 1+x$  for  $|x| < 1$

$$Q_{y,1}(jw)^f = \left(\frac{1}{1+jw}\right)^{2f/p} \rightarrow (1-jf) \times \left(\frac{1-f/p \cdot \ln(w)}{1+f/p \cdot \ln(w)}\right) \rightarrow (1-jf) \times (1-2f/p \cdot \ln(w))$$

When  $1 < \omega < 10^{10}$  and  $f=0.01$ , then the error of this Padé approximation of  $Y_p(j\omega)$  never exceeds 0.7% (and is often much better) and this Taylor approximation never exceeds 1.9%. When the shunt capacitance is modeled via this shaping function then the following approximation applies

$$C_p(jw) \rightarrow C_{p0} \times \left(\frac{1-f/p \cdot \ln(w/w_d)}{1+f/p \cdot \ln(w/w_d)}\right) \rightarrow C_{p0} \times (1-2f/p \cdot \ln(w/w_d))$$

So this model predicts a shunt capacitance which reduces a slightly in value when the frequency increases, and this decrease is roughly constant for each decade in frequency. This can indeed be observed from measurements and is therefore a convenient characteristic of this shaping function. If a small change in capacitance for a change in frequency from  $w_1$  to  $w_2$  is defined as  $\Delta C_p$  then each increase in frequency yields:

$$\frac{\Delta C_p}{C_p} = \left(\frac{C_p(jw_2) - C_p(jw_1)}{C_p(jw)}\right) \rightarrow \left\{ \frac{(-2f/p \cdot \ln(w_2/w_d) + 2f/p \cdot \ln(w_1/w_d))}{(1-2f/p \cdot \ln(w_1/w_d))} \right\} = -\frac{2f}{p} \times \left\{ \frac{\ln(w_2/w_1)}{(1-2f/p \cdot \ln(w_1/w_d))} \right\}$$

$$\frac{\Delta C_p}{C_p} \rightarrow -\frac{2f}{p} \cdot \ln\left(\frac{w_2}{w_1}\right) \rightarrow -\frac{2f}{p \cdot \log_{10}(e)} \cdot \log_{10}\left(\frac{w_2}{w_1}\right)$$

$$\frac{\Delta C_p}{C_p} \rightarrow -f \times 1.47 \cdot \log_{10} \left( \frac{w_2}{w_1} \right)$$

So by using this shaping function,  $C_{p0}$  decreases by about  $(1.47 \times f)$  for each decade in frequency.

### 3.2.2 Example shaping function #2

The function shown in table [\*] also meets the shaping requirements very well. The numerical values illustrates how close they are met over many decades of  $w$  and the results are very similar to the previous one.

	$Q_{Y,2}(jw, q) = \left( \frac{1}{1 + jw + q \cdot (jw)^2} \right)^{1/p}$		
$w$	$abs\{Q_{Y,2}(jw)\}$	$arg\{Q_{Y,2}(jw)\}+1$	$[Q_{Y,2}(jw)]^f$ for $f = 0.01$
1	1.38e-1	6.38e-04	0.9759 -0.0120i
10	3.19e-2	6.37e-05	0.9585 -0.0118i
100	7.37e-3	6.37e-06	0.9413 -0.0116i
1k	1.70e-3	6.37e-07	0.9245 -0.0114i
10k	3.93e-4	6.37e-08	0.9080 -0.0112i
100k	9.07e-5	6.37e-09	0.8918 -0.0110i
1M	2.09e-5	6.37e-10	0.8758 -0.0108i
10M	4.84e-6	6.37e-11	0.8602 -0.0106i
100M	1.12e-6	6.37e-12	0.8448 -0.0104i
1G	2.58e-7	6.37e-13	0.8297 -0.0102i
10G	5.95e-8	6.36e-14	0.8149 -0.0100i

A simple Padé or even a Taylor approximation can predict these numerical values very close as well. For  $w \gg 1$  the following applies:

$$Q_{Y,2}(jw, q)^f = \exp\left(f \cdot \ln(Q_y)\right) = \exp\left(\frac{f}{p} \cdot \ln\left(\frac{1}{1 + jw + q \cdot (jw)^2}\right)\right)$$

$$Q_{Y,2}(jw, q)^f \rightarrow \exp\left(-\frac{f}{p} \cdot \ln(q(jw)^2)\right) = \exp\left(-\frac{2f}{p} \cdot \left(\ln(w \cdot \sqrt{q}) + \frac{jp}{2}\right)\right)$$

$$Q_{Y,2}(jw, q)^f \rightarrow \exp\left(-\frac{2f}{p} \cdot \ln(w \cdot \sqrt{q}) - jf\right) = \exp(-jf) \times \exp\left(-\frac{2f}{p} \cdot \ln(w \cdot \sqrt{q})\right)$$

Padé approximation:  $\exp(x) \rightarrow (1+x/2)/(1-x/2)$  for  $|x| < 1$   
 Taylor approximation:  $\exp(x) \rightarrow 1+x$  for  $|x| < 1$

$$Q_{Y,2}(jw)^f = \left(\frac{1}{1 + jw + q \cdot (jw)^2}\right)^{2f/p} \rightarrow (1 - jf) \times \left(\frac{1 - f/p \cdot \ln(w \cdot \sqrt{q})}{1 + f/p \cdot \ln(w \cdot \sqrt{q})}\right) \rightarrow (1 - jf) \times (1 - 2f/p \cdot \ln(w \cdot \sqrt{q}))$$

When  $1 < w < 10^{10}$  and  $f=0.01$  and  $q=500$ , then the error of this Padé approximation of  $Y_p(jw)$  never exceeds about 1.2% (often much better) and this Taylor approximation at 2.5%. When the shunt capacitance is modeled via this shaping function then the following approximation also applies:

$$C_p(jw) \rightarrow C_{p0} \times \left(\frac{1 - f/p \cdot \ln(w/w_d \cdot \sqrt{q})}{1 + f/p \cdot \ln(w/w_d \cdot \sqrt{q})}\right) \rightarrow C_{p0} \times (1 - 2f/p \cdot \ln(w/w_d \cdot \sqrt{q}))$$

So this model predicts a shunt capacitance which also reduces a slightly in value when the frequency increases, and this decrease is roughly constant for each decade in frequency. This can indeed be observed from measurements and is therefore a convenient characteristic of this shaping function. If a small change in capacitance for a change in frequency from  $w_1$  to  $w_2$  is defined as  $\Delta C_p$  then each increase in frequency yields:

$$\frac{\Delta C_p}{C_p} = \left( \frac{C_p(jw_2) - C_p(jw_1)}{C_p(jw)} \right) \rightarrow \left\{ \frac{(-2f/p \cdot \ln(w_2/w_d \cdot \sqrt{q}) + 2f/p \cdot \ln(w_1/w_d \cdot \sqrt{q}))}{(1 - 2f/p \cdot \ln(w_1/w_d \cdot \sqrt{q}))} \right\}$$

$$\frac{\Delta C_p}{C_p} \rightarrow -\frac{2f}{p} \times \left\{ \frac{\ln(w_2/w_1)}{(1 - 2f/p \cdot \ln(w_1/w_d \cdot \sqrt{q}))} \right\}$$

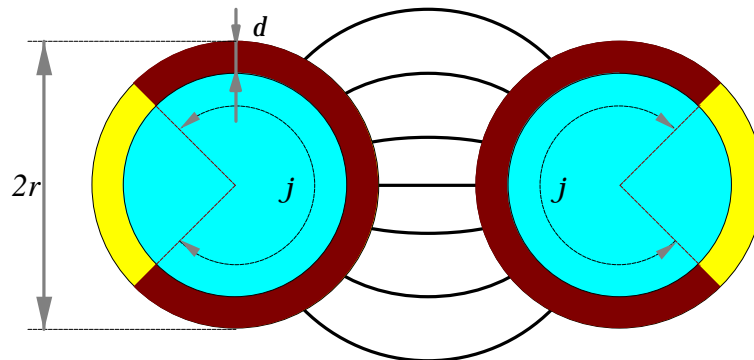
$$\frac{\Delta C_p}{C_p} \rightarrow -\frac{2f}{p} \cdot \ln\left(\frac{w_2}{w_1}\right) \rightarrow -\frac{2f}{p \cdot \log_{10}(e)} \cdot \log_{10}\left(\frac{w_2}{w_1}\right) \approx -f \times 1.47 \cdot \log_{10}\left(\frac{w_2}{w_1}\right)$$

$$\frac{\Delta C_p}{C_p} \approx -f \times 1.47 \cdot \log_{10}\left(\frac{w_2}{w_1}\right)$$

So this model also predicts a change in shunt capacitance or a change in frequency. And by using this shaping function,  $C_{p0}$  also decreases by about  $(1.47 \times f)$  for each decade in frequency. Therefore the added complexity of this second shaping function is hardly worth the effort for considering.

### 3.3 Finding starting values for skin frequency

The break frequency  $w_s$  for describing the frequency dependency of the loop resistance  $R_s(j\omega) \rightarrow R_{s0} \cdot \sqrt{\omega/\omega_s}$  can effectively be estimated as  $w_s = q_H \cdot w_{s0}$  where  $q_H$  is an empirical correction factor and where  $w_{s0} = 4p \cdot R_{s0}/m_b$ . This can easily be demonstrated via an over-simplified geometric model of a (twisted) wire pair and a simple well-known formula for the skin depth. The AC current density in a conductor decreases exponentially from its value at the surface, and most of it vanishes at a depth equal to the skin depth  $d(w)$  associated with a given angular frequency  $w$ . For approximating the total current it is adequate to assume that all current density is uniformly distributed within that skin depth. Figure [\*] shows the current density in a cross section of a wire pair, using that approximation. The frequency is assumed to be high enough to let the skin depth  $d(w)$  be small compared to the wire radius  $r$ . The approximation also assumes that the current density is concentrated in a thin slab that does not cover the full wire circumference. It assumes a fragment equal to  $j / (2p)$ , which is less than 100% of the full circumference and which value depends on the geometry of the wire pair. As a result, our over-simplified approximation assumes that all current flows uniformly through a cross section area equal to  $A_{skin}(w) = j \cdot r \times d(w)$ , for frequencies where  $d(w) \ll r$ .



If  $R_{s0}$  represents the DC resistance per unit length of two wires in a loop-back, and if  $R_s(\omega)$  represents the associated AC loop resistance per unit length, then  $R_s(\omega)$  becomes for frequencies where the skin effect is significant and  $d(w) \ll r$ :

$$R_s(w) \rightarrow R_{s0} \cdot \frac{A_{wire}}{A_{skin}(w)} = R_{s0} \cdot \frac{p \cdot r^2}{(j \cdot r) \times d(w)}$$

$$r = \frac{1}{2} \times (R_{s0} \times A_{wire}) = \frac{R_{s0}}{2} \times p \cdot r^2 \quad = \text{DC resistivity per unit length of a single metallic wire}$$

$$d(w) \approx \sqrt{\frac{2 \cdot r}{w \cdot m_0}} = \sqrt{\frac{R_{s0} \cdot p \cdot r^2}{w \cdot m_0}} \quad = \text{skin depth at angular frequency } w, \text{ where}$$

$$R_s(w) \rightarrow R_{s0} \cdot \frac{p \cdot r^2}{j \cdot r} \cdot \sqrt{\frac{w \cdot m_0}{R_{s0} \cdot p \cdot r^2}} = R_{s0} \cdot \frac{p}{j} \cdot \sqrt{\frac{w \cdot m_0}{p \cdot R_{s0}}} = R_{s0} \cdot \sqrt{\frac{p \cdot w \cdot m_0}{j^2 \cdot R_{s0}}}$$

$$R_s(w) \rightarrow R_{s0} \cdot \frac{2p}{j} \sqrt{\frac{w \cdot m_0}{4p \cdot R_{s0}}}$$

$$\text{Let } w_{s0} \stackrel{\text{def}}{=} \left( \frac{4p \cdot R_{s0}}{m_0} \right), \text{ where } m_0 = 4\pi \cdot 10^{-7} \text{ [H/m]}$$

$$\text{let } q_H \stackrel{\text{def}}{=} \frac{j}{2p} \leq 1$$

$$R_s(w) \rightarrow \frac{R_{s0}}{q_H} \cdot \sqrt{\frac{w}{w_{s0}}} = R_{s0} \cdot \sqrt{\frac{w}{w_s}}$$

$$w_s = q_H^2 \cdot w_{s0}$$

Values for the empirical correction factor  $q_H$  are typically in the order of 0.5-1 (meaning that  $j$  is between  $p$  and  $2p$ ) and  $m_0 = 4\pi \cdot 10^{-7}$  [H/m].

## 4 MODELING HIGH QUALITY, CAT 5 CABLING

The first cabling being modelled is a cable with 4 twisted wire pairs and a common shielding. It is a cable with high quality twists (category 5 quality or better), so that crosstalk between other wire pairs is kept to a minimum. This cabling is typically used for interconnecting 1 Gb/s Ethernet equipment with 100Ω source and load impedances.

A cable of about 300m on a drum was cut into three individual pieces of different lengths, to create different sections named as “232m”, “61m” and “10m”. Further details are described in [\*].



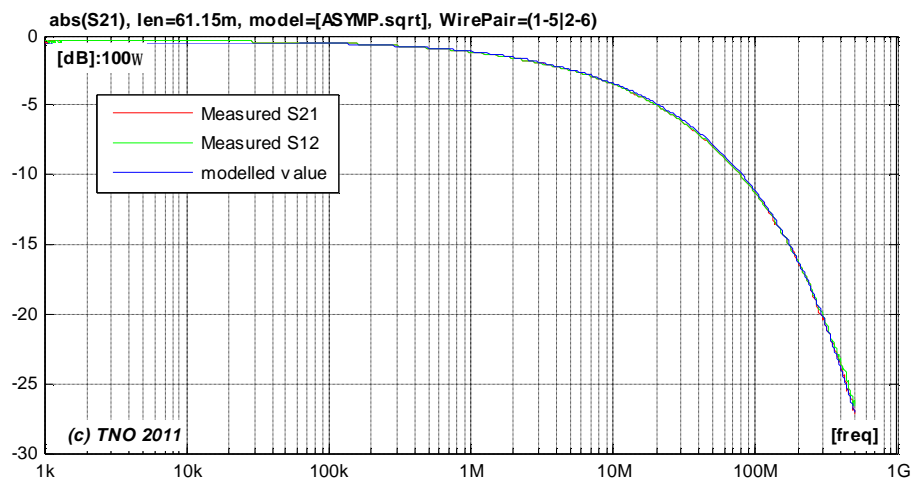
We extracted parameter values for each cable section and each wire pair being measured, for each shaping function of the proposed models. The results are very similar and therefore we show them only for wirepair #1 of the 61m section, using model [ASYMP.sqrt], based on the shaping functions  $Q_{Z,\text{sqrt}}(j\omega)$  and  $Q_{Y,1}(j\omega)$ .

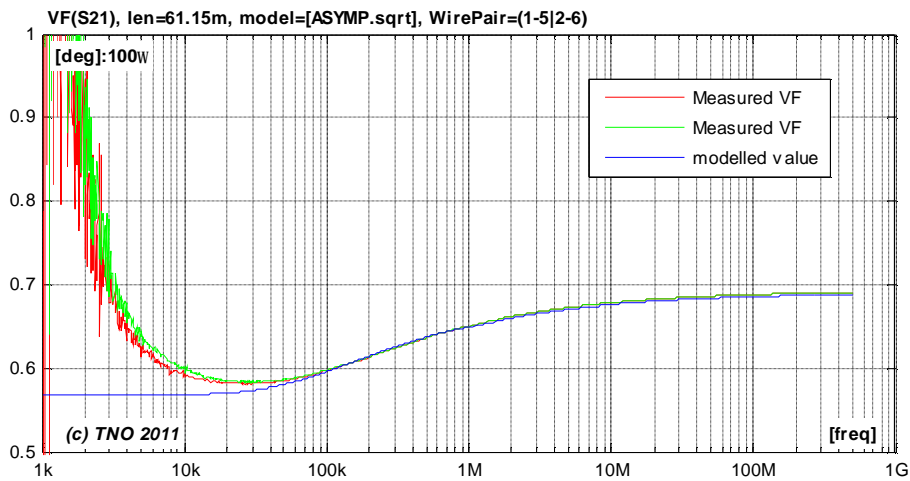
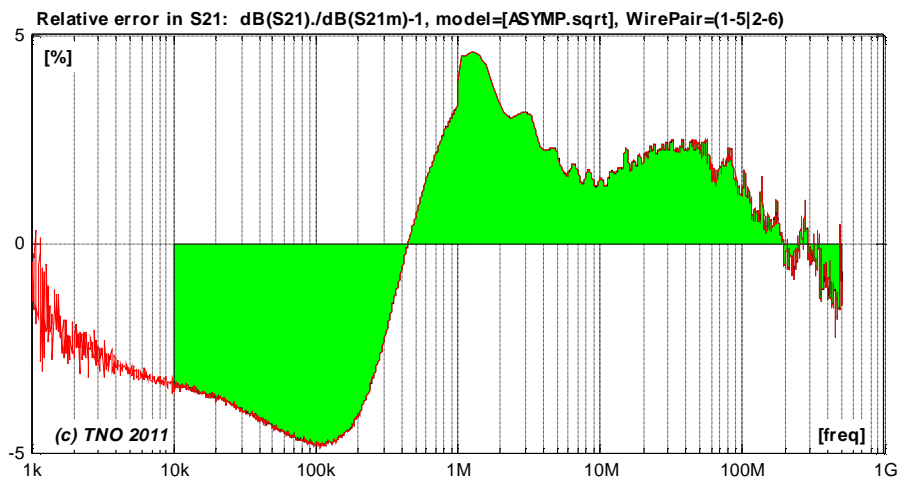
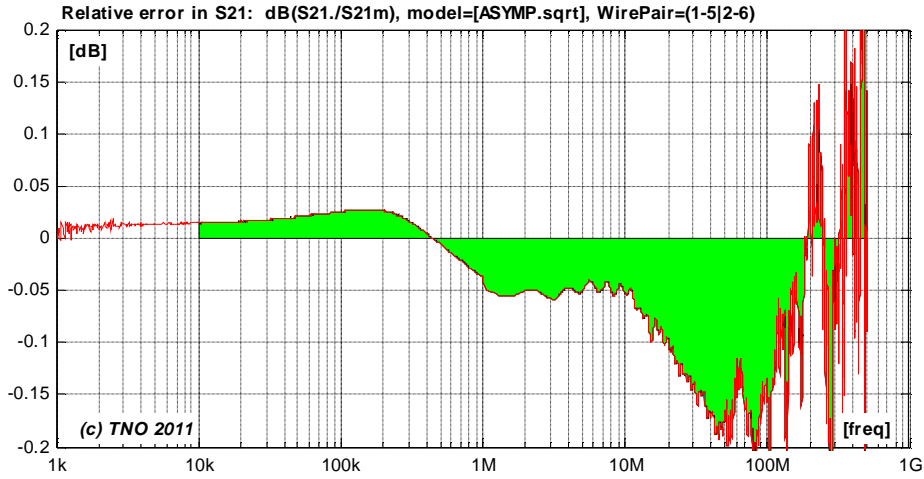
### 4.1 Match with two-port parameters

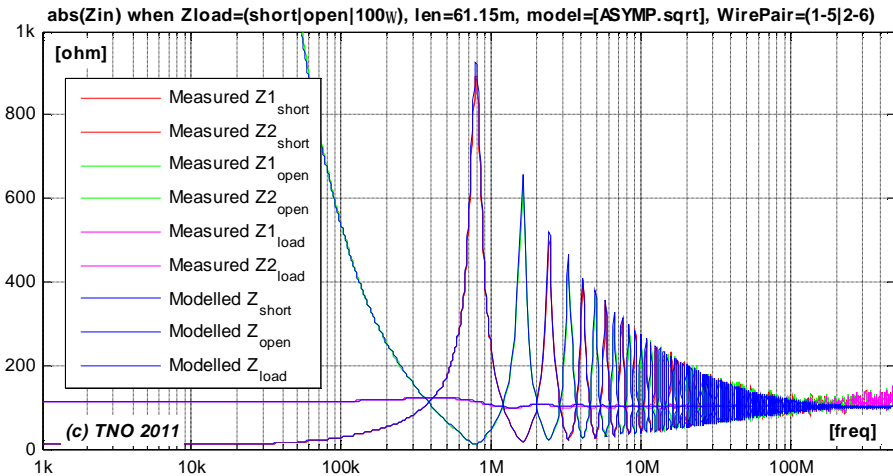
Figure [\*] to [\*] show for the same wire pair how close the two-port cable parameters of the model are matching the values calculated from the measurements.

- $S_{21}=S_{12}$  represents the transmission through the cable when terminated and powered from 100Ω.
- The velocity factor  $h_{VF}$  (or simply VF) is essentially another way to express the phase of  $S_{21}$ . It represents the traveling speed of signals through the cable, as a percentage of the speed of light.
- The input impedances are evaluated for different termination impedances: a short, a load of 100Ω and an open end.

The cable transfer measurements show an excellent match up to 500 MHz.







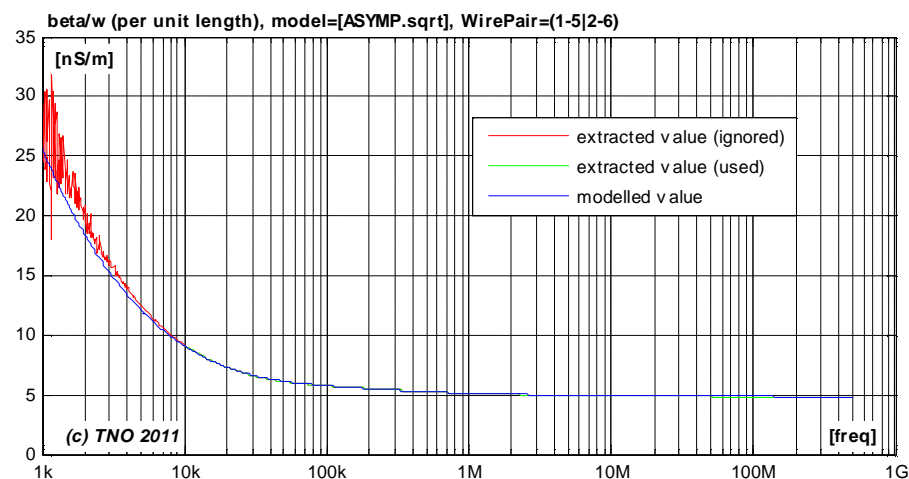
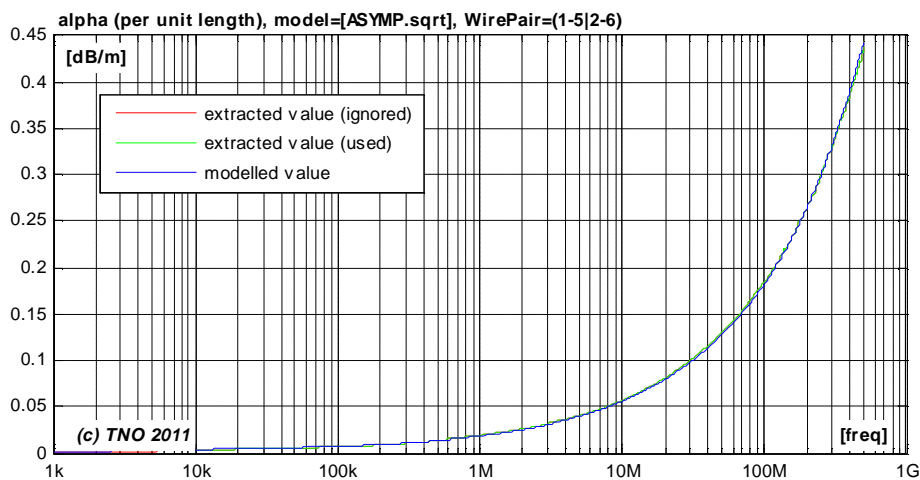
### 4.2 Match with secondary cable parameters (per unit length)

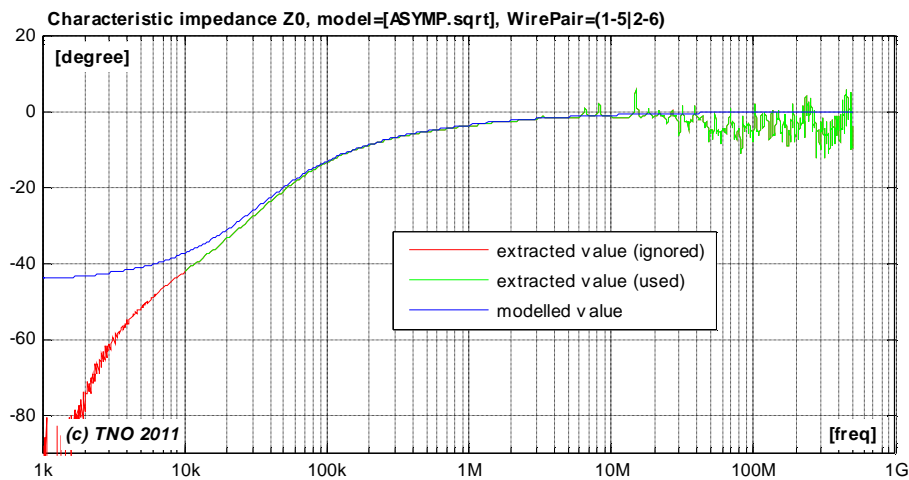
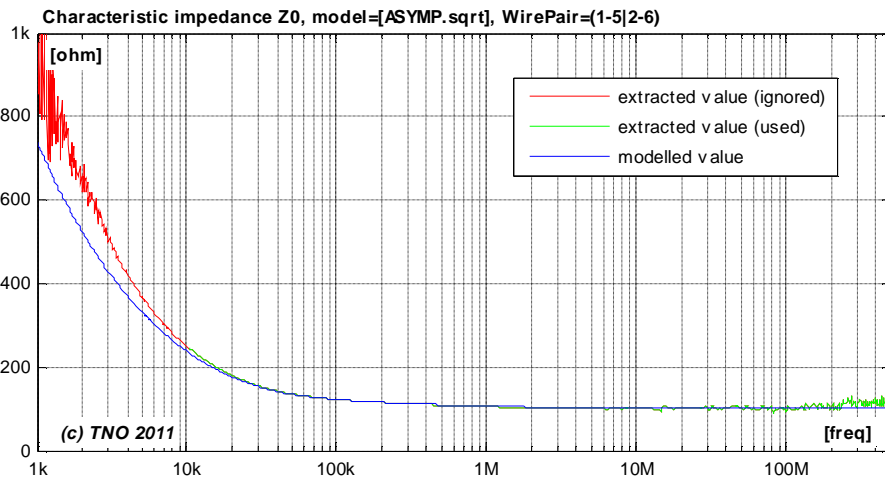
Figure [\*] to [\*] show for the same wire pair how close the secondary cable parameters ( $a$ ,  $b$ ,  $Z_0$ ) of the model are matching the values calculated from the measurements.

$$g(w) = \sqrt{Z_s(w) \cdot Y_p(w)}$$

$$Z_0(w) = \sqrt{Z_s(w) / Y_p(w)}$$

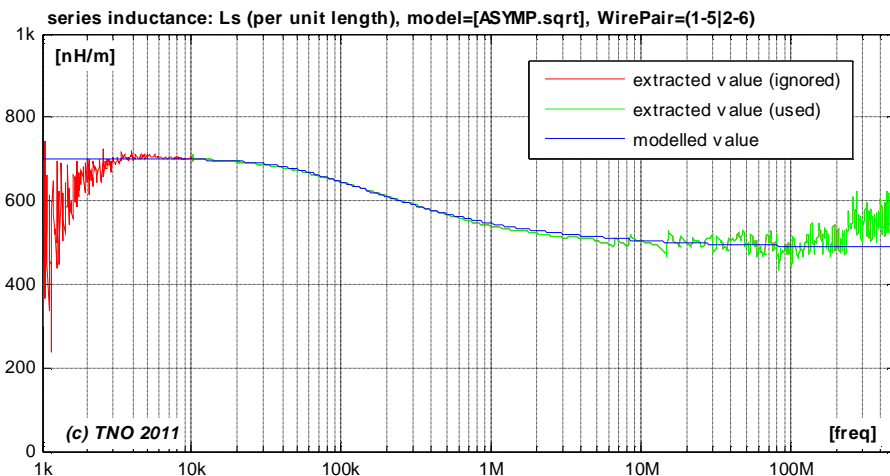
where  $a(w) = \text{real}\{g(w)\}$  and  $b(w) = \text{imag}\{g(w)\}$

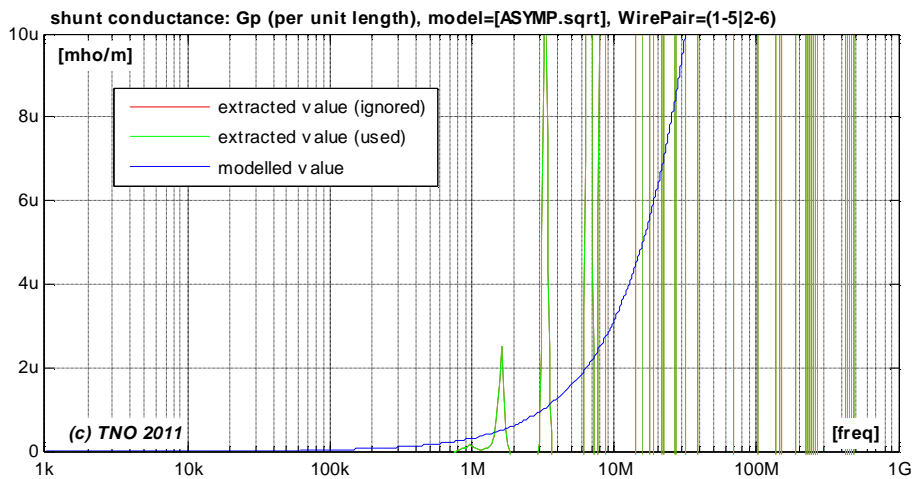
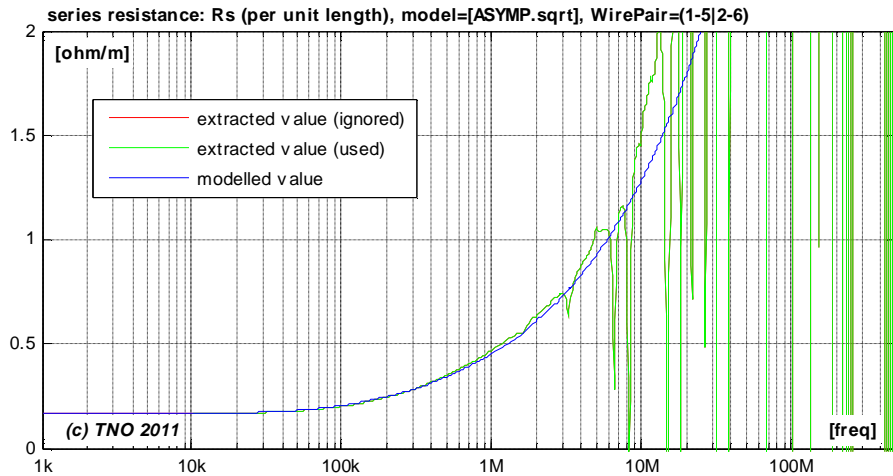
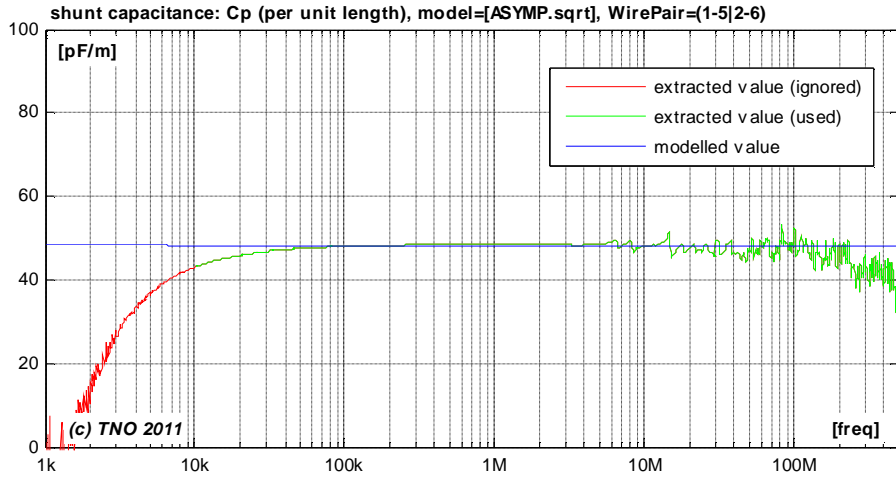




### 4.3 Match with primary cable parameters (per unit length)

Figure [\*] to [\*] show how close the primary cable parameters ( $L_s$ ,  $C_p$ ,  $R_s$ ,  $G_p$ ) of the model are matching the values calculated from the measurements.





## 4.4 Extracted parameter values for various models and sections

We extracted parameter values from each cable section and each wire pair being measured, for each shaping function of the proposed models. Each of them will be a slightly different, and all results are summarized below.

### 4.4.1 Loop section of 232m

HQ_CAT5	Loops\HQ_CAT5\2009_10_23_232m\ Name="232 m", Length=235.000 [m], wire pair 1, diff(1-5 2-6)
[ASYMP.sqrt]	Z0_inf=98.000000; VF=0.695448; Rs0=164.500000e-3; qL=2.150000; qH=0.823405; Phi=0.691283e-3; Fd=1.000000; Band=(10kHz .. 300MHz), Len=235[m], Err_S21dB:(E1=0.85%,E2=1.25%), Err_mix=0.0002351
[ASYMP.sqrt.rat]	Z0_inf=98.000000; VF=0.694347; Rs0=164.500000e-3; qL=2.150000; qH=0.852756; qX=0.523673; qY=0.690146; Phi=0.933130e-3; Fd=1.000000; Band=(10kHz .. 300MHz), Len=235[m], Err_S21dB:(E1=0.84%,E2=1.07%), Err_mix=0.0002307
[ASYMP.bessel]	Z0_inf=98.000000; VF=0.694700; Rs0=164.500000e-3; qL=2.150000; qH=0.841450; Phi=0.849462e-3; Fd=1.000000; Band=(10kHz .. 300MHz), Len=235[m], Err_S21dB:(E1=1.16%,E2=1.78%), Err_mix=0.0002398
[ASYMP.hyp]	Z0_inf=98.000000; VF=0.694436; Rs0=164.500000e-3; qL=2.150000; qH=0.847823; Phi=0.905776e-3; Fd=1.000000; Band=(10kHz .. 300MHz), Len=235[m], Err_S21dB:(E1=1.32%,E2=2.08%), Err_mix=0.0002433
[ASYMP.mix]	Z0_inf=98.000000; VF=0.695293; Rs0=164.500000e-3; qL=2.150000; qH=0.826900; Phi=0.724926e-3; Fd=1.000000; qB=0.123549; Band=(10kHz .. 300MHz), Len=235[m], Err_S21dB:(E1=0.87%,E2=1.27%), Err_mix=0.0002350

HQ_CAT5	Loops\HQ_CAT5\2009_10_23_232m\ Name="232 m", Length=235.000 [m], wire pair 2, diff(3-7 4-8)
[ASYMP.sqrt]	Z0_inf=98.000000; VF=0.688141; Rs0=167.300000e-3; qL=2.150000; qH=0.832450; Phi=0.733386e-3; Fd=1.000000; Band=(10kHz .. 300MHz), Len=235[m], Err_S21dB:(E1=0.96%,E2=1.40%), Err_mix=0.0002741
[ASYMP.sqrt.rat]	Z0_inf=98.000000; VF=0.687274; Rs0=167.300000e-3; qL=2.150000; qH=0.857917; qX=0.548238; qY=0.661893; Phi=0.928568e-3; Fd=1.000000; Band=(10kHz .. 300MHz), Len=235[m], Err_S21dB:(E1=0.88%,E2=1.13%), Err_mix=0.0002686
[ASYMP.bessel]	Z0_inf=98.000000; VF=0.687611; Rs0=167.300000e-3; qL=2.150000; qH=0.847226; Phi=0.846514e-3; Fd=1.000000; Band=(10kHz .. 300MHz), Len=235[m], Err_S21dB:(E1=1.20%,E2=1.87%), Err_mix=0.0002770
[ASYMP.hyp]	Z0_inf=98.000000; VF=0.687186; Rs0=167.300000e-3; qL=2.150000; qH=0.856686; Phi=0.939923e-3; Fd=1.000000; Band=(10kHz .. 300MHz), Len=235[m], Err_S21dB:(E1=1.40%,E2=2.17%), Err_mix=0.0002795
[ASYMP.mix]	Z0_inf=98.000000; VF=0.688161; Rs0=167.300000e-3; qL=2.150000; qH=0.834110; Phi=0.735977e-3; Fd=1.000000; qB=0.199056; Band=(10kHz .. 300MHz), Len=235[m], Err_S21dB:(E1=0.92%,E2=1.39%), Err_mix=0.0002737

### 4.4.2 Loop section of 61m

HQ_CAT5	Loops\HQ_CAT5\2009_10_23_61m\ Name="61 m", Length=61.150 [m], wire pair 1, diff(1-5 2-6)
[ASYMP.sqrt]	Z0_inf=100.000000; VF=0.685777; Rs0=166.700000e-3; qL=2.150000; qH=0.836789; Phi=1.038058e-3; Fd=1.000000; Band=(10kHz .. 500MHz), Len=61.15[m], Err_S21dB:(E1=1.69%,E2=2.09%), Err_mix=0.0006158
[ASYMP.sqrt.rat]	Z0_inf=100.000000; VF=0.685128; Rs0=166.700000e-3; qL=2.150000; qH=0.862124; qX=0.500991; qY=0.683900; Phi=1.186592e-3; Fd=1.000000; Band=(10kHz .. 500MHz), Len=61.15[m], Err_S21dB:(E1=1.36%,E2=1.71%), Err_mix=0.0006113
[ASYMP.bessel]	Z0_inf=100.000000; VF=0.685314; Rs0=166.700000e-3; qL=2.150000; qH=0.852862; Phi=1.139609e-3; Fd=1.000000; Band=(10kHz .. 500MHz), Len=61.15[m], Err_S21dB:(E1=1.84%,E2=2.48%), Err_mix=0.0006166
[ASYMP.hyp]	Z0_inf=100.000000; VF=0.685153; Rs0=166.700000e-3; qL=2.150000; qH=0.858514; Phi=1.175273e-3; Fd=1.000000; Band=(10kHz .. 500MHz), Len=61.15[m], Err_S21dB:(E1=1.93%,E2=2.72%), Err_mix=0.0006176
[ASYMP.mix]	Z0_inf=100.000000; VF=0.685700; Rs0=166.700000e-3; qL=2.150000; qH=0.838760; Phi=1.042901e-3; Fd=1.000000; qB=0.268441; Band=(10kHz .. 500MHz), Len=61.15[m], Err_S21dB:(E1=1.60%,E2=2.06%), Err_mix=0.0006156

HQ_CAT5	Loops\HQ_CAT5\2009_10_23_61m\ Name="61 m", Length=61.150 [m], wire pair 2, diff(3-7 4-8)
[ASYMP.sqrt]	Z0_inf=100.000000; VF=0.690742; Rs0=166.000000e-3; qL=2.150000; qH=0.838860; Phi=1.073253e-3; Fd=1.000000; Band=(10kHz .. 500MHz), Len=61.15[m], Err_S21dB:(E1=1.72%,E2=2.11%), Err_mix=0.0005893
[ASYMP.sqrt.rat]	Z0_inf=100.000000; VF=0.689975; Rs0=166.000000e-3; qL=2.150000; qH=0.868594; qX=0.500000; qY=0.802424; Phi=1.257137e-3; Fd=1.000000; Band=(10kHz .. 500MHz), Len=61.15[m], Err_S21dB:(E1=1.47%,E2=1.78%), Err_mix=0.0005846
[ASYMP.bessel]	Z0_inf=100.000000; VF=0.690275; Rs0=166.000000e-3; qL=2.150000; qH=0.855680; Phi=1.180998e-3; Fd=1.000000; Band=(10kHz .. 500MHz), Len=61.15[m], Err_S21dB:(E1=1.77%,E2=2.27%), Err_mix=0.0005888
[ASYMP.hyp]	Z0_inf=100.000000; VF=0.690109; Rs0=166.000000e-3; qL=2.150000; qH=0.861387; Phi=1.217206e-3; Fd=1.000000; Band=(10kHz .. 500MHz), Len=61.15[m], Err_S21dB:(E1=1.85%,E2=2.45%), Err_mix=0.0005893
[ASYMP.mix]	Z0_inf=100.000000; VF=0.690577; Rs0=166.000000e-3; qL=2.150000; qH=0.845672; Phi=1.110470e-3; Fd=1.000000; qB=0.453616; Band=(10kHz .. 500MHz), Len=61.15[m], Err_S21dB:(E1=1.62%,E2=2.02%), Err_mix=0.0005883

### 4.4.3 Loop section of 10m

HQ_CAT5	Loops\HQ_CAT5\2009_10_23_10m\ Name="10 m", Length=10.210 [m], wire pair 1, diff(1-5 2-6)
[ASYMP.sqrt]	Z0_inf=99.000000; VF=0.693682; Rs0=166.000000e-3; qL=2.050000; qH=0.851537; Phi=1.324103e-3; Fd=1.000000; Band=(20kHz .. 300MHz), Len=10.21[m], Err_S21dB:(E1=5.01%,E2=8.28%), Err_mix=0.0008992
[ASYMP.sqrt.rat]	Z0_inf=99.000000; VF=0.692663; Rs0=166.000000e-3; qL=2.050000; qH=0.883724; qX=0.500000; qY=0.500000; Phi=1.561312e-3; Fd=1.000000; Band=(20kHz .. 300MHz), Len=10.21[m], Err_S21dB:(E1=4.66%,E2=7.60%), Err_mix=0.0008847
[ASYMP.bessel]	Z0_inf=99.000000; VF=0.693114; Rs0=166.000000e-3; qL=2.050000; qH=0.867711; Phi=1.439815e-3; Fd=1.000000; Band=(20kHz .. 300MHz), Len=10.21[m], Err_S21dB:(E1=5.46%,E2=8.91%), Err_mix=0.0009061
[ASYMP.hyp]	Z0_inf=99.000000; VF=0.692929; Rs0=166.000000e-3; qL=2.050000; qH=0.873156; Phi=1.478415e-3; Fd=1.000000; Band=(20kHz .. 300MHz), Len=10.21[m], Err_S21dB:(E1=5.60%,E2=9.13%), Err_mix=0.0009081
[ASYMP.mix]	Z0_inf=99.000000; VF=0.693750; Rs0=166.000000e-3; qL=2.050000; qH=0.850271; Phi=1.309394e-3; Fd=1.000000; qB=0.000740; Band=(20kHz .. 300MHz), Len=10.21[m], Err_S21dB:(E1=5.01%,E2=8.28%), Err_mix=0.0008992

HQ_CAT5	Loops\HQ_CAT5\2009_10_23_10m\ Name="10 m", Length=10.210 [m], wire pair 2, diff(3-7 4-8)
[ASYMP.sqrt]	Z0_inf=99.000000; VF=0.688767; Rs0=170.000000e-3; qL=2.100000; qH=0.869927; Phi=1.191904e-3; Fd=1.000000; Band=(20kHz .. 300MHz), Len=10.21[m], Err_S21dB:(E1=4.57%,E2=7.63%), Err_mix=0.0008340
[ASYMP.sqrt.rat]	Z0_inf=99.000000; VF=0.687822; Rs0=170.000000e-3; qL=2.100000; qH=0.901533; qX=0.500000; qY=0.500000; Phi=1.415260e-3; Fd=1.000000; Band=(20kHz .. 300MHz), Len=10.21[m], Err_S21dB:(E1=4.25%,E2=7.00%), Err_mix=0.0008203
[ASYMP.bessel]	Z0_inf=99.000000; VF=0.688215; Rs0=170.000000e-3; qL=2.100000; qH=0.886178; Phi=1.305381e-3; Fd=1.000000; Band=(20kHz .. 300MHz), Len=10.21[m], Err_S21dB:(E1=5.04%,E2=8.20%), Err_mix=0.0008403
[ASYMP.hyp]	Z0_inf=99.000000; VF=0.688035; Rs0=170.000000e-3; qL=2.100000; qH=0.891667; Phi=1.343427e-3; Fd=1.000000; Band=(20kHz .. 300MHz), Len=10.21[m], Err_S21dB:(E1=5.20%,E2=8.40%), Err_mix=0.0008422
[ASYMP.mix]	Z0_inf=99.000000; VF=0.688822; Rs0=170.000000e-3; qL=2.100000; qH=0.868914; Phi=1.179744e-3; Fd=1.000000; qB=0.002384; Band=(20kHz .. 300MHz), Len=10.21[m], Err_S21dB:(E1=4.58%,E2=7.63%), Err_mix=0.0008340

#### 4.4.4 Virtual loop section of 2´232m in cascade

By evaluating a mathematical cascade of the two wire pairs of the 232m section, a two-port “measurement” of 2x232m is emulated.

HQ_CAT5	Loops\HQ_CAT5\2009_10_23_232m Name="casc:2*(232)", Length=470.000 [m], 2-port parameters
[ASYMP.sqrt]	Z0_inf=98.000000; VF=0.691623; Rs0=165.900000e-3; qL=2.150000; qH=0.828111; Phi=0.716425e-3; Fd=1.000000 Band=(10kHz .. 300MHz), Len=470[m], Err_S21dB:(E1=0.94%,E2=1.39%), Err_mix=0.0002431
[ASYMP.sqrt.rat]	Z0_inf=98.000000; VF=0.690464; Rs0=165.900000e-3; qL=2.150000; qH=0.859450; qX=0.500000; qY=0.722636; Phi=0.973846e-3; Fd=1.000000; Band=(10kHz .. 300MHz), Len=470[m], Err_S21dB:(E1=0.93%,E2=1.18%), Err_mix=0.0002376
[ASYMP.bessel]	Z0_inf=98.000000; VF=0.690893; Rs0=165.900000e-3; qL=2.150000; qH=0.846146; Phi=0.872335e-3; Fd=1.000000; Band=(10kHz .. 300MHz), Len=470[m], Err_S21dB:(E1=1.21%,E2=1.84%), Err_mix=0.0002471
[ASYMP.hyp]	Z0_inf=98.000000; VF=0.690639; Rs0=165.900000e-3; qL=2.150000; qH=0.852464; Phi=0.927203e-3; Fd=1.000000; Band=(10kHz .. 300MHz), Len=470[m], Err_S21dB:(E1=1.36%,E2=2.11%), Err_mix=0.0002503
[ASYMP.mix]	Z0_inf=98.000000; VF=0.691664; Rs0=165.900000e-3; qL=2.150000; qH=0.829503; Phi=0.718536e-3; Fd=1.000000; qB=0.176989; Band=(10kHz .. 300MHz), Len=470[m], Err_S21dB:(E1=0.90%,E2=1.36%), Err_mix=0.0002430

#### 4.5 Common reference model for this CAT5 cable

All asymptotic models in the previous section are predicting the measured cable characteristics very close, and model [ASYMP.sqrt.rat] appeared to provide the closest match and therefore that one is the preferred choice for modeling this cable.

Since the reference model should describe any section of this cable type, its parameter values should be a pragmatic average of the values extracted for each section. The mathematical cascade of the two wire pairs of the 232m section can serve as such average

Therefore the following asymptotic model is proposed to serve as reference model for this cable type:

HQ_CAT5	Parameters of reference model
[ASYMP.sqrt.rat]	Z0_inf=98.000000; VF=0.690464; Rs0=165.900000e-3; qL=2.150000; qH=0.859450; qX=0.500000; qY=0.722636; Phi=0.973846e-3; Fd=1.000000;

Model, with square root of rational function, 8+1 parameters

$$[Z_s, Y_p] = \text{Model}(Z_{0\infty}, \eta_{VF}, R_{s0}, q_L, q_H, q_x, q_y, f, f_d)$$

$$Z_s(j\omega) = j\omega \cdot L_{s\infty} + R_{s0} \times \left( 1 - q_s \cdot q_x + \text{sqr}t \left( q_s^2 \cdot q_x^2 + 2 \cdot \frac{j\omega}{w_s} \cdot \left( \frac{q_s^2 + j\omega/w_s \cdot q_y}{q_s^2/q_x + j\omega/w_s \cdot q_y} \right) \right) \right)$$

$$Y_p(j\omega) = j\omega \cdot C_{p0} \times \left( 1 + \frac{j\omega}{w_d} \right)^{-2 \cdot f/p}$$

Where:

$$L_{s\infty} = \frac{1}{h_{VF} \cdot c_0} \times Z_{0\infty}$$

$$C_{p0} = \frac{1}{h_{VF} \cdot c_0} \times \frac{1}{Z_{0\infty}}$$

$$q_s = \frac{1}{q_H \cdot q_L}$$

$$w_s = q_H^2 \cdot w_{s0} = q_H^2 \cdot \left( \frac{4p \cdot R_{s0}}{m_0} \right)$$

$$w_d = 2p \cdot f_d$$

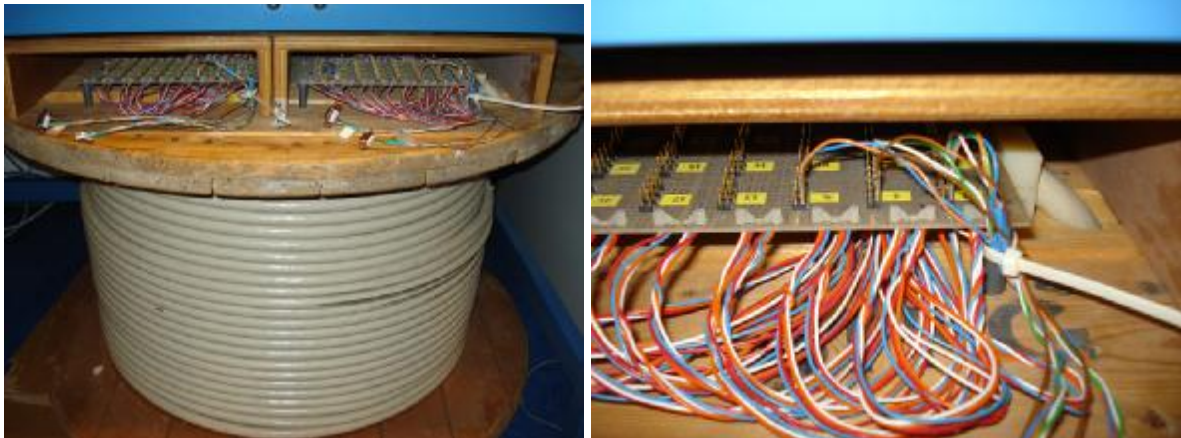
$$c_0 = 3 \cdot 10^8 \text{ [m/s]}$$

$$m_0 = 4\pi \cdot 10^{-7} \text{ [H/m]}$$

## 5 MODELING MEDIUM QUALITY CABLING FOR TELEPHONY

Another cable being modeled is a cable with 30 twisted quads (each with two wire pairs or 4 wires) and a common shielding. It is a cable with medium quality twists, so that crosstalk between other wire pairs is kept to a minimum. This cabling is typically used in buildings for offering telephony services to different locations in that building.

Further details are described in [\*].



We extracted parameter values for different wire-pairs within the 378m cable, for each shaping function of the proposed models. The results are very similar and therefore we show them only for wirepair #1 using model [ASYMP.sqrt.rat], based on the shaping functions  $Q_{z,\text{sqrt,rat}}(j\omega)$  and  $Q_{y,1}(j\omega)$ .

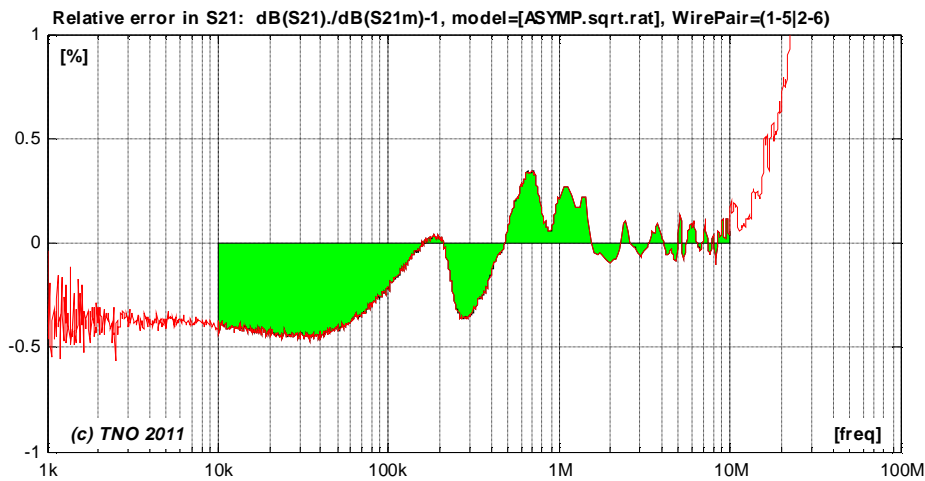
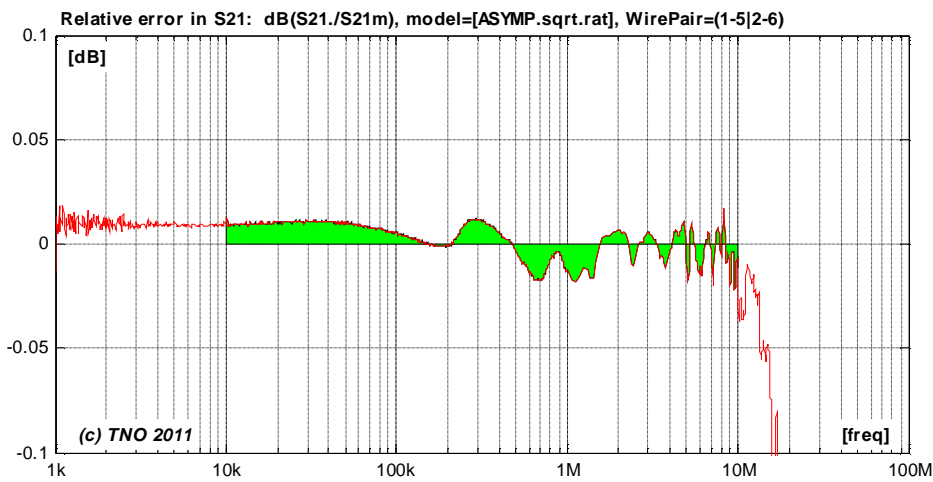
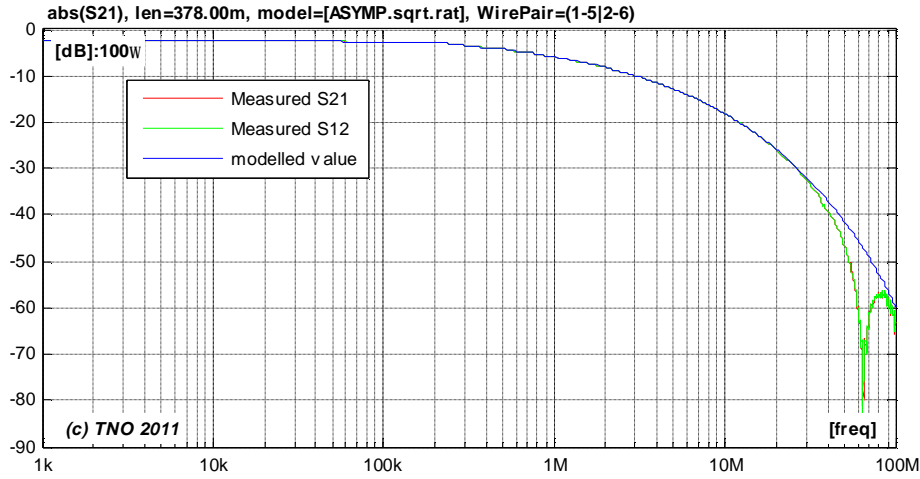
### 5.1 Match with two-port parameters

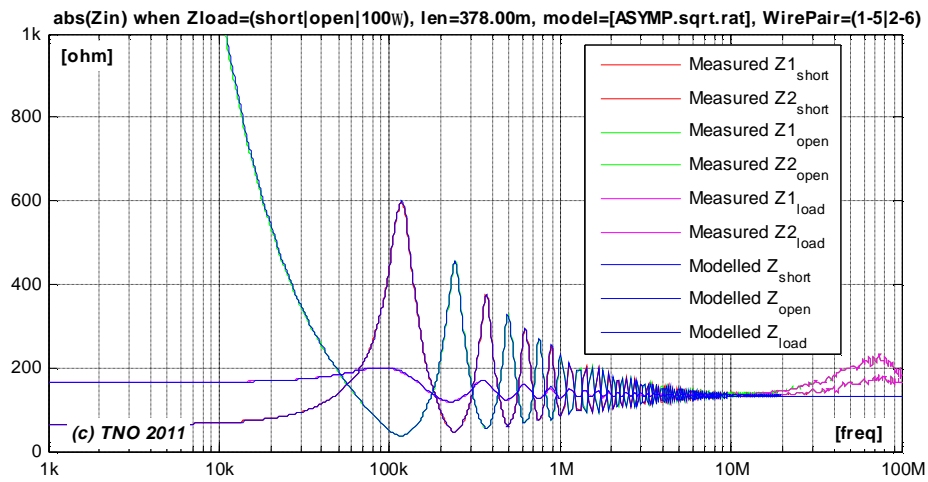
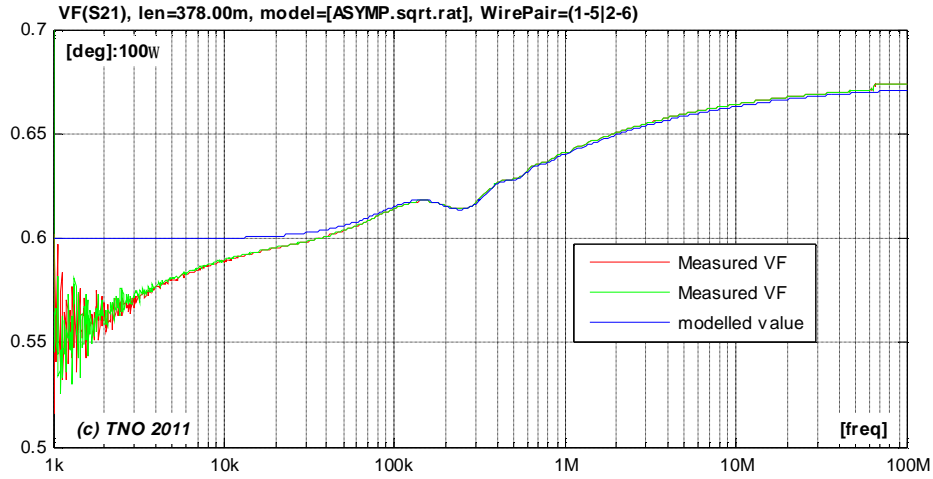
Figure [\*] to [\*] show for the same wire pair how close the two-port cable parameters of the model are matching the values calculated from the measurements.

- $S_{21}=S_{12}$  represents the transmission through the cable when terminated and powered from  $100\Omega$ .
- The velocity factor  $h_{VF}$  (or simply VF) is essentially another way to express the phase of  $S_{21}$ . It represents the traveling speed of signals through the cable, as a percentage of the speed of light.
- The input impedances are evaluated for different termination impedances: a short, a load of  $100\Omega$  and an open end.

The cable transfer measurements show some resonant behavior near 65MHz, which is currently not well understood. Above 100MHz the transmission becomes a bit random in nature (not shown here), which is assumed to be caused by the imperfect homogeneous construction of the twisted-pair cable. Those aspects can never be covered by a perfect homogeneous model.

But if these notches are modeled separately in a deterministic manner then the result may be applicable to about 100MHz. Such a refinement is left for further study.





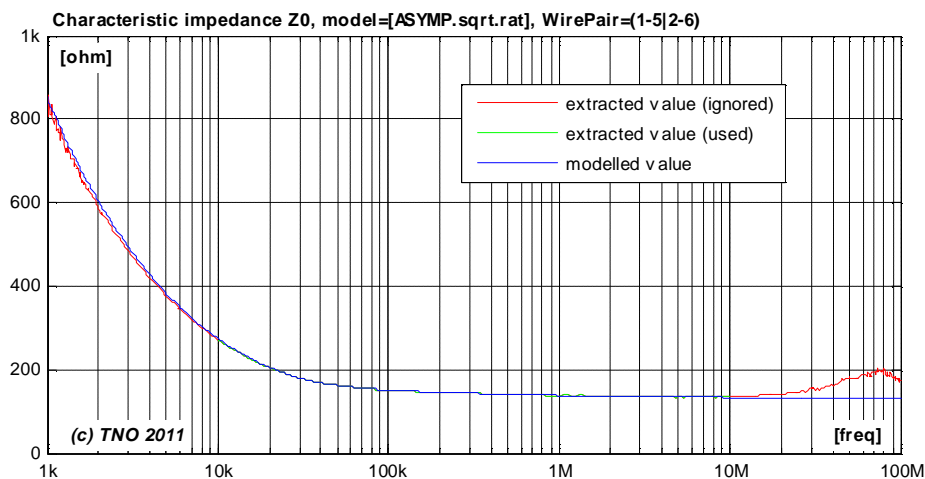
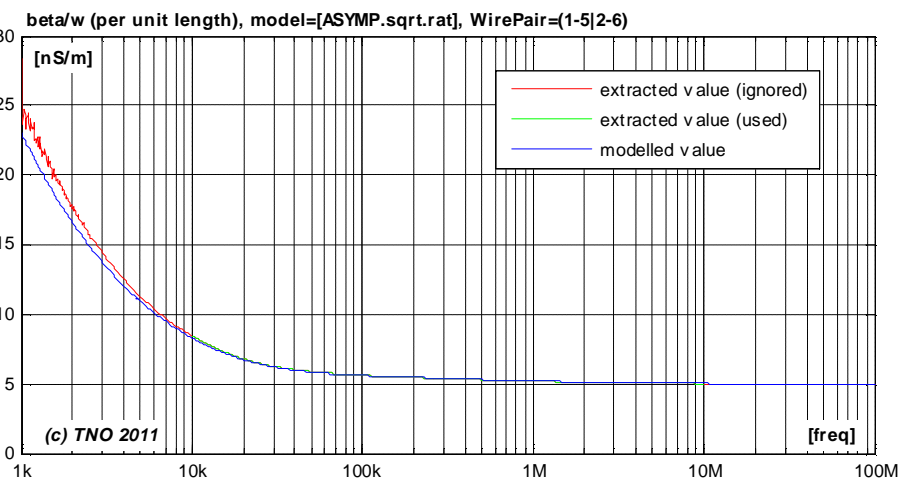
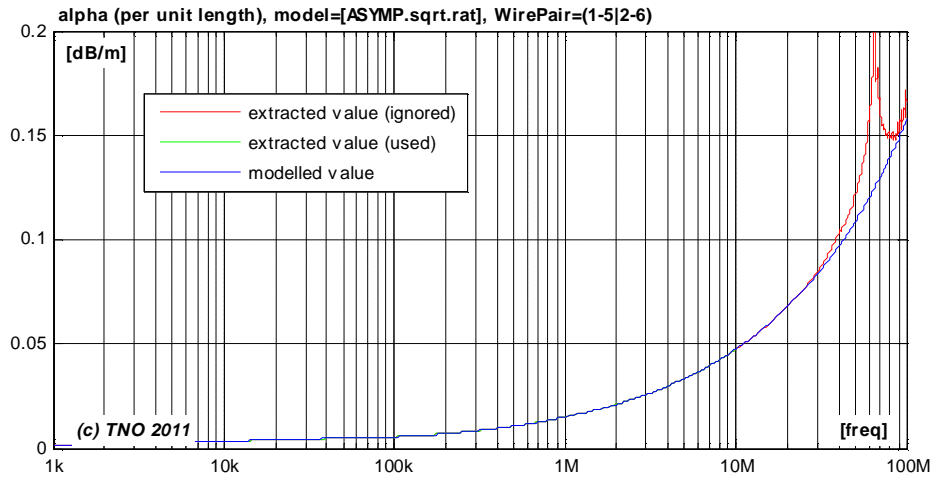
## 5.2 Match with secondary cable parameters (per unit length)

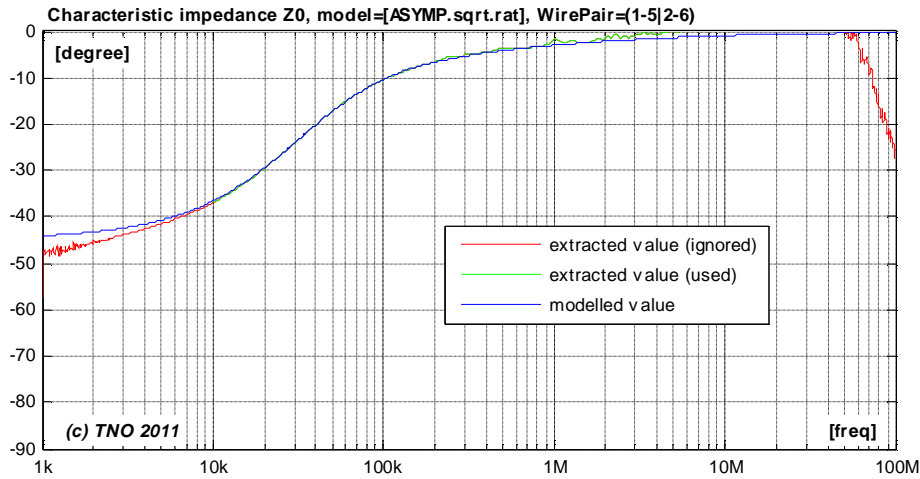
Figure [\*] to [\*] show for the same wire pair how close the secondary cable parameters ( $a$ ,  $b$ ,  $Z_0$ ) of the model are matching the values calculated from the measurements.

$$g(w) = \sqrt{Z_s(w) \cdot Y_p(w)}$$

where  $a(w) = \text{real}\{g(w)\}$  and  $b(w) = \text{imag}\{g(w)\}$

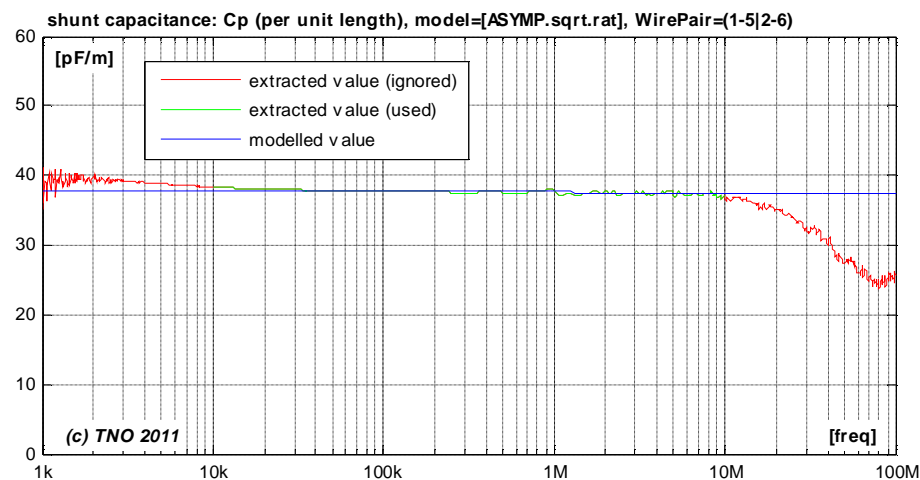
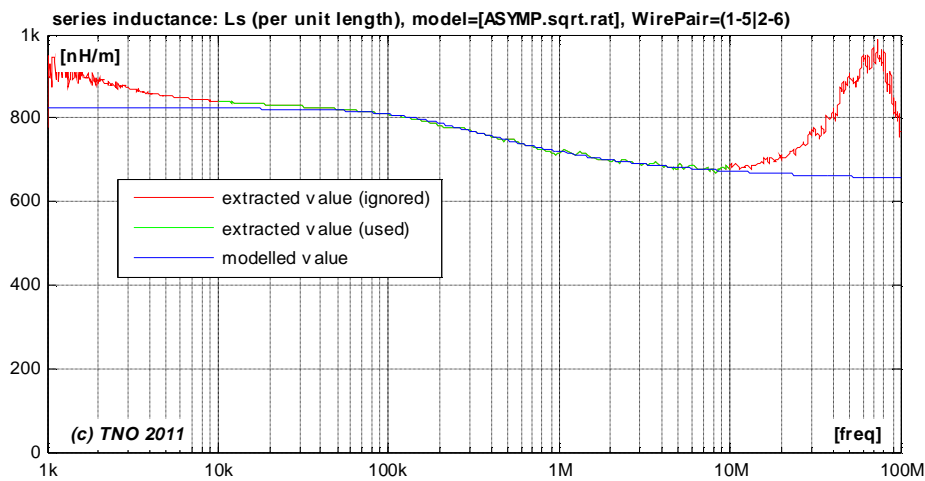
$$Z_0(w) = \sqrt{Z_s(w) / Y_p(w)}$$

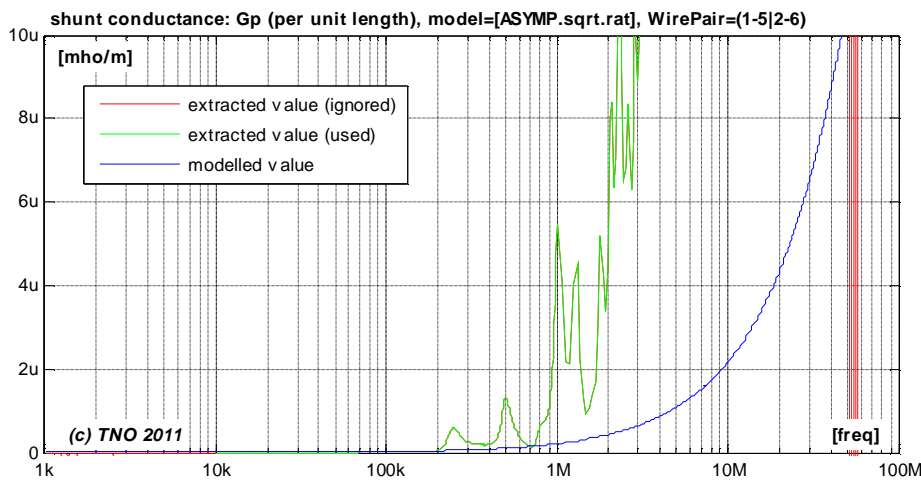
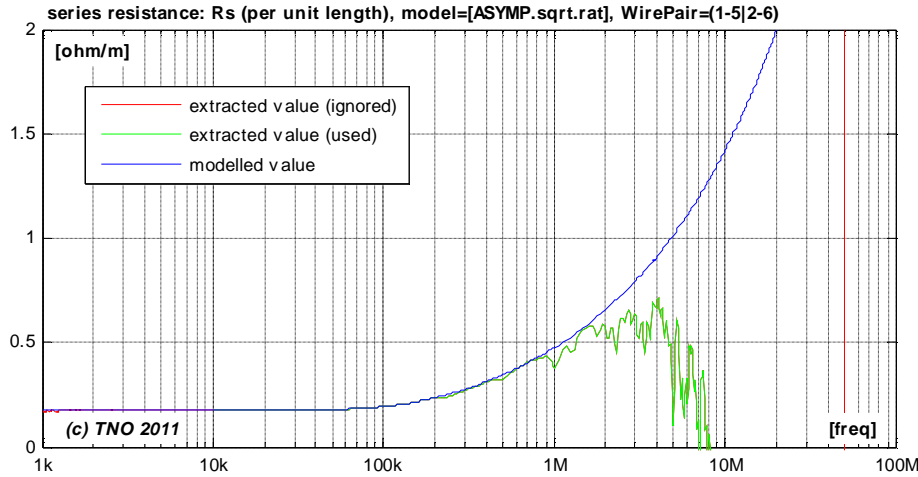




### 5.3 Match with primary cable parameters (per unit length)

Figure [\*] to [\*] show how close the primary cable parameters ( $L_s$ ,  $C_p$ ,  $R_s$ ,  $G_p$ ) of the model are matching the values calculated from the measurements.





## 5.4 Extracted parameters for various models and sections

We extracted parameter values from each wire pair being measured, for each shaping function of the proposed models. Each of them will be a slightly different, and all results are summarized below.

### 5.4.1 Quad #1, 378m

MQ_TelCable_30q	Loops\MQ_TelCable_30quad\2010_01_27_quad_1\ Name="quad 1", Length=378.000 [m], wire pair 1, diff(1-5 2-6)
[ASYMP.sqrt]	$Z0\_inf=131.327281$ ; $VF=0.674816$ ; $Rs0=172.400000e-3$ ; $qL=1.853645$ ; $qH=0.705787$ ; $\Phi=0.000001e-3$ ; $Fd=1.000000$ Band=(10kHz .. 10MHz), Len=378[m], Err_S21dB:(E1=1.03%,E2=1.18%), Err_mix=0.0001393
[ASYMP.sqrt.rat]	$Z0\_inf=131.056172$ ; $VF=0.671482$ ; $Rs0=172.400000e-3$ ; $qL=1.742162$ ; $qH=0.753511$ ; $qX=0.740625$ ; $qY=1.031628$ ; $\Phi=0.799537e-3$ ; $Fd=1.000000$ ; Band=(10kHz .. 10MHz), Len=378[m], Err_S21dB:(E1=0.23%,E2=0.28%), Err_mix=0.0000767
[ASYMP.bessel]	$Z0\_inf=130.845541$ ; $VF=0.668888$ ; $Rs0=172.400000e-3$ ; $qL=1.661718$ ; $qH=0.765084$ ; $\Phi=1.473453e-3$ ; $Fd=1.000000$ ; Band=(10kHz .. 10MHz), Len=378[m], Err_S21dB:(E1=0.47%,E2=0.59%), Err_mix=0.0001012
[ASYMP.hyp]	$Z0\_inf=130.262751$ ; $VF=0.661636$ ; $Rs0=172.400000e-3$ ; $qL=1.579410$ ; $qH=0.821221$ ; $\Phi=3.406321e-3$ ; $Fd=1.000000$ Band=(10kHz .. 10MHz), Len=378[m], Err_S21dB:(E1=0.74%,E2=0.91%), Err_mix=0.0001308
[ASYMP.mix]	$Z0\_inf=131.316277$ ; $VF=0.674329$ ; $Rs0=172.400000e-3$ ; $qL=1.761940$ ; $qH=0.723265$ ; $\Phi=0.064137e-3$ ; $Fd=1.000000$ ; $qB=0.411059$ ; Band=(10kHz .. 10MHz), Len=378[m], Err_S21dB:(E1=0.26%,E2=0.30%), Err_mix=0.0000828

MQ_TelCable_30q	Loops\MQ_TelCable_30quad\2010_01_27_quad_1\ Name="quad 1", Length=378.000 [m], wire pair 2, diff(3-7 4-8)
[ASYMP.sqrt]	Z0_inf=131.306458; VF=0.674736; Rs0=172.800000e-3; qL=1.848934; qH=0.705754; Phi=0.000000e-3; Fd=1.000000; Band=(10kHz .. 10MHz), Len=378[m], Err_S21dB:(E1=1.05%,E2=1.20%), Err_mix=0.0001512
[ASYMP.sqrt.rat]	Z0_inf=131.006131; VF=0.670483; Rs0=172.800000e-3; qL=1.726749; qH=0.758375; qX=0.737548; qY=1.069096; Phi=1.036873e-3; Fd=1.000000; Band=(10kHz .. 10MHz), Len=378[m], Err_S21dB:(E1=0.27%,E2=0.34%), Err_mix=0.0000942
[ASYMP.bessel]	Z0_inf=130.926826; VF=0.669173; Rs0=172.800000e-3; qL=1.662737; qH=0.762509; Phi=1.355073e-3; Fd=1.000000; Band=(10kHz .. 10MHz), Len=378[m], Err_S21dB:(E1=0.49%,E2=0.61%), Err_mix=0.0001144
[ASYMP.hyp]	Z0_inf=130.340583; VF=0.662255; Rs0=172.800000e-3; qL=1.580490; qH=0.816602; Phi=3.227102e-3; Fd=1.000000; Band=(10kHz .. 10MHz), Len=378[m], Err_S21dB:(E1=0.77%,E2=0.94%), Err_mix=0.0001382
[ASYMP.mix]	Z0_inf=131.206859; VF=0.673596; Rs0=172.800000e-3; qL=1.753145; qH=0.726573; Phi=0.249688e-3; Fd=1.000000; qB=0.405535; Band=(10kHz .. 10MHz), Len=378[m], Err_S21dB:(E1=0.30%,E2=0.36%), Err_mix=0.0001002

### 5.4.2 Quad #2, 378m

MQ_TelCable_30q	Loops\MQ_TelCable_30quad\2010_02_04_quad_2\ Name="quad 2", Length=378.000 [m], wire pair 1, diff(1-5 2-6)
[ASYMP.sqrt]	Z0_inf=130.630627; VF=0.673434; Rs0=170.000000e-3; qL=1.855891; qH=0.701574; Phi=0.000000e-3; Fd=1.000000; Band=(10kHz .. 10MHz), Len=378[m], Err_S21dB:(E1=1.18%,E2=1.33%), Err_mix=0.0001683
[ASYMP.sqrt.rat]	Z0_inf=130.648571; VF=0.673159; Rs0=170.000000e-3; qL=1.781432; qH=0.719228; qX=0.846382; qY=1.115441; Phi=0.003920e-3; Fd=1.000000; Band=(10kHz .. 10MHz), Len=378[m], Err_S21dB:(E1=0.55%,E2=0.62%), Err_mix=0.0001250
[ASYMP.bessel]	Z0_inf=130.121347; VF=0.668153; Rs0=170.000000e-3; qL=1.667027; qH=0.757731; Phi=1.320525e-3; Fd=1.000000; Band=(10kHz .. 10MHz), Len=378[m], Err_S21dB:(E1=0.52%,E2=0.63%), Err_mix=0.0001360
[ASYMP.hyp]	Z0_inf=129.902623; VF=0.664494; Rs0=170.000000e-3; qL=1.612063; qH=0.791282; Phi=2.288347e-3; Fd=1.000000; Band=(10kHz .. 10MHz), Len=378[m], Err_S21dB:(E1=0.87%,E2=1.07%), Err_mix=0.0001677
[ASYMP.mix]	Z0_inf=130.741728; VF=0.673081; Rs0=170.000000e-3; qL=1.764346; qH=0.717959; Phi=0.010885e-3; Fd=1.000000; qB=0.428300 Band=(10kHz .. 10MHz), Len=378[m], Err_S21dB:(E1=0.42%,E2=0.51%), Err_mix=0.0001235

MQ_TelCable_30q	Loops\MQ_TelCable_30quad\2010_02_04_quad_2\ Name="quad 2", Length=378.000 [m], wire pair 2, diff(3-7 4-8)
[ASYMP.sqrt]	Z0_inf=130.529280; VF=0.673394; Rs0=169.000000e-3; qL=1.856076; qH=0.700148; Phi=0.000000e-3; Fd=1.000000; Band=(10kHz .. 10MHz), Len=378[m], Err_S21dB:(E1=1.25%,E2=1.42%), Err_mix=0.0001710
[ASYMP.sqrt.rat]	Z0_inf=130.525717; VF=0.672988; Rs0=169.000000e-3; qL=1.764049; qH=0.722307; qX=0.810638; qY=1.154892; Phi=0.013145e-3; Fd=1.000000 Band=(10kHz .. 10MHz), Len=378[m], Err_S21dB:(E1=0.49%,E2=0.57%), Err_mix=0.0001232
[ASYMP.bessel]	Z0_inf=130.126277; VF=0.668231; Rs0=169.000000e-3; qL=1.669674; qH=0.755228; Phi=1.296623e-3; Fd=1.000000 Band=(10kHz .. 10MHz), Len=378[m], Err_S21dB:(E1=0.50%,E2=0.62%), Err_mix=0.0001349
[ASYMP.hyp]	Z0_inf=129.444340; VF=0.659864; Rs0=169.000000e-3; qL=1.580709; qH=0.816992; Phi=3.516236e-3; Fd=1.000000 Band=(10kHz .. 10MHz), Len=378[m], Err_S21dB:(E1=0.75%,E2=0.88%), Err_mix=0.0001583
[ASYMP.mix]	Z0_inf=130.693124; VF=0.672979; Rs0=169.000000e-3; qL=1.764647; qH=0.716382; Phi=0.010869e-3; Fd=1.000000; qB=0.432182 Band=(10kHz .. 10MHz), Len=378[m], Err_S21dB:(E1=0.47%,E2=0.56%), Err_mix=0.0001244

### 5.4.3 Quad #5, 378m

MQ_TelCable_30q	LoopsMQ_TelCable_30quad\2010_02_04_quad_5\ Name="quad 5", Length=378.000 [m], wire pair 1, diff(1-5 2-6)
[ASYMP.sqrt]	Z0_inf=134.759146; VF=0.677618; Rs0=170.700000e-3; qL=1.833362; qH=0.706222; Phi=0.319882e-3; Fd=1.000000 Band=(10kHz .. 10MHz), Len=378[m], Err_S21dB:(E1=1.40%,E2=1.59%), Err_mix=0.0002086
[ASYMP.sqrt.rat]	Z0_inf=134.579759; VF=0.674795; Rs0=170.700000e-3; qL=1.694756; qH=0.748945; qX=0.743244; qY=1.242665; Phi=0.927541e-3; Fd=1.000000 Band=(10kHz .. 10MHz), Len=378[m], Err_S21dB:(E1=0.51%,E2=0.63%), Err_mix=0.0001586
[ASYMP.bessel]	Z0_inf=134.257242; VF=0.671299; Rs0=170.700000e-3; qL=1.639755; qH=0.767998; Phi=1.857306e-3; Fd=1.000000 Band=(10kHz .. 10MHz), Len=378[m], Err_S21dB:(E1=0.55%,E2=0.66%), Err_mix=0.0001661
[ASYMP.hyp]	Z0_inf=133.811610; VF=0.665797; Rs0=170.700000e-3; qL=1.570190; qH=0.814400; Phi=3.313799e-3; Fd=1.000000 Band=(10kHz .. 10MHz), Len=378[m], Err_S21dB:(E1=0.78%,E2=0.90%), Err_mix=0.0001846
[ASYMP.mix]	Z0_inf=134.526005; VF=0.674593; Rs0=170.700000e-3; qL=1.705228; qH=0.741227; Phi=1.015589e-3; Fd=1.000000; qB=0.517773 Band=(10kHz .. 10MHz), Len=378[m], Err_S21dB:(E1=0.58%,E2=0.70%), Err_mix=0.0001609

MQ_TelCable_30q	LoopsMQ_TelCable_30quad\2010_02_04_quad_5\ Name="quad 5", Length=378.000 [m], wire pair 2, diff(3-7 4-8)
[ASYMP.sqrt]	Z0_inf=133.419498; VF=0.678091; Rs0=170.000000e-3; qL=1.808778; qH=0.710935; Phi=0.283682e-3; Fd=1.000000 Band=(10kHz .. 10MHz), Len=378[m], Err_S21dB:(E1=1.35%,E2=1.49%), Err_mix=0.0002070
[ASYMP.sqrt.rat]	Z0_inf=133.405002; VF=0.678573; Rs0=170.000000e-3; qL=1.716534; qH=0.730892; qX=0.799088; qY=1.168938; Phi=0.060949e-3; Fd=1.000000 Band=(10kHz .. 10MHz), Len=378[m], Err_S21dB:(E1=0.49%,E2=0.59%), Err_mix=0.0001529
[ASYMP.bessel]	Z0_inf=133.049738; VF=0.674725; Rs0=170.000000e-3; qL=1.635491; qH=0.757896; Phi=1.062722e-3; Fd=1.000000 Band=(10kHz .. 10MHz), Len=378[m], Err_S21dB:(E1=0.54%,E2=0.64%), Err_mix=0.0001687
[ASYMP.hyp]	Z0_inf=132.736701; VF=0.670896; Rs0=170.000000e-3; qL=1.578488; qH=0.793366; Phi=2.056457e-3; Fd=1.000000 Band=(10kHz .. 10MHz), Len=378[m], Err_S21dB:(E1=0.85%,E2=1.04%), Err_mix=0.0002001
[ASYMP.mix]	Z0_inf=133.361145; VF=0.678143; Rs0=170.000000e-3; qL=1.709399; qH=0.729153; Phi=0.196901e-3; Fd=1.000000; qB=0.473781 Band=(10kHz .. 10MHz), Len=378[m], Err_S21dB:(E1=0.46%,E2=0.57%), Err_mix=0.0001542

### 5.4.4 Virtual loop section of 6 × 378m in cascade

By evaluating a mathematical cascade of the six wire pairs being measured, a two-port “measurement” of 6×378m = 2268m is emulated.

MQ_TelCable_30q	LoopsMQ_TelCable_30quad\2010_01_27 Name="casc:2*(q1,q2,q5)", Length=2268.000 [m], 2-port parameters
[ASYMP.sqrt]	Z0_inf=132.350917; VF=0.675774; Rs0=170.500000e-3; qL=1.871028; qH=0.701937; Phi=0.005175e-3; Fd=1.000000 Band=(10kHz .. 10MHz), Len=2268[m], Err_S21dB:(E1=1.12%,E2=1.25%), Err_mix=0.0001474
[ASYMP.sqrt.rat]	Z0_inf=132.348256; VF=0.675449; Rs0=170.500000e-3; qL=1.789725; qH=0.725776; qX=0.799306; qY=1.030832; Phi=0.005222e-3; Fd=1.000000 Band=(10kHz .. 10MHz), Len=2268[m], Err_S21dB:(E1=0.39%,E2=0.56%), Err_mix=0.0000989
[ASYMP.bessel]	Z0_inf=131.879170; VF=0.669967; Rs0=170.500000e-3; qL=1.676987; qH=0.760143; Phi=1.447322e-3; Fd=1.000000 Band=(10kHz .. 10MHz), Len=2268[m], Err_S21dB:(E1=0.75%,E2=0.93%), Err_mix=0.0001264
[ASYMP.hyp]	Z0_inf=131.567028; VF=0.666431; Rs0=170.500000e-3; qL=1.619331; qH=0.794170; Phi=2.409237e-3; Fd=1.000000 Band=(10kHz .. 10MHz), Len=2268[m], Err_S21dB:(E1=1.13%,E2=1.36%), Err_mix=0.0001629
[ASYMP.mix]	Z0_inf=132.301728; VF=0.675370; Rs0=170.500000e-3; qL=1.777906; qH=0.718488; Phi=0.049967e-3; Fd=1.000000; qB=0.403924 Band=(10kHz .. 10MHz), Len=2268[m], Err_S21dB:(E1=0.42%,E2=0.59%), Err_mix=0.0001005

## 5.5 Common reference model for this cable

All asymptotic models in the previous section are predicting the measured cable characteristics very close, and the models [ASYMP.sqrt.rat], [ASYMP.bessel] and [ASYMP.mix] are providing the closest match. However, the tiny improvement of these model may not justify the additional complexity over the simplest one of this subset being [ASYMP.sqrt.rat], and therefore that one is the preferred choice for modeling this cable.

Since the reference model should describe any wire pair of this cable type, its parameter values should be a pragmatic average of the values extracted for each section. The mathematical cascade of the six wire pairs being measured can serve as such average  
Therefore the following asymptotic model is proposed to serve as reference model for this cable type:

MQ TelCable_30q	Parameters of reference model
[ASYMP.sqrt.rat]	Z0_inf=132.348256; VF=0.675449; Rs0=170.500000e-3; qL=1.789725; qH=0.725776; qX=0.799306; qY=1.030832; Phi=0.005222e-3; Fd=1.000000

*Model, with square root of rational function, 8+1 parameters*

$[Z_s, Y_p] = \text{Model}(Z_{0L}, \eta_{VF}, R_{s0}, q_L, q_H, q_x, q_y, f, f_d)$
$Z_s(j\omega) = j\omega \cdot L_{s\infty} + R_{s0} \times \left( 1 - q_s \cdot q_x + \text{sqrt} \left( q_s^2 \cdot q_x^2 + 2 \cdot \frac{j\omega}{w_s} \cdot \left( \frac{q_s^2 + j\omega/w_s \cdot q_y}{q_s^2/q_x + j\omega/w_s \cdot q_y} \right) \right) \right)$ $Y_p(j\omega) = j\omega \cdot C_{p0} \times \left( 1 + \frac{j\omega}{w_d} \right)^{-2 \cdot f/p}$

Where:

$$L_{s\infty} = \frac{1}{h_{VF} \cdot c_0} \times Z_{0\infty}$$

$$C_{p0} = \frac{1}{h_{VF} \cdot c_0} \times \frac{1}{Z_{0\infty}}$$

$$q_s = \frac{1}{q_H \cdot q_L}$$

$$w_s = q_H^2 \cdot w_{s0} = q_H^2 \cdot \left( \frac{4p \cdot R_{s0}}{m_0} \right)$$

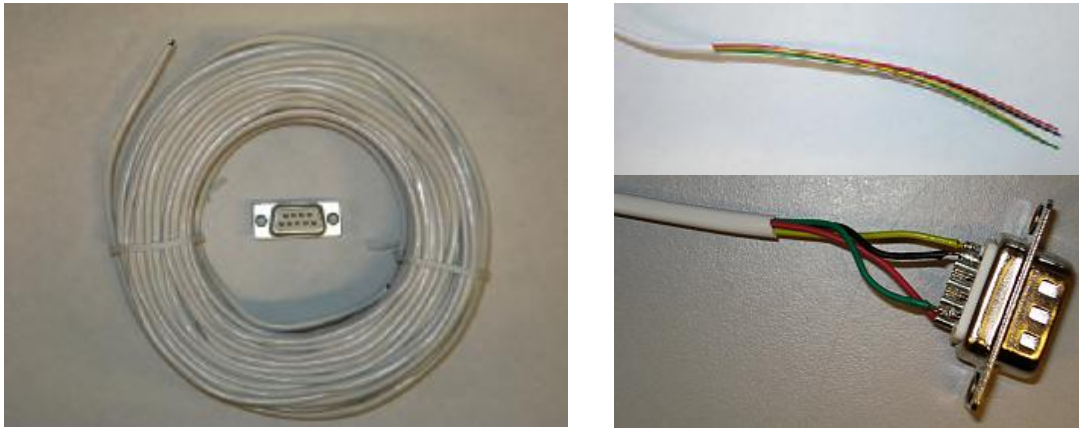
$$w_d = 2p \cdot f_d$$

$$c_0 = 3 \cdot 10^8 \text{ [m/s]}$$

$$m_0 = 4\pi \cdot 10^{-7} \text{ [H/m].}$$

## 6 MODELING LOW QUALITY CABLING FOR TELEPHONY

Another cable being modeled is the kind of cabling found in consumer shops (“Gamma” in this example), being sold as “telephony cabling”. In general these cables are of undefined quality. Due to the lack of any twisting, and due to the irregular geometry of the distance between the wires, it may not be of any surprise that the quality of this cabling is very low. Further details are described in [\*].



We extracted parameter values for different wire-pairs of this cable (all 50m long), for each shaping function of the proposed models. The results are very similar and therefore we show them only for wirepair #1 using model [ASYMP.sqrt.rat], based on the shaping functions  $Q_{Z,\text{sqrt.rat}}(j\omega)$  and  $Q_{Y,1}(j\omega)$ .

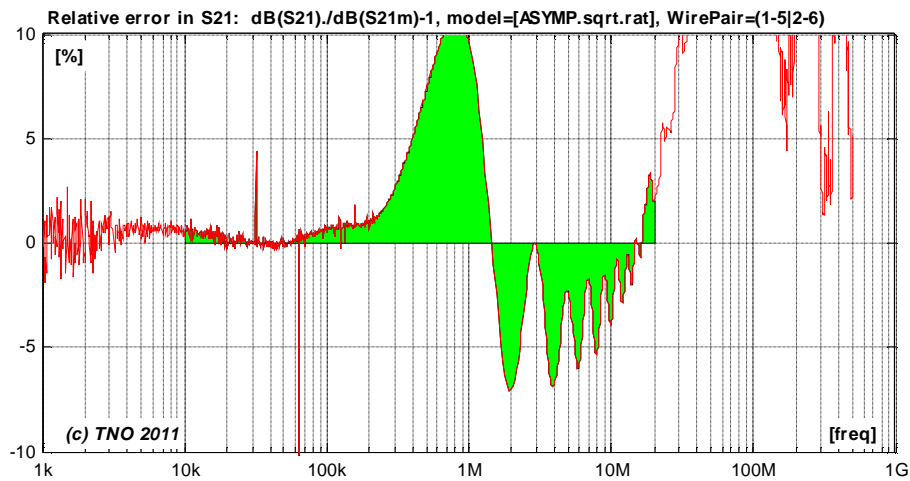
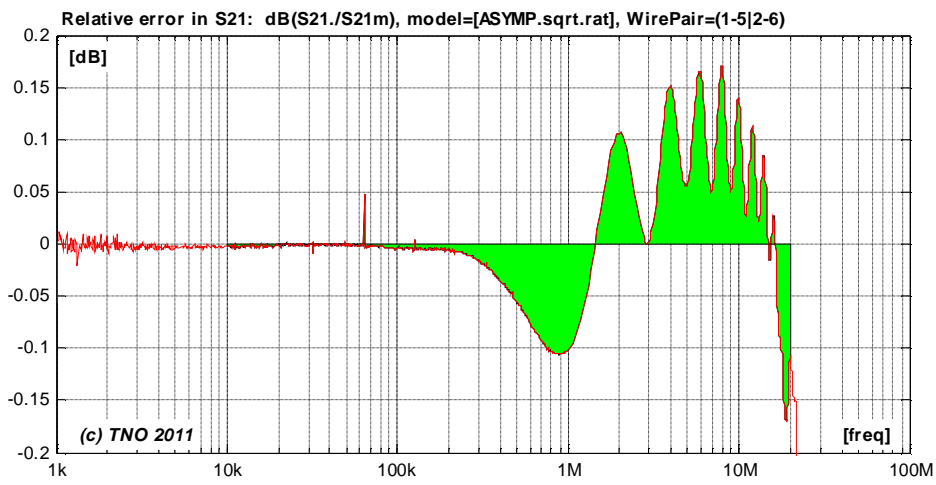
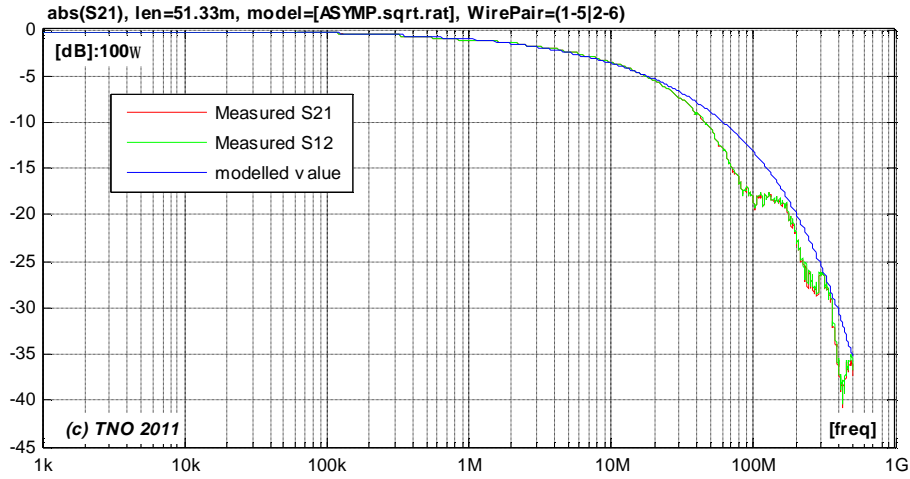
### 6.1 Match with two-port parameters

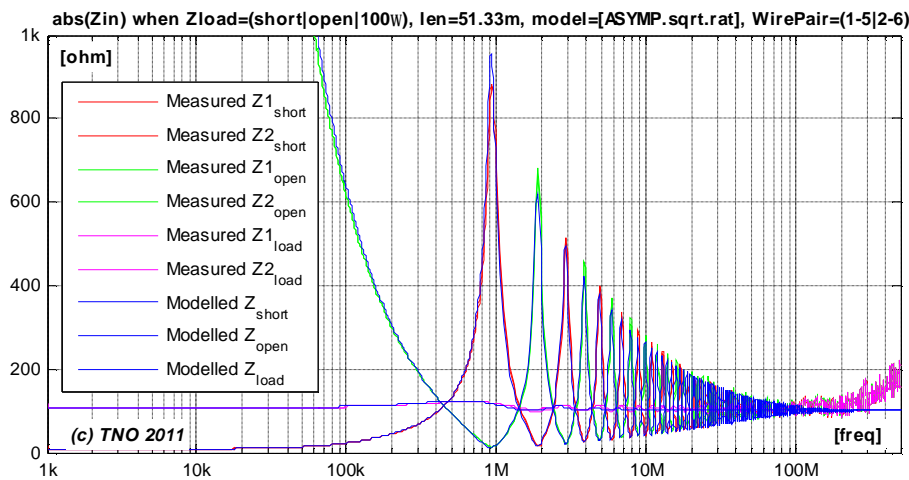
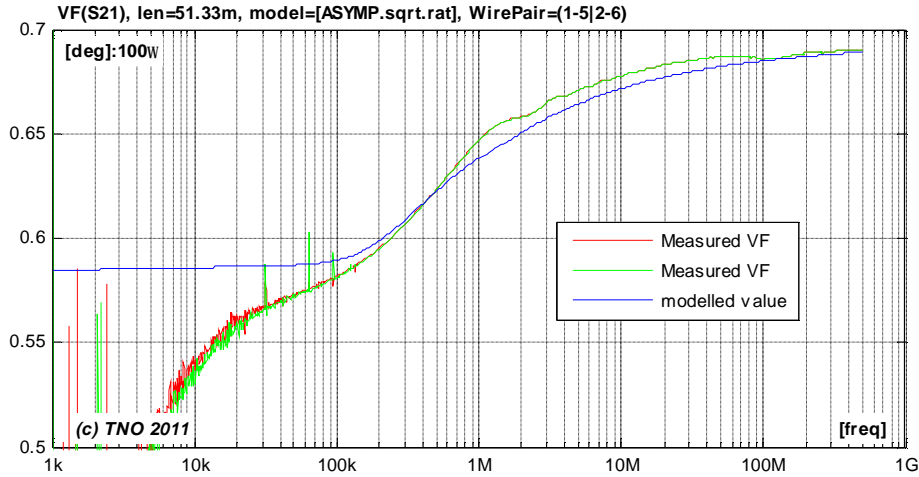
Figure [\*] to [\*] show for the same wire pair how close the two-port cable parameters of the model are matching the values calculated from the measurements.

- $S_{21}=S_{12}$  represents the transmission through the cable when terminated and powered from  $100\Omega$ .
- The velocity factor  $h_{VF}$  (or simply VF) is essentially another way to express the phase of  $S_{21}$ . It represents the traveling speed of signals through the cable, as a percentage of the speed of light.
- The input impedances are evaluated for different termination impedances: a short, a load of  $100\Omega$  and an open end.

The cable transfer measurements show some resonant behavior near 100, 270 and 420MHz, which is currently not well understood. Above 40MHz the transmission becomes a bit random in nature, which is assumed to be caused by the imperfect homogeneous construction of the twisted-pair cable. Those aspects can never be covered by a perfect homogeneous model.

But if these notches are modeled separately in a deterministic manner and if the model is augmented with random variations above 30 MHz, then the result may be applicable to hundreds of MHz. Such a refinement is left for further study.





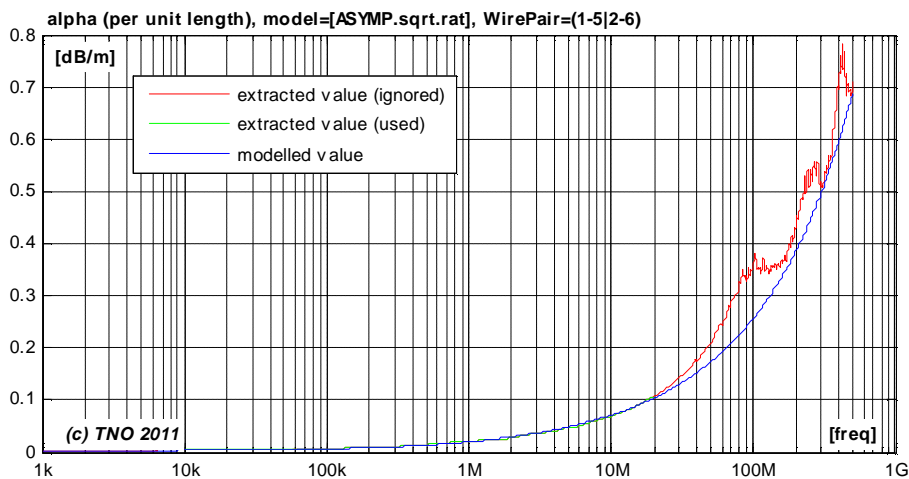
## 6.2 Match with secondary cable parameters (per unit length)

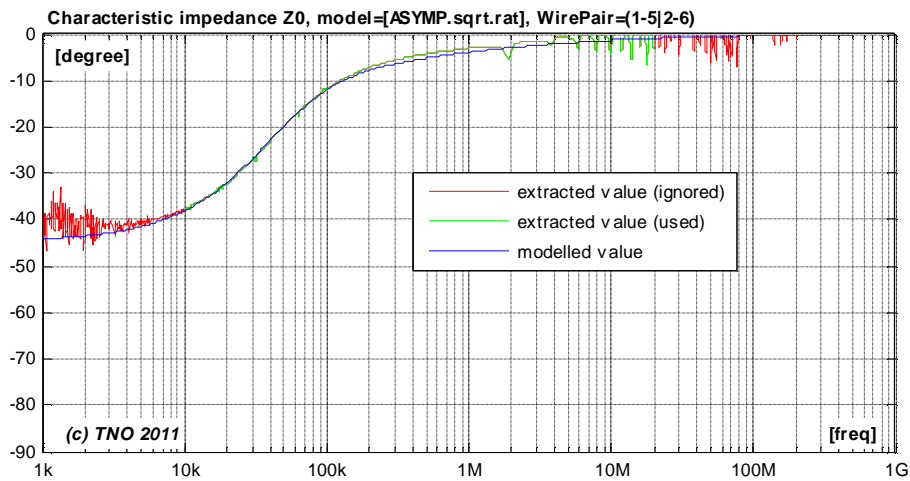
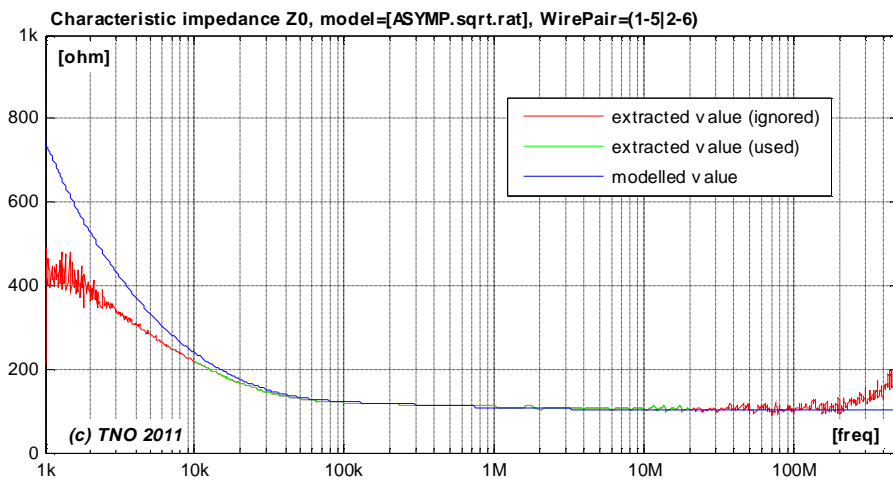
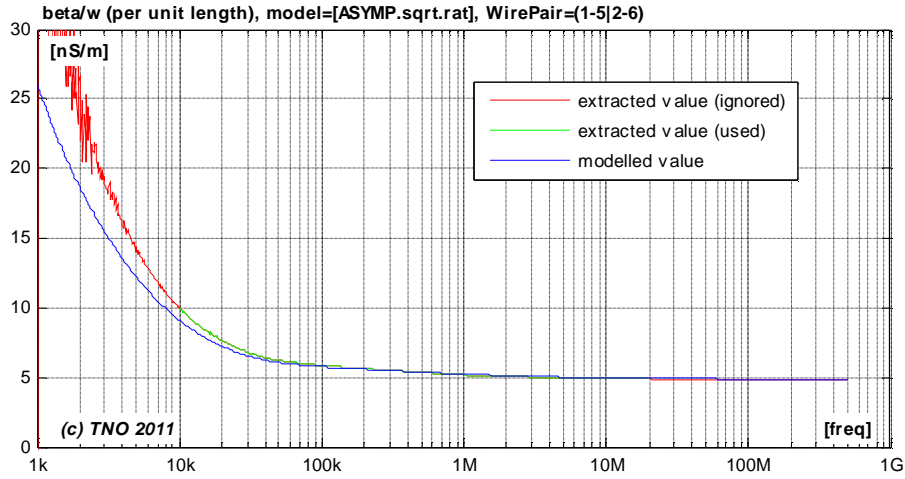
Figure [\*] to [\*] show for the same wire pair how close the secondary cable parameters ( $a$ ,  $b$ ,  $Z_0$ ) of the model are matching the values calculated from the measurements.

$$g(w) = \sqrt{Z_s(w) \cdot Y_p(w)}$$

where  $a(w) = \text{real}\{g(w)\}$  and  $b(w) = \text{imag}\{g(w)\}$

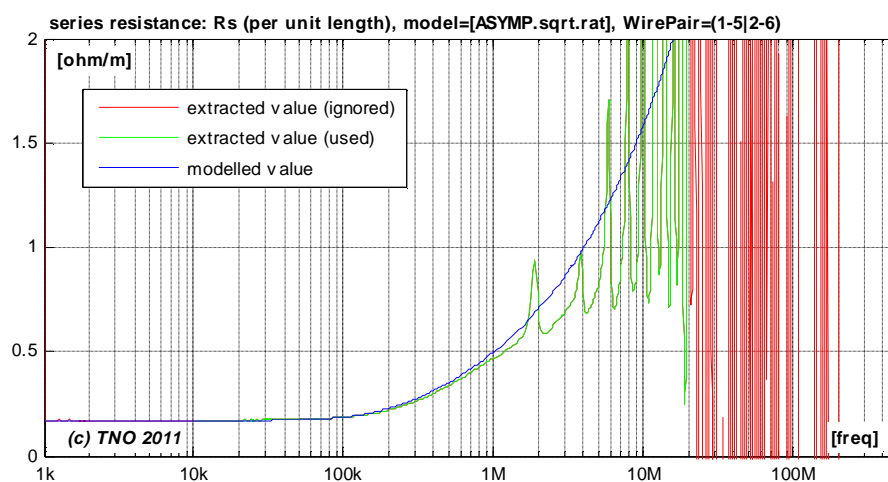
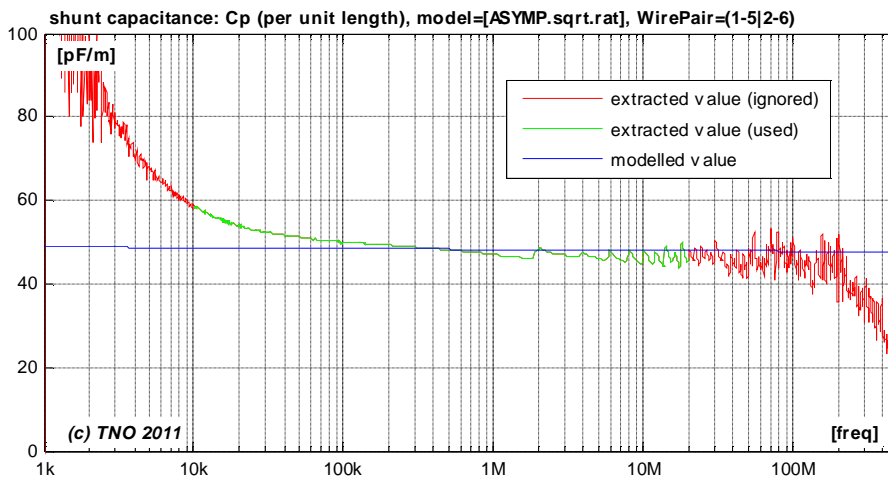
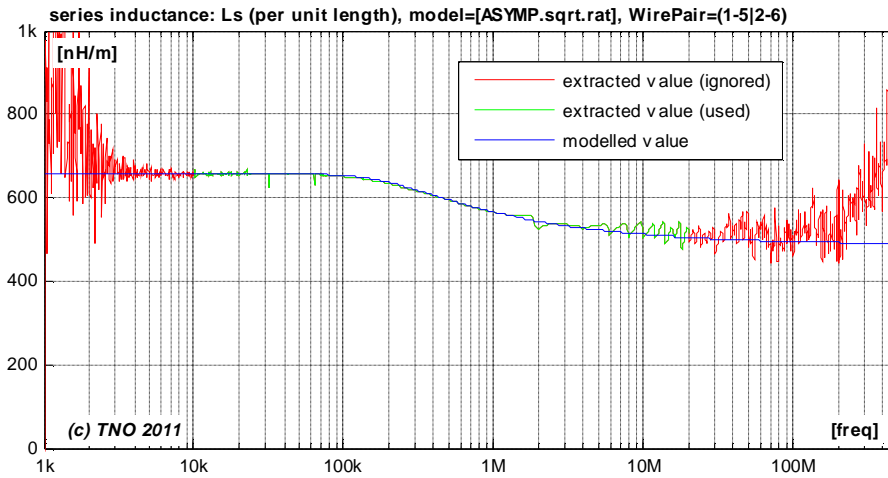
$$Z_0(w) = \sqrt{Z_s(w) / Y_p(w)}$$

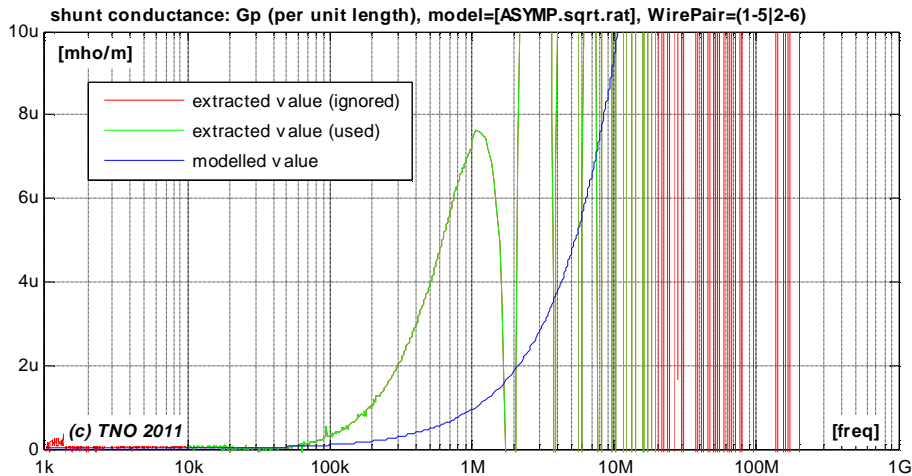




### 6.3 Match with primary cable parameters (per unit length)

Figure [\*] to [\*] show how close the primary cable parameters ( $L_s$ ,  $C_p$ ,  $R_s$ ,  $G_p$ ) of the model are matching the values calculated from the measurements.





## 6.4 Extracted parameters for various models and sections

### 6.4.1 Loop section of 50m

LQ_Gamma	Loops\LQ_GAMMA\2009_01_29_50m\ Name="50 m", Length=51.330 [m], wire pair 1, diff(1-5 2-6)
[ASYMP.sqrt]	Z0_inf=98.360020; VF=0.673560; Rs0=170.600000e-3; qL=1.700000; qH=0.650000; Phi=4.352154e-3; Fd=1.000000 Band=(10kHz .. 20MHz), Len=51.33[m], Err_S21dB:(E1=3.29%,E2=5.58%), Err_mix=0.0005910
[ASYMP.sqrt.rat]	Z0_inf=99.108537; VF=0.678032; Rs0=170.600000e-3; qL=1.700000; qH=0.650000; qX=0.767736; qY=1.499999; Phi=3.113495e-3; Fd=1.000000 Band=(10kHz .. 20MHz), Len=51.33[m], Err_S21dB:(E1=2.52%,E2=3.90%), Err_mix=0.0005432
[ASYMP.bessel]	Z0_inf=99.185757; VF=0.678458; Rs0=170.600000e-3; qL=1.700000; qH=0.650000; Phi=3.002227e-3; Fd=1.000000 Band=(10kHz .. 20MHz), Len=51.33[m], Err_S21dB:(E1=2.59%,E2=3.67%), Err_mix=0.0005393
[ASYMP.hyp]	Z0_inf=99.458729; VF=0.680066; Rs0=170.600000e-3; qL=1.700000; qH=0.649999; Phi=2.569681e-3; Fd=1.000000 Band=(10kHz .. 20MHz), Len=51.33[m], Err_S21dB:(E1=2.67%,E2=3.44%), Err_mix=0.0005521
[ASYMP.mix]	Z0_inf=99.112534; VF=0.678064; Rs0=170.600000e-3; qL=1.700000; qH=0.650000; Phi=3.110619e-3; Fd=1.000000; qB=0.683898 Band=(10kHz .. 20MHz), Len=51.33[m], Err_S21dB:(E1=2.69%,E2=3.82%), Err_mix=0.0005424

LQ_Gamma	Loops\LQ_GAMMA\2009_01_29_50m\ Name="50 m", Length=51.330 [m], wire pair 2, diff(3-7 4-8)
[ASYMP.sqrt]	Z0_inf=97.337557; VF=0.678768; Rs0=171.000000e-3; qL=1.700000; qH=0.650000; Phi=4.325711e-3; Fd=1.000000 Band=(10kHz .. 20MHz), Len=51.33[m], Err_S21dB:(E1=3.15%,E2=5.00%), Err_mix=0.0005492
[ASYMP.sqrt.rat]	Z0_inf=98.006632; VF=0.682795; Rs0=171.000000e-3; qL=1.700000; qH=0.649996; qX=0.793131; qY=1.499999; Phi=3.213621e-3; Fd=1.000000 Band=(10kHz .. 20MHz), Len=51.33[m], Err_S21dB:(E1=2.27%,E2=3.52%), Err_mix=0.0005108
[ASYMP.bessel]	Z0_inf=98.155977; VF=0.683750; Rs0=171.000000e-3; qL=1.700000; qH=0.650000; Phi=2.971606e-3; Fd=1.000000 Band=(10kHz .. 20MHz), Len=51.33[m], Err_S21dB:(E1=2.24%,E2=3.16%), Err_mix=0.0005084
[ASYMP.hyp]	Z0_inf=98.416863; VF=0.685400; Rs0=171.000000e-3; qL=1.699997; qH=0.650000; Phi=2.519088e-3; Fd=1.000000 Band=(10kHz .. 20MHz), Len=51.33[m], Err_S21dB:(E1=2.28%,E2=2.99%), Err_mix=0.0005249
[ASYMP.mix]	Z0_inf=98.002694; VF=0.682882; Rs0=171.000000e-3; qL=1.699997; qH=0.650000; Phi=3.211455e-3; Fd=1.000000; qB=0.608307 Band=(10kHz .. 20MHz), Len=51.33[m], Err_S21dB:(E1=2.42%,E2=3.41%), Err_mix=0.0005093

### 6.4.2 Virtual loop section of 2´50m in cascade

By evaluating a mathematical cascade of the two wire pairs being measured, a two-port “measurement” of 2x50m = 100m is emulated.

LQ_Gamma	Loops\LQ_GAMMA\2009_01_29_50m\
[ASYMP.sqrt]	Z0_inf=97.652129; VF=0.676733; Rs0=170.800000e-3; qL=1.700000; qH=0.650000; Phi=4.215157e-3; Fd=1.000000 Band=(10kHz .. 20MHz), Len=102.66[m], Err_S21dB:(E1=3.25%,E2=5.28%), Err_mix=0.0005682
[ASYMP.sqrt.rat]	Z0_inf=98.369783; VF=0.681182; Rs0=170.800000e-3; qL=1.700000; qH=0.650000; qX=0.777307; qY=1.500000; Phi=3.023930e-3; Fd=1.000000 Band=(10kHz .. 20MHz), Len=102.66[m], Err_S21dB:(E1=2.52%,E2=3.82%), Err_mix=0.0005230
[ASYMP.bessel]	Z0_inf=98.494574; VF=0.681572; Rs0=170.800000e-3; qL=1.698995; qH=0.650000; Phi=2.920440e-3; Fd=1.000000 Band=(10kHz .. 20MHz), Len=102.66[m], Err_S21dB:(E1=2.60%,E2=3.60%), Err_mix=0.0005195
[ASYMP.hyp]	Z0_inf=98.730794; VF=0.683436; Rs0=170.800000e-3; qL=1.700000; qH=0.650000; Phi=2.404522e-3; Fd=1.000000 Band=(10kHz .. 20MHz), Len=102.66[m], Err_S21dB:(E1=2.68%,E2=3.49%), Err_mix=0.0005330
[ASYMP.mix]	Z0_inf=98.396627; VF=0.681125; Rs0=170.800000e-3; qL=1.700000; qH=0.650000; Phi=3.031579e-3; Fd=1.000000; qB=0.656508 Band=(10kHz .. 20MHz), Len=102.66[m], Err_S21dB:(E1=2.71%,E2=3.80%), Err_mix=0.0005215

## 6.5 Common reference model for this cable

All asymptotic models in the previous section are predicting the measured cable characteristics very close, and the models [ASYMP.sqrt.rat], [ASYMP.bessel] and [ASYMP.mix] are providing the closest match. However, the tiny improvement within this set of models may not justify the additional complexity over the simplest one of this subset being [ASYMP.sqrt.rat]. Therefore that one is the preferred choice for modeling this cable.

Since the reference model should describe any wire pair of this cable type, its parameter values should be a pragmatic average of the values extracted for each wire pair. The mathematical cascade of the two wire pairs being measured can serve as such average. Therefore the following asymptotic model is proposed to serve as reference model for this cable type:

LQ_Gamma	Parameters of reference model
[ASYMP.sqrt.rat]	Z0_inf=98.369783; VF=0.681182; Rs0=170.800000e-3; qL=1.700000; qH=0.650000; qX=0.777307; qY=1.500000; Phi=3.023930e-3; Fd=1.000000

Model, with square root of rational function, 8+1 parameters

$$[Z_s, Y_p] = \text{Model}(Z_{0L}, \eta_{VF}, R_{s0}, q_L, q_H, q_x, q_y, f, f_d)$$

$$Z_s(j\omega) = j\omega \cdot L_{s\infty} + R_{s0} \times \left( 1 - q_s \cdot q_x + \text{sqrt} \left( q_s^2 \cdot q_x^2 + 2 \cdot \frac{j\omega}{w_s} \cdot \left( \frac{q_s^2 + j\omega/w_s \cdot q_y}{q_s^2/q_x + j\omega/w_s \cdot q_y} \right) \right) \right)$$

$$Y_p(j\omega) = j\omega \cdot C_{p0} \times \left( 1 + \frac{j\omega}{w_d} \right)^{-2 \cdot f/p}$$

Where:

$$L_{s\infty} = \frac{1}{h_{VF} \cdot c_0} \times Z_{0\infty}$$

$$C_{p0} = \frac{1}{h_{VF} \cdot c_0} \times \frac{1}{Z_{0\infty}}$$

$$q_s = \frac{1}{q_H \cdot q_L}$$

$$w_s = q_H^2 \cdot w_{s0} = q_H^2 \cdot \left( \frac{4p \cdot R_{s0}}{m_0} \right)$$

$$w_d = 2p \cdot f_d$$

$$c_0 = 3 \cdot 10^8 \text{ [m/s]}$$

$$m_0 = 4\pi \cdot 10^{-7} \text{ [H/m]}$$

## 7 MODELING KPN ACCES CABLING FOR TELEPHONY

Another cable being modeled a cable with many twisted quads (each with two wire pairs or 4 wires) and a common shielding. It is a cable with medium quality twists, so that crosstalk between other wire pairs is kept to a minimum. This cabling is typically within the Netherlands by KPN for offering telephony services, and the cable can be found underground as well as in buildings. Further details are to be described in an update of [\*].

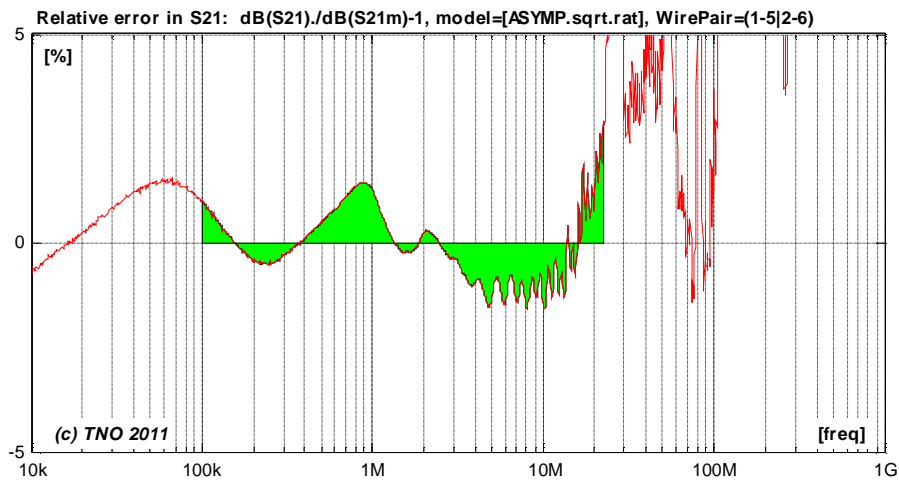
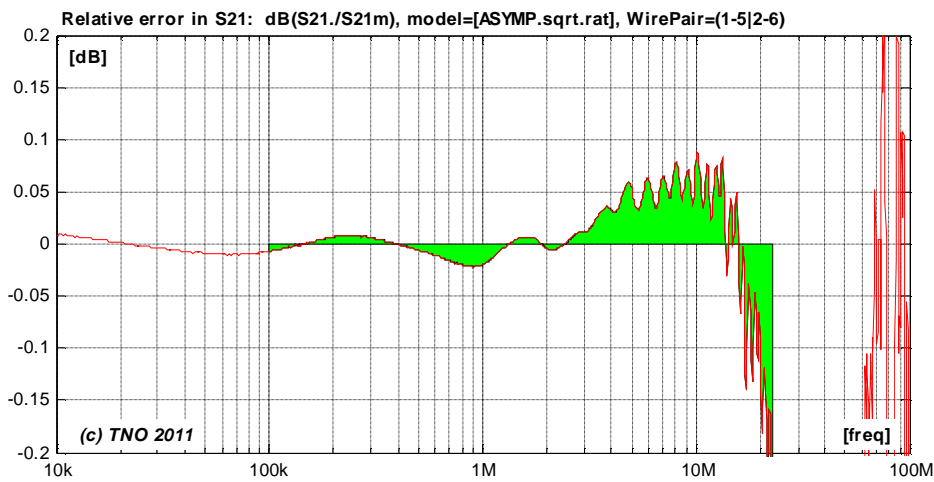
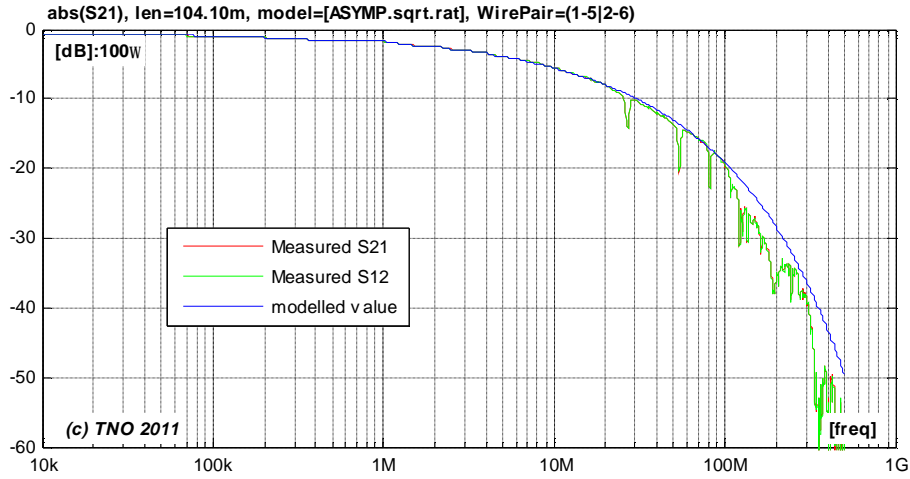


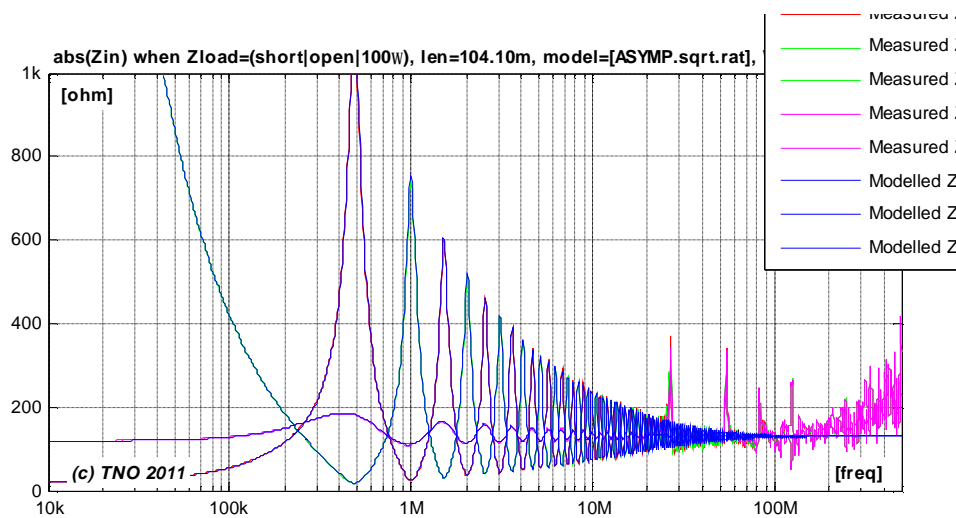
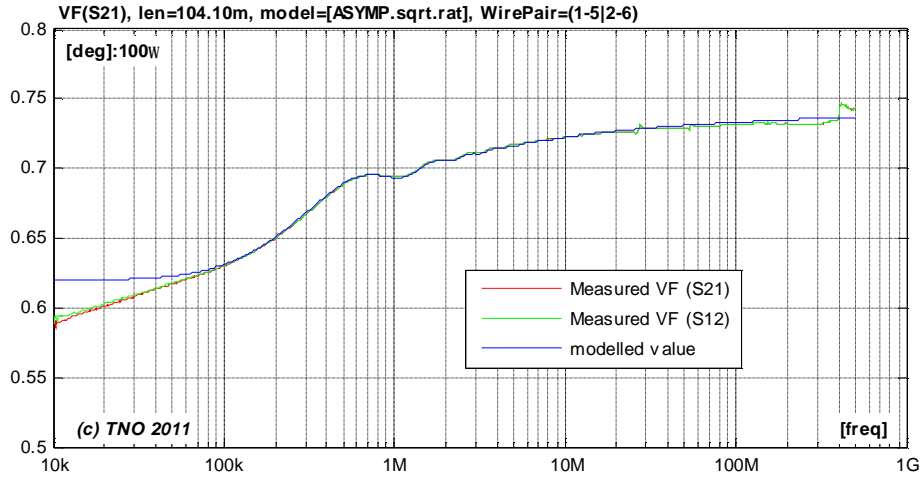
### 7.1 Match with two-port parameters

Figure [\*] to [\*] show for the same wire pair how close the two-port cable parameters of the model are matching the values calculated from the measurements.

- $S_{21}=S_{12}$  represents the transmission through the cable when terminated and powered from  $100\Omega$ .
- The velocity factor  $v_{VF}$  (or simply VF) is essentially another way to express the phase of  $S_{21}$ . It represents the traveling speed of signals through the cable, as a percentage of the speed of light.
- The input impedances are evaluated for different termination impedances: a short, a load of  $100\Omega$  and an open end.

The cable transfer measurements show some resonant behavior near 27, 54 and 81.5MHz, which is currently not well understood. If these notches are modeled separately in a deterministic manner the result may be considered as very good up to 100 MHz. Above 100MHz the transmission becomes a bit random in nature, which is assumed to be caused by the imperfect homogeneous construction of the twisted-pair cable. Those aspects can never be covered by a perfect homogeneous model but if the model is augmented with random variations above 100 MHz, then the result may be applicable to hundreds of MHz. Such a refinement is left for further study.





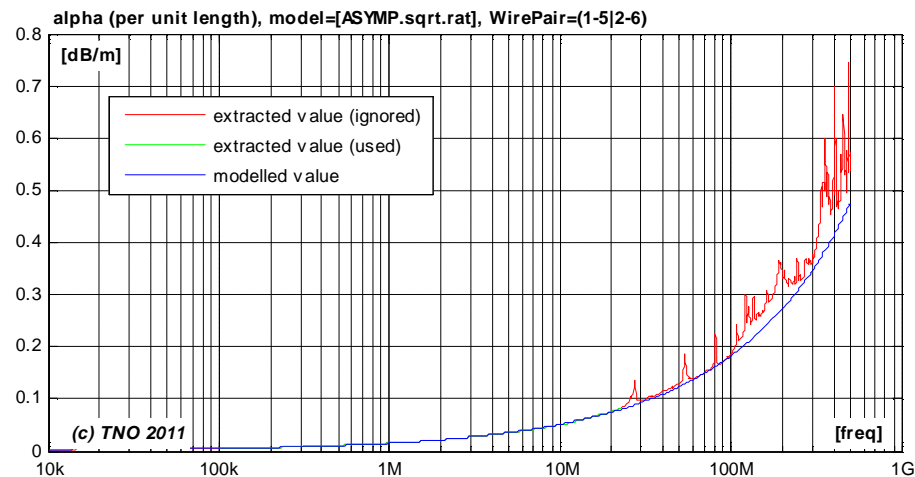
## 7.2 Match with secondary cable parameters (per unit length)

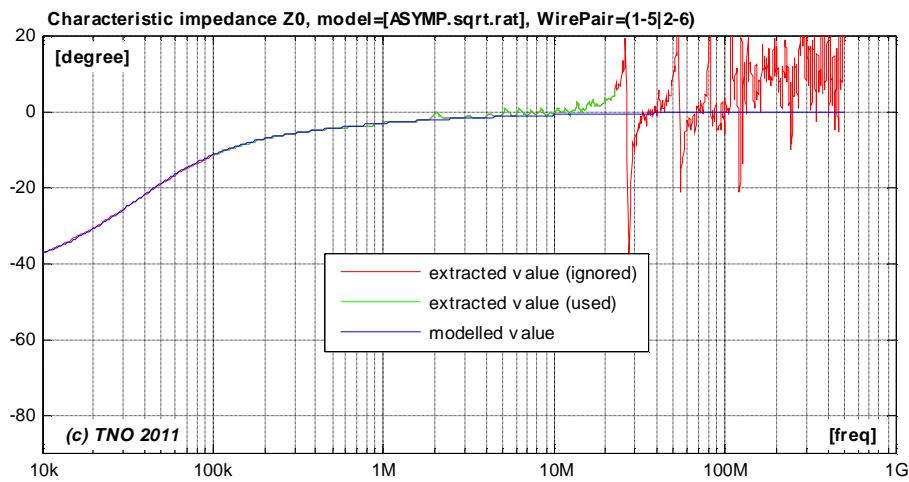
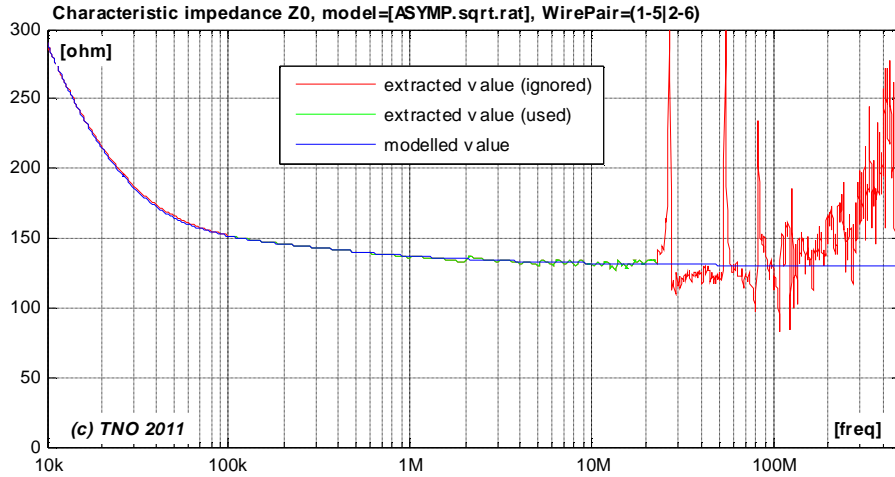
Figure [\*] to [\*] show for the same wire pair how close the secondary cable parameters ( $a$ ,  $b$ ,  $Z_0$ ) of the model are matching the values calculated from the measurements.

$$g(w) = \sqrt{Z_s(w) \cdot Y_p(w)}$$

where  $a(w) = \text{real}\{g(w)\}$  and  $b(w) = \text{imag}\{g(w)\}$

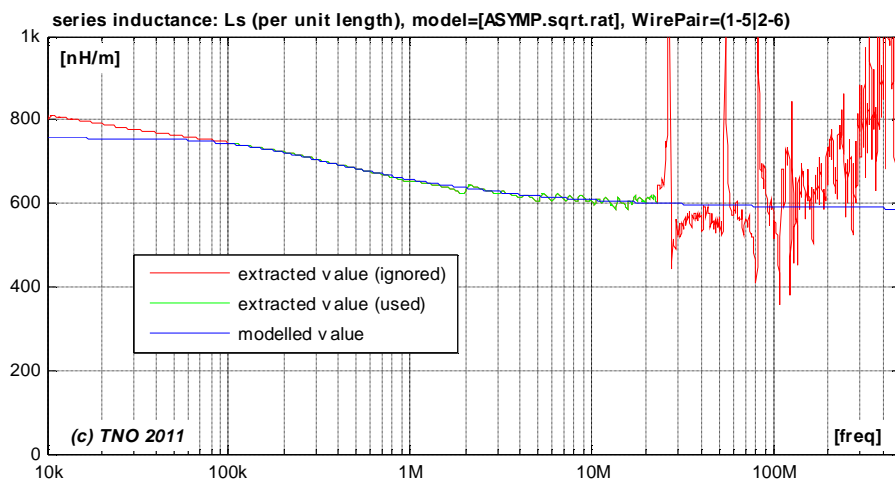
$$Z_0(w) = \sqrt{Z_s(w) / Y_p(w)}$$

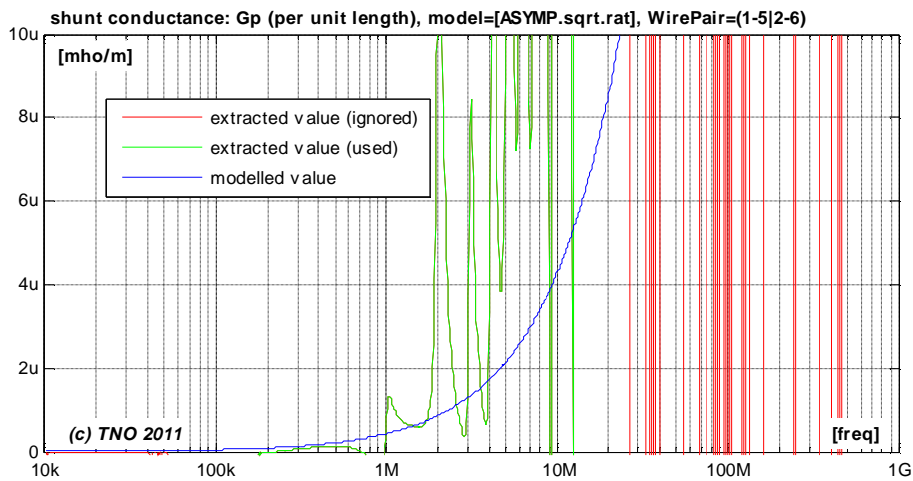
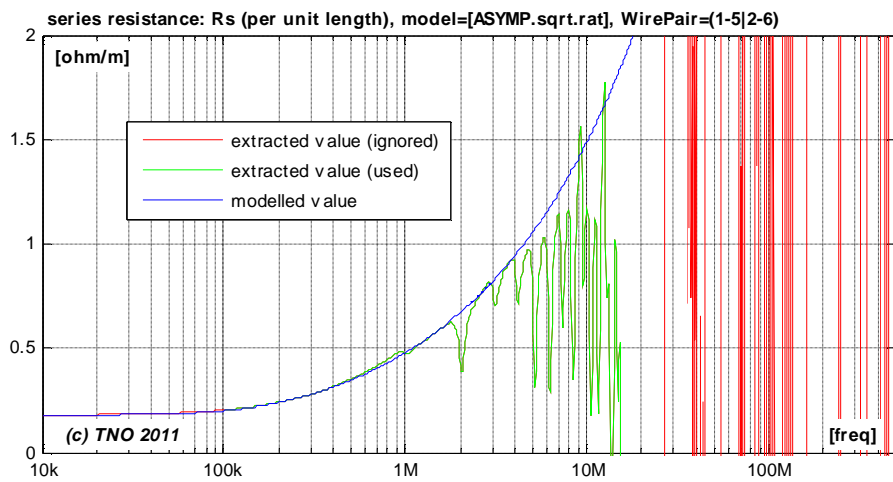
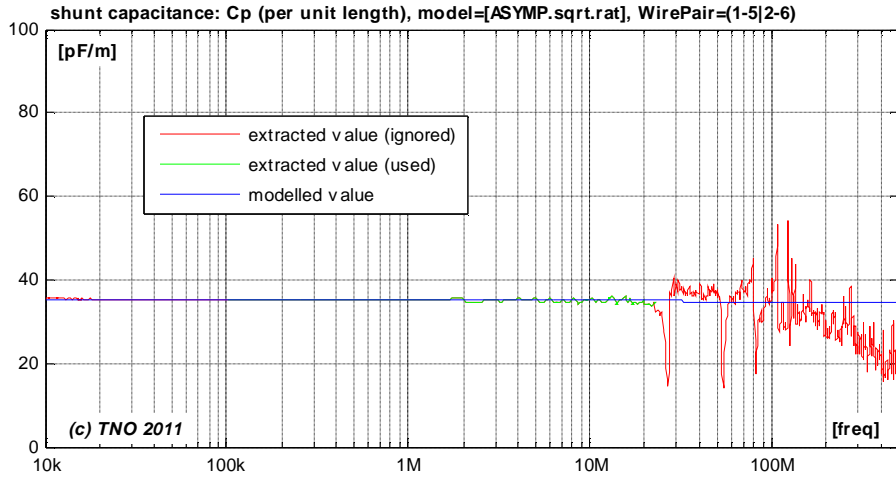




### 7.3 Match with primary cable parameters (per unit length)

Figure [\*] to [\*] show how close the primary cable parameters ( $L_s$ ,  $C_p$ ,  $R_s$ ,  $G_p$ ) of the model are matching the values calculated from the measurements.





## 7.4 Extracted parameters for various models and wire pairs

### 7.4.1 Individual wire pairs (104.1m)

KPN_acc	Loops\KPN_cable_100m\2011_04_12_in_quad\ Name="104 m, sloppy connections", Length=104.100 [m], wire pair 1, diff(1-5 2-6)
[ASYMP.sqrt]	Z0_inf=128.097249; VF=0.730647; Rs0=180.000000e-3; qL=1.776974; qH=0.700000; Phi=1.723894e-3; Fd=1.000000 Band=(100kHz .. 23MHz), Len=104.1[m], Err_S21dB:(E1=0.83%,E2=0.98%), Err_mix=0.0001806
[ASYMP.sqrt.rat]	Z0_inf=128.009539; VF=0.729667; Rs0=180.000000e-3; qL=1.716635; qH=0.709968; qX=0.928581; qY=1.350286; Phi=1.952262e-3; Fd=1.000000 Band=(100kHz .. 23MHz), Len=104.1[m], Err_S21dB:(E1=0.69%,E2=0.86%), Err_mix=0.0001682
[ASYMP.bessel]	Z0_inf=128.044496; VF=0.728462; Rs0=180.000000e-3; qL=1.600955; qH=0.729999; Phi=2.199294e-3; Fd=1.000000 Band=(100kHz .. 23MHz), Len=104.1[m], Err_S21dB:(E1=1.36%,E2=1.59%), Err_mix=0.0002119
[ASYMP.hyp]	Z0_inf=128.146542; VF=0.728133; Rs0=180.000000e-3; qL=1.570343; qH=0.740000; Phi=2.259818e-3; Fd=1.000000 Band=(100kHz .. 23MHz), Len=104.1[m], Err_S21dB:(E1=2.07%,E2=2.34%), Err_mix=0.0002840
[ASYMP.mix]	Z0_inf=128.035771; VF=0.729702; Rs0=180.000000e-3; qL=1.715401; qH=0.709940; Phi=1.946530e-3; Fd=1.000000; qB=0.213403 Band=(100kHz .. 23MHz), Len=104.1[m], Err_S21dB:(E1=0.64%,E2=0.81%), Err_mix=0.0001633

KPN_acc	Loops\KPN_cable_100m\2011_04_12_in_quad\ Name="104 m, sloppy connections", Length=104.100 [m], wire pair 2, diff(3-7 4-8)
[ASYMP.sqrt]	Z0_inf=128.992550; VF=0.733484; Rs0=180.000000e-3; qL=1.878735; qH=0.718636; Phi=1.092212e-3; Fd=1.000000 Band=(100kHz .. 23MHz), Len=104.1[m], Err_S21dB:(E1=0.91%,E2=1.08%), Err_mix=0.0002006
[ASYMP.sqrt.rat]	Z0_inf=128.883665; VF=0.732092; Rs0=180.000000e-3; qL=1.738748; qH=0.740000; qX=0.799140; qY=1.159570; Phi=1.359060e-3; Fd=1.000000 Band=(100kHz .. 23MHz), Len=104.1[m], Err_S21dB:(E1=0.39%,E2=0.52%), Err_mix=0.0001623
[ASYMP.bessel]	Z0_inf=128.781316; VF=0.731343; Rs0=180.000000e-3; qL=1.679316; qH=0.750000; Phi=1.552343e-3; Fd=1.000000 Band=(100kHz .. 23MHz), Len=104.1[m], Err_S21dB:(E1=0.62%,E2=0.96%), Err_mix=0.0001786
[ASYMP.hyp]	Z0_inf=128.645692; VF=0.729227; Rs0=180.000000e-3; qL=1.629254; qH=0.769972; Phi=2.032830e-3; Fd=1.000000 Band=(100kHz .. 23MHz), Len=104.1[m], Err_S21dB:(E1=1.08%,E2=1.53%), Err_mix=0.0002137
[ASYMP.mix]	Z0_inf=128.790756; VF=0.731949; Rs0=180.000000e-3; qL=1.739861; qH=0.739727; Phi=1.423810e-3; Fd=1.000000; qB=0.478880 Band=(100kHz .. 23MHz), Len=104.1[m], Err_S21dB:(E1=0.45%,E2=0.60%), Err_mix=0.0001647

KPN_acc	Loops\KPN_cable_100m\2011_04_13_in_quad\ Name="104 m, sloppy connections", Length=104.100 [m], wire pair 1, diff(1-5 2-6)
[ASYMP.sqrt]	Z0_inf=128.362817; VF=0.730930; Rs0=181.000000e-3; qL=1.777641; qH=0.701769; Phi=1.774774e-3; Fd=1.000000; Band=(100kHz .. 23MHz), Len=104.1[m], Err_S21dB:(E1=0.84%,E2=1.01%), Err_mix=0.0001727
[ASYMP.sqrt.rat]	Z0_inf=128.015993; VF=0.730409; Rs0=181.000000e-3; qL=1.725212; qH=0.710000; qX=0.937220; qY=1.499928; Phi=1.882539e-3; Fd=1.000000 Band=(100kHz .. 23MHz), Len=104.1[m], Err_S21dB:(E1=0.72%,E2=0.88%), Err_mix=0.0001586
[ASYMP.bessel]	Z0_inf=128.069486; VF=0.729376; Rs0=181.000000e-3; qL=1.607402; qH=0.730000; Phi=2.095960e-3; Fd=1.000000 Band=(100kHz .. 23MHz), Len=104.1[m], Err_S21dB:(E1=1.38%,E2=1.62%), Err_mix=0.0002108
[ASYMP.hyp]	Z0_inf=127.967350; VF=0.727345; Rs0=181.000000e-3; qL=1.568820; qH=0.750000; Phi=2.553904e-3; Fd=1.000000 Band=(100kHz .. 23MHz), Len=104.1[m], Err_S21dB:(E1=1.93%,E2=2.21%), Err_mix=0.0002617
[ASYMP.mix]	Z0_inf=128.048168; VF=0.730592; Rs0=181.000000e-3; qL=1.723555; qH=0.709868; Phi=1.858341e-3; Fd=1.000000; qB=0.199880 Band=(100kHz .. 23MHz), Len=104.1[m], Err_S21dB:(E1=0.66%,E2=0.84%), Err_mix=0.0001545

KPN_acc	Loops\KPN_cable_100m\2011_04_13_in_quad\ Name="104 m, sloppy connections", Length=104.100 [m], wire pair 2, diff(3-7 4-8)
[ASYMP.sqrt]	Z0_inf=129.036329; VF=0.733851; Rs0=180.000000e-3; qL=1.858274; qH=0.718387; Phi=1.081230e-3; Fd=1.000000 Band=(100kHz .. 23MHz), Len=104.1[m], Err_S21dB:(E1=0.93%,E2=1.10%), Err_mix=0.0001881
[ASYMP.sqrt.rat]	Z0_inf=128.928509; VF=0.732707; Rs0=180.000000e-3; qL=1.708993; qH=0.740000; qX=0.795307; qY=1.204047; Phi=1.343333e-3; Fd=1.000000 Band=(100kHz .. 23MHz), Len=104.1[m], Err_S21dB:(E1=0.41%,E2=0.56%), Err_mix=0.0001406
[ASYMP.bessel]	Z0_inf=128.810843; VF=0.731779; Rs0=180.000000e-3; qL=1.659287; qH=0.750000; Phi=1.535790e-3; Fd=1.000000 Band=(100kHz .. 23MHz), Len=104.1[m], Err_S21dB:(E1=0.59%,E2=0.94%), Err_mix=0.0001552
[ASYMP.hyp]	Z0_inf=128.677794; VF=0.729729; Rs0=180.000000e-3; qL=1.611634; qH=0.770000; Phi=1.999998e-3; Fd=1.000000 Band=(100kHz .. 23MHz), Len=104.1[m], Err_S21dB:(E1=1.05%,E2=1.51%), Err_mix=0.0001930
[ASYMP.mix]	Z0_inf=128.699252; VF=0.731347; Rs0=180.000000e-3; qL=1.704435; qH=0.747459; Phi=1.651742e-3; Fd=1.000000; qB=0.540237 Band=(100kHz .. 23MHz), Len=104.1[m], Err_S21dB:(E1=0.47%,E2=0.64%), Err_mix=0.0001438

KPN_acc	Loops\KPN_cable_100m\2011_04_12_out_quad\ Name="104 m, sloppy connections", Length=104.100 [m], wire pair 1, diff(1-5 2-6)
[ASYMP.sqrt]	Z0_inf=128.341127; VF=0.730797; Rs0=180.000000e-3; qL=1.769236; qH=0.698142; Phi=1.723227e-3; Fd=1.000000 Band=(100kHz .. 23MHz), Len=104.1[m], Err_S21dB:(E1=0.88%,E2=1.05%), Err_mix=0.0001835
[ASYMP.sqrt.rat]	Z0_inf=127.998158; VF=0.729849; Rs0=180.000000e-3; qL=1.690344; qH=0.710000; qX=0.911426; qY=1.479891; Phi=1.932238e-3; Fd=1.000000 Band=(100kHz .. 23MHz), Len=104.1[m], Err_S21dB:(E1=0.72%,E2=0.89%), Err_mix=0.0001644
[ASYMP.bessel]	Z0_inf=128.016934; VF=0.728483; Rs0=180.000000e-3; qL=1.589540; qH=0.729977; Phi=2.222165e-3; Fd=1.000000 Band=(100kHz .. 23MHz), Len=104.1[m], Err_S21dB:(E1=1.30%,E2=1.56%), Err_mix=0.0001991
[ASYMP.hyp]	Z0_inf=128.108733; VF=0.728222; Rs0=180.000000e-3; qL=1.560293; qH=0.740000; Phi=2.270081e-3; Fd=1.000000 Band=(100kHz .. 23MHz), Len=104.1[m], Err_S21dB:(E1=2.01%,E2=2.29%), Err_mix=0.0002699
[ASYMP.mix]	Z0_inf=127.849641; VF=0.728304; Rs0=180.000000e-3; qL=1.685004; qH=0.720000; Phi=2.287921e-3; Fd=1.000000; qB=0.289900 Band=(100kHz .. 23MHz), Len=104.1[m], Err_S21dB:(E1=0.62%,E2=0.78%), Err_mix=0.0001496

KPN_acc	Loops\KPN_cable_100m\2011_04_12_out_quad\ Name="104 m, sloppy connections", Length=104.100 [m], wire pair 2, diff(3-7 4-8)
[ASYMP.sqrt]	Z0_inf=122.789185; VF=0.723361; Rs0=180.000000e-3; qL=1.865213; qH=0.740000; Phi=1.985993e-3; Fd=1.000000 Band=(100kHz .. 23MHz), Len=104.1[m], Err_S21dB:(E1=1.18%,E2=1.41%), Err_mix=0.0002160
[ASYMP.sqrt.rat]	Z0_inf=122.776078; VF=0.722065; Rs0=180.000000e-3; qL=1.713740; qH=0.770000; qX=0.693019; qY=0.987824; Phi=2.253774e-3; Fd=1.000000 Band=(100kHz .. 23MHz), Len=104.1[m], Err_S21dB:(E1=0.28%,E2=0.38%), Err_mix=0.0001345
[ASYMP.bessel]	Z0_inf=122.741965; VF=0.722503; Rs0=180.000000e-3; qL=1.643969; qH=0.760000; Phi=2.172226e-3; Fd=1.000000 Band=(100kHz .. 23MHz), Len=104.1[m], Err_S21dB:(E1=0.54%,E2=0.84%), Err_mix=0.0001504
[ASYMP.hyp]	Z0_inf=122.618963; VF=0.720531; Rs0=180.000000e-3; qL=1.596784; qH=0.780000; Phi=2.626279e-3; Fd=1.000000 Band=(100kHz .. 23MHz), Len=104.1[m], Err_S21dB:(E1=0.97%,E2=1.39%), Err_mix=0.0001792
[ASYMP.mix]	Z0_inf=122.749361; VF=0.722620; Rs0=180.000000e-3; qL=1.679230; qH=0.755909; Phi=2.151006e-3; Fd=1.000000; qB=0.607773 Band=(100kHz .. 23MHz), Len=104.1[m], Err_S21dB:(E1=0.48%,E2=0.65%), Err_mix=0.0001444

### 7.4.2 Virtual loop section of 6 × 100m in cascade

By evaluating a mathematical cascade of the six wire pairs being measured, a two-port “measurement” of about 6×100m = 600m is emulated.

KPN_acc	
[ASYMP.sqrt]	Z0_inf=125.708208; VF=0.731326; Rs0=180.000000e-3; qL=1.770935; qH=0.720000; Phi=1.388412e-3; Fd=1.000000 Band=(100kHz .. 23MHz), Len=624.6[m], Err_S21dB:(E1=1.12%,E2=1.38%), Err_mix=0.0002104
[ASYMP.sqrt.rat]	Z0_inf=125.636455; VF=0.729623; Rs0=180.000000e-3; qL=1.666050; qH=0.740000; qX=0.848761; qY=1.207166; Phi=1.762056e-3; Fd=1.000000 Band=(100kHz .. 23MHz), Len=624.6[m], Err_S21dB:(E1=0.57%,E2=0.70%), Err_mix=0.0001906
[ASYMP.bessel]	Z0_inf=125.445917; VF=0.727385; Rs0=180.000000e-3; qL=1.577390; qH=0.760000; Phi=2.274088e-3; Fd=1.000000 Band=(100kHz .. 23MHz), Len=624.6[m], Err_S21dB:(E1=0.68%,E2=0.89%), Err_mix=0.0002073
[ASYMP.hyp]	Z0_inf=125.517628; VF=0.727092; Rs0=180.000000e-3; qL=1.541717; qH=0.770000; Phi=2.326011e-3; Fd=1.000000 Band=(100kHz .. 23MHz), Len=624.6[m], Err_S21dB:(E1=1.41%,E2=1.68%), Err_mix=0.0002580
[ASYMP.mix]	Z0_inf=125.516807; VF=0.727666; Rs0=180.000000e-3; qL=1.643239; qH=0.750000; Phi=2.195307e-3; Fd=1.000000; qB=0.448007 Band=(100kHz .. 23MHz), Len=624.6[m], Err_S21dB:(E1=0.43%,E2=0.51%), Err_mix=0.0001877

## 7.5 Common reference model for this cable

All asymptotic models in the previous section are predicting the measured cable characteristics very close, and the models [ASYMP.sqrt.rat], [ASYMP.bessel] and [ASYMP.mix] are providing the closest match. However, the tiny improvement of these model may not justify the additional complexity over the simplest one of this subset being [ASYMP.sqrt.rat], and therefore that one is the preferred choice for modeling this cable.

Since the reference model should describe any wire pair of this cable type, its parameter values should be a pragmatic average of the values extracted for each wire pair. The mathematical cascade of the six wire pairs being measured can serve as such average.

Therefore the following asymptotic model is proposed to serve as reference model for this cable type:

KPN_acc	Parameters of reference model
[ASYMP.sqrt.rat]	Z0_inf=125.636455; VF=0.729623; Rs0=180.000000e-3; qL=1.666050; qH=0.740000; qX=0.848761; qY=1.207166; Phi=1.762056e-3; Fd=1.000000

Model, with square root of rational function, 8+1 parameters

$$[Z_s, Y_p] = \text{Model}(Z_{0\infty}, \eta_{VF}, R_{s0}, q_L, q_H, q_x, q_y, f, f_d)$$

$$Z_s(j\omega) = j\omega \cdot L_{s\infty} + R_{s0} \times \left( 1 - q_s \cdot q_x + \text{sqr}t \left( q_s^2 \cdot q_x^2 + 2 \cdot \frac{j\omega}{w_s} \cdot \left( \frac{q_s^2 + j\omega/w_s \cdot q_y}{q_s^2/q_x + j\omega/w_s \cdot q_y} \right) \right) \right)$$

$$Y_p(j\omega) = j\omega \cdot C_{p0} \times \left( 1 + \frac{j\omega}{w_d} \right)^{-2 \cdot f/p}$$

Where:

$$L_{s\infty} = \frac{1}{h_{VF} \cdot c_0} \times Z_{0\infty}$$

$$C_{p0} = \frac{1}{h_{VF} \cdot c_0} \times \frac{1}{Z_{0\infty}}$$

$$q_s = \frac{1}{q_H \cdot q_L}$$

$$w_s = q_H^2 \cdot w_{s0} = q_H^2 \cdot \left( \frac{4p \cdot R_{s0}}{m_0} \right)$$

$$w_d = 2p \cdot f_d$$

$$c_0 = 3 \cdot 10^8 \text{ [m/s]}$$

$$m_0 = 4\pi \cdot 10^{-7} \text{ [H/m]}$$

## 8 REFERENCES

### TO BE ELABORATED

- Private communications with Jo Musson (retired from Marconi) during 2006-2007
- ETSI cable reference document
- BT, KPN, MAR model etc
- Cable model in ITU standards
- ITU contribution on cable measurements
- Causality relations